

เส้นใยอิเล็กทรอนิกส์ของคาร์บอนนาโนทิวบ์-ไนลอน6 คอมพอสิตเป็นตัวดูดซับ
ในการสกัดด้วยวัฏภาคของแข็งสำหรับการตรวจวัดพอลิไซคลิกแอโรแมติกไฮโดรคาร์บอน



บทคัดย่อและแฟ้มข้อมูลฉบับเต็มของวิทยานิพนธ์ตั้งแต่ปีการศึกษา 2554 ที่ให้บริการในคลังปัญญาจุฬาฯ (CUIR)
เป็นแฟ้มข้อมูลของนิสิตเจ้าของวิทยานิพนธ์ ที่ส่งผ่านทางบัณฑิตวิทยาลัย

The abstract and full text of theses from the academic year 2011 in Chulalongkorn University Intellectual Repository (CUIR)
are the thesis authors' files submitted through the University Graduate School.

วิทยานิพนธ์นี้เป็นส่วนหนึ่งของการศึกษาตามหลักสูตรปริญญาวิทยาศาสตรมหาบัณฑิต
สาขาวิชาปิโตรเคมีและวิทยาศาสตร์พอลิเมอร์
คณะวิทยาศาสตร์ จุฬาลงกรณ์มหาวิทยาลัย
ปีการศึกษา 2558
ลิขสิทธิ์ของจุฬาลงกรณ์มหาวิทยาลัย

ELECTROSPUN CARBON NANOTUBE-NYLON6 COMPOSITE FIBERS
AS SOLID PHASE EXTRACTION SORBENT FOR DETERMINATION OF
POLYCYCLIC AROMATIC HYDROCARBONS

Mr. Sirisak Tharasiripaitoon



A Thesis Submitted in Partial Fulfillment of the Requirements
for the Degree of Master of Science Program in Petrochemistry and Polymer Science

Faculty of Science

Chulalongkorn University

Academic Year 2015

Copyright of Chulalongkorn University

Thesis Title ELECTROSPUN CARBON NANOTUBE-NYLON6
COMPOSITE FIBERS AS SOLID PHASE EXTRACTION
SORBENT FOR DETERMINATION OF POLYCYCLIC
AROMATIC HYDROCARBONS

By Mr. Sirisak Tharasiripaitoon

Field of Study Petrochemistry and Polymer Science

Thesis Advisor Assistant Professor Puttaruksa Varanusupakul,
Ph.D.

Accepted by the Faculty of Science, Chulalongkorn University in Partial
Fulfillment of the Requirements for the Master's Degree

.....Dean of the Faculty of Science
(Associate Professor Polkit Sangvanich, Ph.D.)

THESIS COMMITTEE

.....Chairman
(Assistant Professor Warinthorn Chavasiri, Ph.D.)

.....Thesis Advisor
(Assistant Professor Puttaruksa Varanusupakul, Ph.D.)

.....Examiner
(Associate Professor Chawalit Ngamcharussrivichai, Ph.D.)

.....External Examiner
(Natthida Sriboonvorakul, Ph.D.)

ศิริศักดิ์ ธาราศิริไพฑูรย์ : เส้นใยอีเล็กโทรสปินของคาร์บอนนาโนทิวบ์-ไนลอน6 คอมพอสิตเป็นตัวดูดซับในการสกัดด้วยวัฏภาคของแข็งสำหรับการตรวจวัดพอลิไซคลิกแอโรแมติกไฮโดรคาร์บอน (ELECTROSPUN CARBON NANOTUBE-NYLON6 COMPOSITE FIBERS AS SOLID PHASE EXTRACTION SORBENT FOR DETERMINATION OF POLYCYCLIC AROMATIC HYDROCARBONS) อ.ที่ปรึกษาวิทยานิพนธ์หลัก: ผศ. ดร.พุทธรักษา วรานุศูภากุล, 94 หน้า.

ในงานวิจัยนี้ได้เตรียมเส้นใยอีเล็กโทรสปินของคาร์บอนนาโนทิวบ์-ไนลอน6 คอมพอสิตเพื่อใช้เป็นตัวดูดซับในการสกัดด้วยวัฏภาคของแข็ง โดยการเติมคาร์บอนนาโนทิวบ์ช่วยให้ประสิทธิภาพในการสกัดพอลิไซคลิกแอโรแมติกไฮโดรคาร์บอนดีขึ้น ได้ตรวจสอบลักษณะเฉพาะของแผ่นเส้นใยที่เตรียมได้ด้วยเทคนิค SEM, TEM, DSC, TGA และ การดูดซับแก๊สไนโตรเจนพบว่าขนาดเส้นผ่านศูนย์กลางของเส้นใยอยู่ในช่วง 59-117 นาโนเมตร และมีพื้นที่ผิวของเส้นใยอีเล็กโทรสปินของคาร์บอนนาโนทิวบ์-ไนลอน6 คอมพอสิต และเส้นใยอีเล็กโทรสปินของไนลอน6 เท่ากับ 148 และ 139 ตารางเมตรต่อกรัม ตามลำดับเมื่อความเข้มข้นของสารละลายไนลอน6 เพิ่มขึ้นทำให้เส้นใยมีขนาดใหญ่ขึ้น แต่การเพิ่มระยะทางระหว่างปลายเชื่อมกับตัวรองรับทำให้ขนาดเส้นผ่านศูนย์กลางมีขนาดเล็กลง คาร์บอนนาโนทิวบ์ที่อยู่ในเส้นใยมีการวางตัวในแนวเดียวกันกับเส้นใยไนลอน6 ซึ่งปริมาณสูงสุดที่สามารถเติมคาร์บอนนาโนทิวบ์ คือ ร้อยละ 0.83 โดยน้ำหนัก เพราะเมื่อมีปริมาณคาร์บอนนาโนทิวบ์มากกว่า ร้อยละ 0.83 โดยน้ำหนัก ส่งผลให้ไม่สามารถขึ้นรูปเป็นเส้นใยได้ จากนั้นนำเส้นใยที่เตรียมได้มา ศึกษาการสกัดพอลิไซคลิกแอโรแมติกไฮโดรคาร์บอนในน้ำพบว่าภาวะที่ได้ประสิทธิภาพสูงสุดเมื่อใช้แผ่นเมมเบรน 4.0 มิลลิกรัม (ร้อยละ 30 โดยน้ำหนักต่อปริมาตร ของไนลอน6 ที่มีการเติมคาร์บอนนาโนทิวบ์ ร้อยละ 0.83 โดยน้ำหนัก) และชะด้วยตัวทำละลายผสมของแอสีโตนกับอะซิโตนไทรล์ในอัตราส่วน 1 ต่อ 1 โดยปริมาตร ปริมาตร 1 มิลลิลิตร ค่าร้อยละการคืนกลับ (%Recovery) ของการสกัดสารในน้ำที่มีการเติมพอลิไซคลิกแอโรแมติกไฮโดรคาร์บอนที่ความเข้มข้น 8 มิลลิกรัมต่อลิตร เท่ากับ ร้อยละ 56.7 ถึง 100.8 และมีค่าส่วนเบี่ยงเบนมาตรฐานสัมพัทธ์ (RSD) น้อยกว่า 5 มีค่าปริมาณต่ำสุดที่สามารถตรวจพบได้ (LOD) และค่าปริมาณต่ำสุดที่สามารถรายงานเป็นตัวเลขได้ (LOQ) อยู่ในช่วง 0.2 ถึง 3.0 และ 0.5 ถึง 6.0 มิลลิกรัมต่อลิตร ตามลำดับ เมื่อนำแผ่นเมมเบรนไปประยุกต์ใช้ในการวิเคราะห์ พอลิไซคลิกแอโรแมติกไฮโดรคาร์บอนในน้ำตัวอย่างจริง พบว่า ค่าร้อยละการคืนกลับของการสกัดสารในน้ำที่มีการเติม พอลิไซคลิกแอโรแมติกไฮโดรคาร์บอนที่ความเข้มข้น 10 มิลลิกรัมต่อลิตร เท่ากับ ร้อยละ 54.2 ถึง 101.6 และเปรียบเทียบวิธีกับงานวิจัยอื่น

สาขาวิชา ปิโตรเคมีและวิทยาศาสตร์พอลิเมอร์
ปีการศึกษา 2558

ลายมือชื่อนิสิต
ลายมือชื่อ อ.ที่ปรึกษาหลัก

5672107323 : MAJOR PETROCHEMISTRY AND POLYMER SCIENCE

KEYWORDS: CARBON NANOTUBES / NYLON6 / ELECTROSPINNING / POLYCYCLIC AROMATIC HYDROCARBONS / SOLID PHASE EXTRACTION

SIRISAK THARASIRIPAITOON: ELECTROSPUN CARBON NANOTUBE-NYLON6 COMPOSITE FIBERS AS SOLID PHASE EXTRACTION SORBENT FOR DETERMINATION OF POLYCYCLIC AROMATIC HYDROCARBONS. ADVISOR: ASST. PROF. PUTTARUKSA VARANUSUPAKUL, Ph.D., 94 pp.

In this work, electrospun carbon nanotubes-Nylon6 (CNTs-Nylon6) composite fibers were prepared in order to apply as an adsorbent for solid phase extraction (SPE). Adding of CNTs is expected to improve the extraction efficiency of electrospun Nylon6 fibers for determination of polycyclic aromatic hydrocarbons (PAHs). The electrospun CNTs-Nylon6 composite fibers were characterized by scanning electron microscopy (SEM), transmission electron microscopy (TEM), differential scanning calorimetry (DSC), thermogravimetric analysis (TGA) and N₂ physisorption measurement. The average diameters of obtained fibers ranged from 59 to 117 nm and the BET specific surface area of the electrospun CNTs-Nylon6 composite nanofibers and Nylon6 was 149 and 139 m²/g, respectively. The increase of Nylon6 concentration led to larger fiber diameters. However, increasing the distance of the needle to the collector resulted in smaller fiber diameters. The CNTs aligned along the long axis of Nylon6 nanofibers. The maximum amount of added CNTs was 0.83 %w/w because non-uniform fibers were formed when the amount of CNTs was more than 0.83 %w/w. The obtained electrospun CNTs-Nylon6 composite fibers were examined as SPE disk for determination of PAHs in water. The optimum conditions for extraction of PAHs were using 4.0 mg of electrospun CNTs-Nylon6 composite fibers prepared from 30 %w/v of Nylon6 and 0.83 %w/w of CNTs and eluted with 1 mL of 1:1 (v/v) mixture of acetone and acetonitrile. The percentage recoveries of the extraction of PAHs from 8 µg/L spiked water at optimum conditions were in the range of 56.7-100.8% with the %RSD less than 5. The MOD and MOQ were 0.2-3.0 µg/L and 0.5-6.0 µg/L, respectively. Finally, the membrane was applied for the analysis of PAHs in real water samples. The percentage recoveries of PAHs at 10 µg/L spiked in the samples ranged from 54.2-101.6% which comparable to other methods.

Field of Study: Petrochemistry and Polymer Science

Science

Student's Signature

Advisor's Signature

Academic Year: 2015

ACKNOWLEDGEMENTS

The author a lot of thanks and appreciate many people for kindly providing the knowledge in this study. My research can be successfully completed with support and helpfulness from my advisor, Assistant Professor Dr. Puttaruksa Varanusupakul who has been giving useful advisements for solving many problems through my experiment. I would like to extend my appreciation to Assistant Professor Dr. Warinthon Chavasiri, Associate Professor Dr. Chawalit Ngamcharussrivichai, and Dr. Natthida Sriboonvorakul for their valuable suggestion as my thesis committees.

Moreover, I would like to thank many people in Chromatography and Separation Research Unit (ChSRU) and members of 1205/1207 laboratory who gave helpfulness for doing my work until my research was completely finished. Thanks for your regards, remission, kindness, listening, and suggestion for the problems about my thesis. I am very glad to have the chance to known and see them.

Finally, I would like to thank my beloved family; father, mother, and my intimate friends for their unlimited supports, love, care, encourage, understanding, and helpfulness.

CONTENTS

	Page
THAI ABSTRACT	iv
ENGLISH ABSTRACT	v
ACKNOWLEDGEMENTS	vi
CONTENTS	vii
LIST OF TABLES	xi
LIST OF FIGURES	xiv
LIST OF ABBREVIATIONS AND SYMBOLS	xvii
CHAPTER I INTRODUCTION	1
1.1 Statement of purpose	1
1.2 Objective of this research	4
1.3 Scopes of this research	5
1.4 Benefits of the research	5
CHAPTER II THEORY	6
2.1 Nylon6	6
2.2 Carbon nanotubes	7
2.3 Electrospinning	8
2.3.1 Electrospinning process	8
2.3.2 Parameters of electrospinning	10
2.3.2.1 Solution parameters	10
2.3.2.1.1 Solution concentration	10
2.3.2.1.2 Viscosity	11
2.3.2.1.3 Surface tension	11

	Page
2.3.2.1.4 Conductivity.....	11
2.3.2.2 Process parameters	12
2.3.2.2.1 Applied electric potential.....	12
2.3.2.2.2 Collector distance	12
2.3.2.2.3 Flow rate/feed rate	12
2.4 Solid-phase extraction (SPE).....	13
2.4.1 Procedure and mechanism of SPE process	13
2.4.2 SPE formats.....	14
2.4.2.1 SPE cartridges.....	14
2.4.2.2 Pipette-tip format in SPE.....	15
2.4.2.3 Stir bar format in SPE	16
2.4.2.4 Disk format in SPE	16
2.4.3 Sorbents in SPE.....	18
2.4.3.1 Silica and bonded silica sorbent.....	18
2.4.3.2 Polymer sorbents.....	19
2.4.3.3 Nanostructured materials.....	19
2.4.3.4 Molecularly imprinted polymers	19
2.5 Analysis of PAHs.....	20
CHAPTER III EXPERIMENTAL.....	21
3.1 Materials	21
3.1.1 Preparation of electrospun CNTs-Nylon6 composite nanofibers by electrospinning technique.....	21
3.1.2 Extraction of PAHs in water.....	21

	Page
3.2 Methodology.....	22
3.2.1 Preparation of electrospun CNTs-Nylon6 composite nanofibers.....	22
3.2.2 Characterization of electrospun CNTs-Nylon6 composite nanofibers.....	23
3.2.2.1 Scanning electron microscopy (SEM).....	23
3.2.2.2 Transmission electron microscopy (TEM).....	23
3.2.2.3 Thermogravimetric analysis (TGA).....	23
3.2.2.4 Differential scanning calorimetry (DSC).....	24
3.2.2.5 Nitrogen physisorption measurement	24
3.2.3 Analysis of PAHs by GC-MS.....	24
3.2.4 Extraction of PAHs by electrospun CNTs-Nylon6 composite nanofibers..	25
3.2.4.1 Preparation of PAHs solutions.....	25
3.2.4.2 Extraction procedure.....	25
3.2.4.3 Optimization of membrane material	26
3.2.4.4 Optimization of types of desorption solvent.....	27
3.2.4.5 Optimization of volume of the desorption solvent	27
3.2.4.6 Optimization of sorbent weight	27
3.2.4.7 Recovery of PAHs extraction.....	28
3.2.4.8 Method of detection (MOD) and method of quantitation (MOQ).....	28
3.2.4.9 Reproducibility.....	28
3.2.5 Extraction of PAHs in water sample	28
CHAPTER IV RESULTS AND DISCUSSION	29
4.1 Optimization and characterization of the electrospun CNTs-Nylon6 composite fibers	29

	Page
4.1.1 Optimization of electrospun CNTs-Nylon6 composite nanofibers.....	29
4.1.1.1 Effect of Nylon6 concentration.....	29
4.1.1.2 Effect of collector distance.....	31
4.1.1.3 Effect of CNTs amount.....	33
4.1.2 Characterization of electrospun CNTs-Nylon6 composite nanofibers.....	35
4.1.2.1 Transmission electron microscopy (TEM).....	35
4.1.2.2 Thermogravimetric analyzer (TGA)	37
4.1.2.3 Differential scanning calorimetry (DSC).....	40
4.1.2.4 Nitrogen physisorption measurement	42
4.2 The extraction of PAHs in water using the electrospun CNTs-Nylon6 composite nanofibers	44
4.2.1 Effect of membrane material.....	44
4.2.2 Desorption solvent.....	48
4.2.3 Volume of the desorption solvent.....	51
4.2.4 Weight of the electrospun CNTs-Nylon6 composite nanofibers	54
4.3 Method validation	58
4.4 Applied the electrospun CNTs-Nylon6 composite nanofibers for determination of PAHs in water samples	62
CHAPTER V CONCLUSIONS.....	71
5.1 Conclusions.....	71
5.2 Suggestion of future work	73
REFERENCES	74
VITA.....	94

LIST OF TABLES

	Page
Table 1.1 Name and structure of some PAHs regulated by EPA [6].	2
Table 2.1 Advantages and disadvantage of Nylon6.....	7
Table 2.2 Comparison of formats in SPE.....	17
Table 3.1 GC condition	24
Table 3.2 MS condition.....	25
Table 3.3 Abbreviations of sorbent.....	27
Table 4.1 Morphology of CNTs-Nylon6 nanofibers at various Nylon6 concentrations.....	30
Table 4.2 Average diameters of electrospun CNTs-Nylon6 composite nanofibers at 30%w/v of Nylon6 and 0.33%w/w of CNTs (n=20).....	31
Table 4.3 The optimum of the collector distance for fabricated electrospun Nylon6 and CNTs-Nylon6 composite nanofibers.	32
Table 4.4 Average diameters of CNTs-Nylon6 composite nanofibers (nm) for the optimum of collector distance. (n=20).....	33
Table 4.5 Thermal properties of nanofibers electrospun from Nylon6 and CNTs/Nylon6 composite.....	40
Table 4.6 Percentage recoveries and standard deviations for the extraction of PAHs from spiked water at 8 µg/L by different sorbents	47
Table 4.7 Percentage recoveries and standard deviations of the extraction of PAHs from spiked water at 8 µg/L by 30N0.83C sorbent and eluting with different solvents.....	50
Table 4.8 Percentage recoveries and standard deviations of extraction PAHs from at 8 µg/L spiked in to Milli-Q water by 30N0.83C sorbent and	

	eluted with different volumes of 1:1 (v/v) mixture of acetone and acetonitrile.	53
Table 4.9	Percentage recoveries and standard deviations of extraction PAHs from at 8 µg/L spiked in to Milli-Q water by different weights of 30N0.83C sorbent.	56
Table 4.10	The optimum condition for the extraction of PAHs in water by electrospun CNTs-Nylon6 composite nanofibers.	57
Table 4.11	Method of detection (MOD) and method of quantitation (MOQ) for developed method.	58
Table 4.12	Percentage recoveries and RSD for the extraction of PAHs from spiked water at 6, 8 and 10 µg/L PAHs (n=10).	59
Table 4.13	Comparison of PAHs recoveries from other researches to our sorbent.	60
Table 4.14	Comparison of method from other researches.	61
Table 4.15	Percentage recoveries of PAHs at 10 µg/L spiked in drinking water sample 1.	62
Table 4.16	Percentage recoveries of PAHs at 10 µg/L spiked in drinking water sample 2.	63
Table 4.17	Percentage recoveries of PAHs at 10 µg/L spiked in drinking water sample 3.	64
Table A-1	Equation and R^2 value of calibration curve for PAHs.	82
Table A-2	Retention time, Peak width and Resolution of PAHs.	86
Table A-3	Determined PAHs concentration in spiked water (8 µg/L) for extraction by different sorbents.	87
Table A-4	Determined PAHs concentration in spiked water (8 µg/L) for extraction by 30N0.83C sorbent as the sorbent and eluting with different desorption solvents.	91

Table A-5	Determined PAHs concentration in spiked water (8 µg/L) for extraction by 30N0.83C sorbent and eluting with different volumes of 1:1 (v/v) mixture of acetone and acetonitrile.....	92
Table A-6	Determined PAHs concentration in spiked water (8 µg/L) for extraction by using different weights of 30N0.83C sorbent and eluting with 1 mL of 1:1 (v/v) mixture of acetone and acetonitrile.	93



LIST OF FIGURES

	Page
Figure 2.1 Ring opening polymerization of caprolactam to Nylon6	6
Figure 2.2 Structure of Nylon6 (Above) and Nylon6,6 (Below)	6
Figure 2.3 Structure of CNTs: (A) SWNTs, (B) MWNTs	8
Figure 2.4 Schematics of set up of electrospinning apparatus (a) a typical vertical set up and (b) a horizontal set up of electrospinning apparatus. [35].....	9
Figure 2.5 The model of polymer solution changing: increasing electric fields are applied [36].....	10
Figure 2.6 Solid phase extraction process.....	13
Figure 2.7 SPE cartridge format [46].....	15
Figure 2.8 SPE pipette-tip format [47].....	15
Figure 2.9 SPE stir bar format [5].....	16
Figure 2.10 SPE disk format [48].....	16
Figure 2.11 Sorbent particles in (A) SPE disk and (B) SPE cartridge [49]	17
Figure 3.1 Schematic of electrospinning apparatus [58].....	22
Figure 3.2 13 mm SPE disk format of electrospun CNTs-Nylon6 composite nanofibers.....	23
Figure 3.3 Filter holder	26
Figure 3.4 Steps of PAHs extraction by electrospun CNTs-Nylon6 composite membrane.....	26
Figure 4.1 SEM images of the electrospun CNTs-Nylon6 composite nanofibers (A) 15% (B) 20% (C) 25% (D) 30% w/v of Nylon6 with 0.2% w/w of CNTs.....	30

Figure 4.2	SEM images of the electrospun CNTs-Nylon6 composite nanofibers 30% w/v of Nylon6 with 0.33% w/w of CNTs, collector distance at (A) 11 cm, (B) 12 cm and (C) 13 cm.....	32
Figure 4.3	SEM images of the electrospun CNTs-Nylon6 composite nanofibers at various concentrations of Nylon6 and CNTs.....	34
Figure 4.4	TEM images of (A) CNTs, (B) pure Nylon6, (C) 25 %w/v and (D) 30 %w/v of Nylon6 with 0.83 %w/w of CNTs.	35
Figure 4.5	The dispersion of CNTs in the electrospun 30 %w/v of Nylon6 fibers with 0.83 %w/w of CNTs nanofibers.....	36
Figure 4.6	TGA curves of (A) 30 %w/v of Nylon6 with CNTs and pure CNTs. The heating speed was 25°C/min. (B) Enlarge image of TGA curves for 30 %w/v of Nylon6 with CNTs at 400-800 °C.....	38
Figure 4.7	TGA curves of (A) 25 %w/v of Nylon6 with CNTs and pure CNTs. The heating speed was 25°C/min. (B) Enlarge image of TGA curves for 25 %w/v of Nylon6 with CNTs at 400-800 °C.....	39
Figure 4.8	DSC thermograms of electrospun CNTs-Nylon6 nanofibers: (A) 25%w/v of Nylon6 and (B) 30%w/v of Nylon6.....	41
Figure 4.9	The nitrogen adsorption-desorption isotherm of (A) the electrospun CNTs-Nylon6 composite nanofibers and (B) the electrospun Nylon6 nanofibers.....	43
Figure 4.10	Percentage recoveries for the extraction of PAHs from spiked water at 8 µg/L by different sorbents.	46
Figure 4.11	Effect of desorption solvent on the extraction of PAHs from spiked water at 8 µg/L.....	49
Figure 4.12	Percentage recoveries of PAHs from at 8 µg/L spiked in to Milli-Q water by extraction with different volumes of 1:1 (v/v) mixture of	

	acetone and acetonitrile for elution. Elute with 1:1 (v/v) mixture of acetone and acetonitrile by different volume.	52
Figure 4.13	Percentage recoveries of PAHs from at 8 µg/L spiked in to Milli-Q water by extraction with different weights of 30N0.83C sorbent and eluted by 1.0 mL of 1:1 (v/v) mixture of acetone and acetonitrile.	55
Figure 4.14	Chromatogram of PAHs from extraction of drinking water sample 1.	65
Figure 4.15	Chromatogram of PAHs from extraction of drinking water sample 1 was spiked PAHs at 10 µg/L.....	66
Figure 4.16	Chromatogram of PAHs from extraction of drinking water sample 2.	67
Figure 4.17	Chromatogram of PAHs from extraction of drinking water sample 2 was spiked PAHs at 10 µg/L.....	68
Figure 4.18	Chromatogram of PAHs from extraction of drinking water sample 3.	69
Figure 4.19	Chromatogram of PAHs from extraction of drinking water sample 3 was spiked PAHs at 10 µg/L.....	70
Figure 5.1	Flow chart of CNTs-Nylon6 composite fibers preparation by electrospinning technique	72
Figure 5.2	Flow chart of extraction of PAHs in water samples	72
Figure A-1	Calibration curve of PAHs analysis by GC-MS	83
Figure A-1	Calibration curve of PAHs analysis by GC-MS (continue).....	84
Figure A-2	GC chromatogram of mixed standard PAHs at 1 mg/L.....	85
Figure A-3	Chromatogram of PAHs from the extraction of 8 µg/L spiked water by C18 SPE.	88
Figure A-4	Chromatogram of PAHs from the extraction of 8 µg/L spiked water by Nylon6 nanofibers (30N).	89
Figure A-5	Chromatogram of PAHs from the extraction of 8 µg/L spiked water by CNTs-Nylon6 composite nanofibers (30N0.33C).	90

LIST OF ABBREVIATIONS AND SYMBOLS

PAHs	Polycyclic aromatic hydrocarbons
SPE	Solid phase extraction
PS	Polystyrene
PAN	Polyacrylonitrile
C18	Octadecyl silica bonded phases
C8	Octyl silica bonded phases
C2	Ethyl silica bonded phases
CH	Cyclohexyl silica bonded phases
PH	Phenyl silica bonded phases
NH ₂	Aminopropyl silica bonded phases
CNTs	Carbon nanotubes
BPA	Bisphenol A
HPLC	High-performance liquid chromatography
GC	Gas chromatography
UV	Ultraviolet
MS	Mass spectrometer
SEM	Scanning electron microscopy
TEM	Transmission electron microscopy
TGA	Thermogravimetric analyzer
DSC	Differential scanning calorimetry
BET	Brunauer, Emmett and Teller
PA6	Polyamide6

K	Kelvin
T _g	Glass transition temperature
T _m	Melt point temperature
°C	Degree Celcius
MIPs	Molecularly imprinted polymers
MeOH	Methanol
ACN	Acetonitrile
mL	Milliliter
μL	Microliter
min	Minute
w/v	Weight by volume
w/w	Weight by weight
v/v	Volume by volume
mm	Millimeter
mg	Milligram
L	liter
MOD	Method of detection
MOQ	Method of quantitation
RSD	Relative standard deviation
cm	Centimeter
nm	Nanometer
ΔH	Enthalpy

CHAPTER I

INTRODUCTION

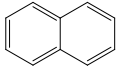
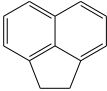
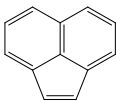
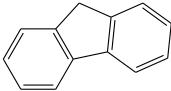
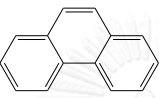
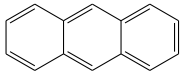
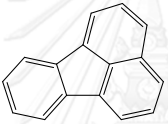
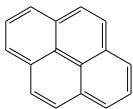

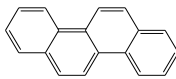
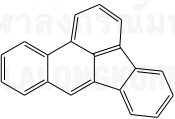
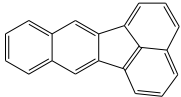
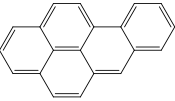
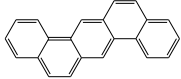
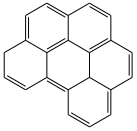
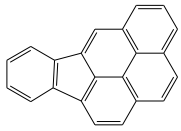
1.1 Statement of purpose

Polycyclic aromatic hydrocarbons (PAHs), an organic compound containing multiple aromatic rings, are produced from an incomplete combustion of organic matter. They are found in fossil fuel, sediment, tar deposits, soil, cooking food, exhaust fumes from cars, smoke and water. PAHs are potentially mutagenic and carcinogen substances and they are also pollutants to the environment [1-4]. Therefore, the amount of PAHs in contaminated water needs to be measured. Some PAHs regulated by Environmental Protection Agency (EPA) are listed in Table 1.1.

PAHs are usually determined by solid phase extraction (SPE) coupled to chromatography because SPE is a simple preparation process, offers a multitude of sorbents and has a high extraction efficiency. Moreover, SPE can also use to concentrate and purify for analysis in one step.

There are two main forms of the sorbent for SPE which are cartridges and disk [5]. SPE disk has particle sizes smaller than SPE cartridges thus it has a large surface area. Moreover, sorbents in SPE disk are usually in fiber form. Therefore, a backpressure in SPE disk is low allowing faster flow rate through the sorbent; hence this type of SPE is suitable for large volume sample. The choice of sorbents for SPE is very important to achieve high enrichment and efficiency for extraction of analytes. In the present, silica and polymer are two types of materials mainly used as a sorbent. Silica is commonly used as particles packed into the column whereas polymer is mostly used as fibers in disk format since polymer has good properties for example light weight, simple synthesis, and good stiffness.

Table 1.1 Name and structure of some PAHs regulated by EPA [6].

Compound	Structure	Compound	Structure
Naphthalene (Na)		Acenaphthene (Ac)	
Acenaphthylene (Ap)		Fluorene (F)	
Phenanthrene (Pa)		Anthracene (A)	
Fluoranthene (Fl)		Pyrene (P)	
Benzo[a]anthracene (BaA)		Chrysene (Ch)	
Benzo[b]fluoranthene (BbF)		Benzo[k]fluoranthene (BkF)	
Benzo[a]pyrene (BaP)		Dibenzo[a,h]anthracene (DBaH)	
Benzo[g,h,i]perylene (BghiP)		Indeno[1,2,3-cd]pyrene (IP)	

Silica particles modified with long chain hydrocarbons were widely studied and applied for SPE extraction of PAHs. For example, Barranco et al. [1] studied the octadecyl (C18) silica bonded phases for extraction of PAHs in edible oil and compared with SPE cartridge of octyl (C8), ethyl (C2), cyclohexyl (CH), phenyl (PH), and aminopropyl (NH₂) silica bonded phases. C18 and C8 sorbents showed the same good recoveries because their polarity was quite non-polar comparing with C2, CH, PH, and NH₂ sorbents.

Moja and Mtunzi [7] used C18 as a SPE sorbent and Kanchanamayoon and Tatrahun [8] compared C18 SPE cartridge (LC-18) with ENVI-18 SPE cartridge for determination of PAHs in water. The C18 cartridge has good extraction efficiency because it can interact with PAHs, which were non-polar compounds better than ENVI-18 cartridge.



In the present, there are many researches used carbon nanotubes (CNTs) as a SPE sorbent because of large surface areas, good adsorption, and a variety of force to interact with analytes, like Van der Waals force, π - π interaction, and electrostatic force [9]. For example, Ma et al. [10] applied CNTs as SPE adsorbent to extract PAHs in water and compared with C18 cartridge. CNTs showed a good extraction efficiency because CNTs could interact with PAHs by π - π interaction and physical adsorption, while C18 cartridge can only interact with PAHs by physical adsorption. Moreover, Gua and Lee [11] reported that the large surface area and the electrostatic properties of CNTs could interact with the aromatic rings of PAHs which facilitated a strong adsorption between PAHs and CNTs. When compared with graphite, granular activated carbon, C2 silica bonded phases, and C18 silica bonded phases, CNTs were a better SPE adsorbent for extraction PAHs in water samples.

There are many works used the polymer nanofiber-based SPE devices [12,13] which fabricated by electrospinning technique. The advantage of nanofibers material is the large specific surface area allowing the reduction of sorbent bed mass while high extraction efficiency is accomplished. Electrospinning technique is a popular method to fabricate fibers because the electrospun fibers have small diameters and high surface area. Thereby, using electrospun fibrous membrane as a sorbent for SPE

is interested. Many polymers were studied such as Nylon6, polystyrene (PS) and polyacrylonitrile (PAN) [14,15].

Xu et al. used electrospun Nylon6 nanofibers as a membrane for extraction of estrogens [16] and phthalate esters in water sample [17]. Average diameters of nanofibers were optimized and a comparison with commercial Nylon6 microporous membrane and C18 silica cartridges was carried out. The results showed that electrospun Nylon6 nanofibrous membrane, as a new adsorbent material had great potential for the enrichment of steroid estrogens in the water samples with good recovery, repeatability, and sensitivity.

Wu et al. [18] applied electrospun Nylon6 fibrous membrane for the determination of bisphenol A (BPA) in plastic bottled drinking water with HPLC-UV. A comparison between the electrospun Nylon6 nanofibrous membrane and commercially available SPE was studied. The electrospun Nylon6 nanofibrous membrane showed a great potential for the enrichment and determination of BPA in water.

As electrospun polymer nanofibrous membrane showed a great practicability as a sorbent in SPE, Nylon6 was interested to fabricate and applied for determination of PAHs in water samples in this work. Moreover, CNTs which had large surface area, good adsorption, and a variety of force to interact with PAHs were added to improve the extraction efficiency. Important parameters influencing fabrication of CNTs-Nylon6 composite nanofibers via electrospinning process were optimized and studied. The applicability of the proposed SPE disk for determination of PAHs in water samples was also examined.

1.2 Objective of this research

The objective of this work is to prepare electrospun CNTs-Nylon6 composite nanofibers in membrane format and used as a sorbent in solid-phase extraction for determination of PAHs in water samples.

1.3 Scopes of this research

- 1.3.1 Electrospun fibrous CNTs-Nylon6 composite nanofibers were prepared by electrospinning technique.
- 1.3.2 The electrospinning factors to fabricate electrospun fibrous CNTs-Nylon6 composite, for example, concentration of Nylon6, collector distance and amount of CNTs were optimized.
- 1.3.3 Electrospun fibrous CNTs-Nylon6 composite nanofibers were studied for extraction of PAHs in water and compared with commercial C18 SPE cartridge.
- 1.3.4 Electrospun fibrous CNTs-Nylon6 composite nanofibers were applied for the determination of PAHs in real water samples.

1.4 Benefits of the research

The research aimed to get an electrospun fibrous CNTs-Nylon6 composite membrane which can be an alternative sorbent for extraction of PAHs in water samples.



CHAPTER II

THEORY

2.1 Nylon6

Nylon6 or polycaprolactam or polyamide6 (PA6) is a polymer developed by Paul Schlack at IG Farben to reproduce the properties of nylon6,6 without violating the patent on its production. Nylon6 is a semi-crystalline polyamide. Nylon6 is not a condensation polymer. Instead, Nylon6 is formed by ring-opening polymerization of caprolactam which has 6 carbons. The ring of caprolactam will break and undergoes polymerization, when caprolactam is heated at about 533 K in an inert atmosphere of nitrogen for about 4-5 hours as Figure 2.1. During polymerization, the amide bond within each caprolactam molecule is broken, with the active groups on each side reforming two new bonds as the monomer becomes portion of the polymer backbone. Dissimilar Nylon6,6, the direction of the amide bond reverses at each bond, all Nylon6 amide bonds lie in the same direction as Figure 2.2.

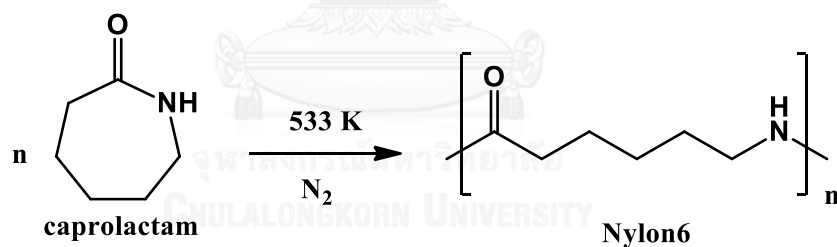


Figure 2.1 Ring opening polymerization of caprolactam to Nylon6

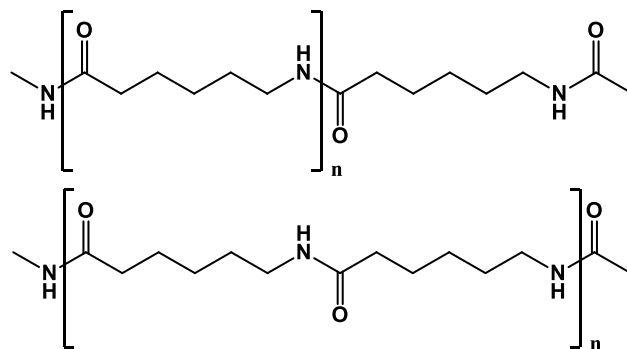


Figure 2.2 Structure of Nylon6 (Above) and Nylon6,6 (Below)

Nylon6 fibers are possessing high tensile strength, elasticity, luster, and tough. They can be a wrinkleproof and highly resistant to abrasion and chemicals such as acids and alkalis. The glass transition temperature (T_g) of Nylon6 is 47 °C which is a solid state at room temperature.

As a result of its high strength, Nylon6 is widely used for gears, fittings, and bearings in automotive industry, as thread in bristles for toothbrushes, surgical sutures, strings for acoustic and classical musical instruments, i.e. guitars, violins, and cellos, and as a material for power tools housings. Nylon6 is also used in the manufacture of a large variety of threads, ropes, filaments, nets, besides hosiery and knitted garments. Table 2.1 summarizes the advantages and disadvantages of Nylon6. In addition, Nylon6 can also be used as a composite with other polymers or materials.

Table 2.1 Advantages and disadvantage of Nylon6

Advantages	Disadvantages
<ul style="list-style-type: none"> • Strength • Toughness • Inflexibility • Abrasion • Chemical resistance 	<ul style="list-style-type: none"> • High water adsorption • Poor chemical resistance to strong and base

2.2 Carbon nanotubes

Carbon nanotubes (CNTs) are allotropes of carbon with tubular nanostructure that individual CNTs naturally align themselves into ropes held together by van der Waals forces, more specifically, pi-stacking. CNTs are divided into two types: single-walled carbon nanotubes (SWNTs) and multi-walled carbon nanotubes (MWNTs) as Figure 2.3. These tubular carbon molecules have unusual properties, which are valuable for nanotechnology, electronics, optics and other fields of materials science and technology. Particularly, thanks to their thermal conductivity, mechanical and electrical properties, CNTs are used with many applications as additives to various

structural materials. For instance, CNTs form a trifling portion of the materials in some baseball bats, golf clubs, and car parts.

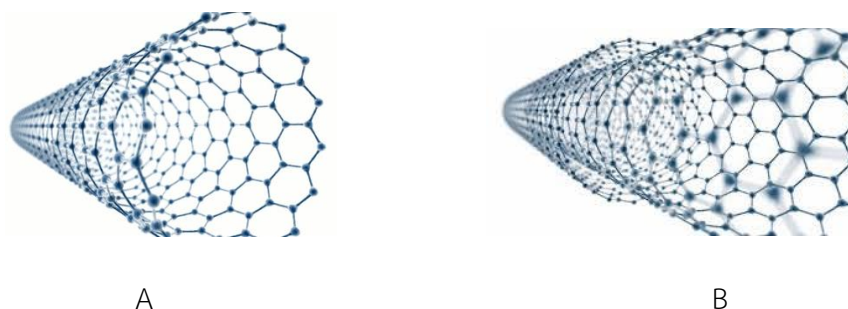


Figure 2.3 Structure of CNTs: (A) SWNTs, (B) MWNTs

Furthermore, CNTs are a good adsorbent because CNTs have high surface areas, length-to-diameter ratio of up to 132,000,000:1, significantly larger than for any other material, can be applied to use with organic and inorganic compounds, and can interact with the analytes by a variety of force such as van der Waals force, π - π interaction, and electrostatic force.

2.3 Electrospinning

2.3.1 Electrospinning process

Nanofibers are a unique class of nanomaterials with interesting properties thanks to their nanoscale diameters and large aspect ratio. They possess good mechanical properties and their surface can be readily modified owing to their high surface area to volume ratio [12]. Nanofibers can be produced with different techniques, for example, template synthesis [19,20], drawing [21-23], phase separation [24,25], and electrospinning [26-28]. Among these techniques, electrospinning is rapidly emerging as a simple and reliable technique for the preparation of smooth nanofibers with controllable morphology from a variety of polymers [29-33]. Electrospinning is a technique which uses electric force to draw charged threads of polymer solutions or polymer melts up to fibers which have

diameters range from a few nanometers to more than 1 of micrometers [34] and a larger surface area than those obtained from conventional spinning processes. These fibers are interesting for such application as electrode materials, biomedical application, optical sensor, pharmaceutical, filter media, and sorbent for SPE.

Basically, an electrospinning system consists of three basic components: a high voltage power supply, a spinneret (such as pipette tip, a capillary with metal needle), and a grounded collecting plate (e.g. a metal screen, stationary plate, or rotating mandrel). Currently, there are two standard electrospinning setups, vertical and horizontal, shown in Figure 2.4.

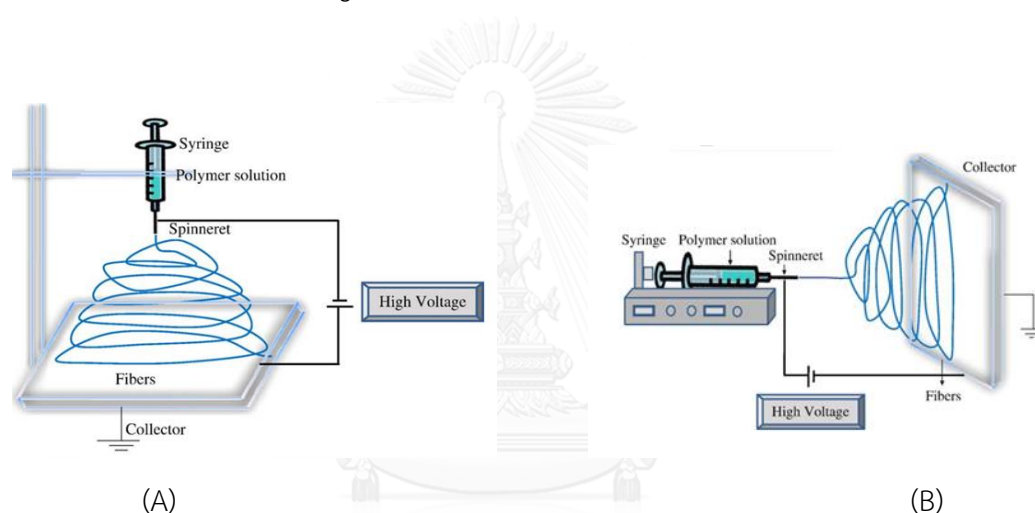


Figure 2.4 Schematics of set up of electrospinning apparatus (a) a typical vertical set up and (b) a horizontal set up of electrospinning apparatus. [35]

In the electrospinning system, a power supply is connected between anode and cathode. At the first stage, voltage is not applied; the surface is the only forces that act on the liquid surface at the outlet of the needle. The shape of the surface is hemispherical in a first approximation. When a positive potential is applied to the solution at the anode, the hemispherical shape of the solution at the needle tip will change to Taylor's cone, which is conical shape. The electrical forces overcome the surface tension forces when the electric field applied reaches a critical value. Eventually, a charged jet of the solution is ejected from the needle tip of the

Taylor cone and an unstable and a rapid whipping of the jet occurs in the space between the needle tip and collector which leads to evaporation of the solvent before falling on the collector, leaving a polymer behind. The Taylor's cone is shown in Figure 2.5.

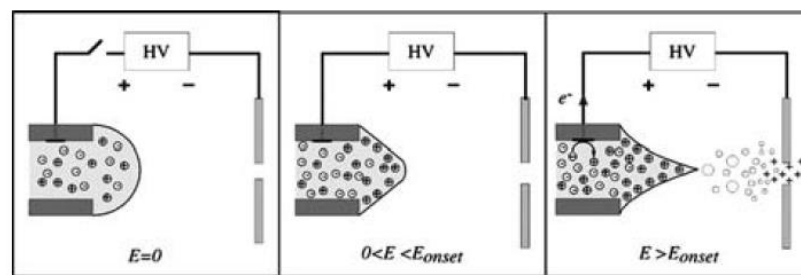


Figure 2.5 The model of polymer solution changing: increasing electric fields are applied [36].

2.3.2 Parameters of electrospinning

The morphology and diameter of electrospun fibers are governed by many parameters, classified into two parameters: solution parameters and process parameters.

2.3.2.1 Solution parameters

2.3.2.1.1 Solution concentration

For fiber formation to occur, a minimum solution concentration is required. It has been found that there should be an optimum solution concentration for the electrospinning process. At low concentrations, beads are formed instead of fibers. As the solution concentration increases, finally uniform fibers with increased diameters are formed because of the higher viscosity. At high concentrations, the formation of continuous fibers is prohibited because of the inability to maintain the flow of the solution at the tip of the needle resulting in the formation of larger fibers.

2.3.2.1.2 Viscosity

Solution viscosity is an important factor in determining the fiber size and morphology of the electrospun fibers. At very low viscosity, the fiber formation is not continuous, whereas, at very high viscosity, it is difficult in the ejection of jets from polymer solution, thus there is a requirement of optimal viscosity for electrospinning.

2.3.2.1.3 Surface tension

Surface tension is a critical factor in the electrospinning process. The formation of droplets, bead and fibers depend on the surface tension of solution. Reducing the surface tension of a nanofibers solution, fibers can be obtained without beads, where, the high surface tension prevents the process of spinning owing to instability of the jets and the generation of sprayed droplets [37]. Different solvents may lead different surface tensions. Moreover, a lower surface tension of the spinning solution helps electrospinning to occur at a lower electric field.

2.3.2.1.4 Conductivity

Solution of zero conductivity cannot be an electrospun. Conductivity of spinning solution is mainly determined by the polymer type, solvent used, and additive such as inorganic salt, ionic organic compound, and nanomaterial. Increasing of conductivity of the spinning solution, there is a significant decrease in the diameter of the electrospun nanofibers, whereas, low conductivity of the spinning solution, there results insufficient elongation of a jet by electrical force to produce uniform fiber, and beads may also be observed. However, highly conductive solutions are extremely unstable in the presence of strong electric fields which results in a broad diameter distribution and beads on the nanofibers.

2.3.2.2 Process parameters

2.3.2.2.1 Applied electric potential

In the electrospinning process, an essential parameter is the applied voltage. After applied voltage, fiber formation will occur; this influences the charges on the solution along with electric field and commences the electrospinning process. Increasing the electric field strength will increase the electrostatic repulsive force on the polymer jet, thus, a higher voltage brings about greater stretching of the solution as well as a stronger electric field. These effects contribute to reduction in the fiber diameter and also rapid evaporation of solvent. Furthermore, at a higher voltage, there is also greater probability of beads formation. Even though diameter and morphology of the fibers depend on the electric potential, other parameters (the flow rate and collector distance) are considered together.

2.3.2.2.2 Collector distance

The distance between the tip and the collector (collector distance) is an important parameter which controls the fiber diameters and morphology because it affects the time spent in the evaporation of the solvent and strength of the electric field [38]. A minimum distance is required to give the sufficient time for fibers to dry before reaching the collector. The diameters of the fibers will be decreased when increased the collector distance, whereas, reducing the collector distance is shorter solvent evaporation time, and increases the electric field strength.

2.3.2.2.3 Flow rate/feed rate

The flow rate is an important parameter which controls transferring of the polymer from the syringe to the collector. Therefore, a lower feed rate is desirable since the solvent will get enough time for evaporation, and will decrease in diameters of the fibers [39]. Conversely, high flow rates result in bead formation on the fibers owing to unavailability of proper drying time prior to

reaching the collector. Accordingly, there should always be an optimum flow rate for spinning.

2.4 Solid-phase extraction (SPE)

Solid phase extraction (SPE) is the most popular used procedure for clean-up [40], extraction, and pre-concentration of trace analytes from environmental [41], clinical [42], biological, food and beverages samples [43,44]. SPE provides low solvent consumption, low costs, reduction of processing time and automation whole process [45].

2.4.1 Procedure and mechanism of SPE process

The SPE process provides samples, which are in solution, free of interfering matrix components, and concentrated enough for detection. This is done in four steps as Figure 2.6.

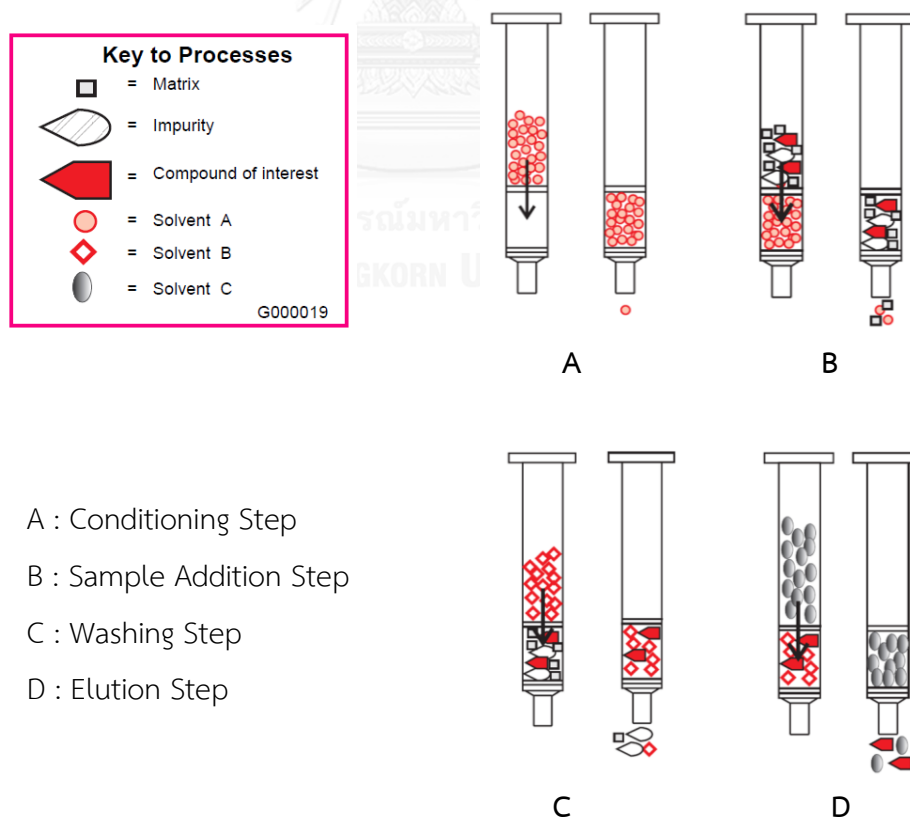


Figure 2.6 Solid phase extraction process

A : Conditioning step

This step is purpose to condition the SPE tube packing. The packing is rinsed with up to one tube-full of solvent before extracting the sample.

B : Sample addition step

The sample is transferred to the tube or reservoir in this step. The sample must be in a form that is compatible with SPE.

C : Washing step

If analytes are retained on the packing, wash off matrix or impurity by using the same solution in which the sample was dissolved, or another solution that will not remove the analytes.

D : Elution step

The last step is elution by rinsing the packing with a small volume of a solution to remove the analytes from SPE and collect the eluate for analysis.

2.4.2 SPE formats

A significant progress in SPE has been observed, including simplification, automation and miniaturization of the original concept because of the development of SPE for target analytes. The production of a wide range of new classes of materials can adsorb various kinds of analytes, enabled the development for obtaining high recovery and enrichment. The formats in SPE are divided four types of sorbent formats; cartridges, pipette-tip, stir bar, and disk.

2.4.2.1 SPE cartridges

The SPE cartridges are small polypropylene or glass open-ended syringe barrels filled with sorbent which is a stationary phase of various types as shown in Figure 2.7. An extraction efficiency depends primarily on the selection of a suitable sorbent, which provides an opportunity to trap all analytes as well as to select the appropriate volume of the column. The SPE cartridge is the most frequently chosen format for the separation and enrichment of analytes which are in

various kinds of samples with different levels of content. The liquid sample can be passed through the cartridge by the gravitational force or by the use of positive pressure using syringes or vacuum pressure. The advantages of SPE cartridge are the capacity to prepare a highly selective tool for the isolation and enrichment of analytes in the laboratory. Moreover, SPE cartridge is possible to combine several columns filled with the same or different types of sorbent that this increases the extraction efficiency and the recovery of target analytes.



Figure 2.7 SPE cartridge format [46]



Figure 2.8 SPE pipette-tip format [47]

2.4.2.2 Pipette-tip format in SPE

SPE pipette-tip format is a miniaturized version of the conventional SPE technique. Sorbent in SPE pipette-tip is packed at the top of a micropipette as shown in Figure 2.8. The extraction procedure of SPE pipette-tip is simple and easy since no specialized equipment is required. The mechanism of transfer of the analytes is the same as that in the conventional SPE technique; the sorbent is washed and preactivated with methanol and water, respectively. Then, the sample solution is passed through the pipette by replicable aspiration and dispensing using the micropipette to increase the recovery. After extraction, the analytes in the sorbent are eluted with the solvent.

2.4.2.3 Stir bar format in SPE

SPE stir bar format is the coating of sorbent on the surface of the magnetic stirring bar as shown in Figure 2.9. The SPE stir bar technique is based on the same principle as that of solid phase microextraction (SPME). The SPE stir bar is immersed in the solution of sample and stirred for the optimal amount of time given the situation. After complete extraction, the SPE stir bar is removed from the sample solution and wiped to dry with a soft tissue. The analytes are thermally desorbed in the injection port of the GC apparatus. For LC analysis, the analytes are desorbed by dipping the SPE stir bar in the solvent.

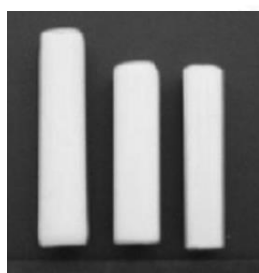


Figure 2.9 SPE stir bar format [5]



Figure 2.10 SPE disk format [48]

2.4.2.4 Disk format in SPE

SPE disk (Figure 2.10) is developed from the SPE cartridge to redress limitations inherent in cartridges, especially in regard to isolation and enrichment of analytes from samples of large volume. The sorption materials used of columns and disks are the same and the principle of SPE disk is based on SPE cartridge. The sorbent particles of SPE disks are much smaller than SPE cartridges as shown in Figure 2.11. Using SPE disk which has a small diameter of sorbent and short sample path results in an increased extraction efficiency and makes it possible to eliminate some of the disadvantages experienced with using SPE cartridges. Furthermore, the SPE disk has many more particles which imply that it has high surface area and the kinetic of sorption is quicker of the SPE disk than the SPE cartridge hence the SPE disk is appropriate for the separation of trace analytes in

large volume of sample resulting from the high fluid permeability and adsorption ability.

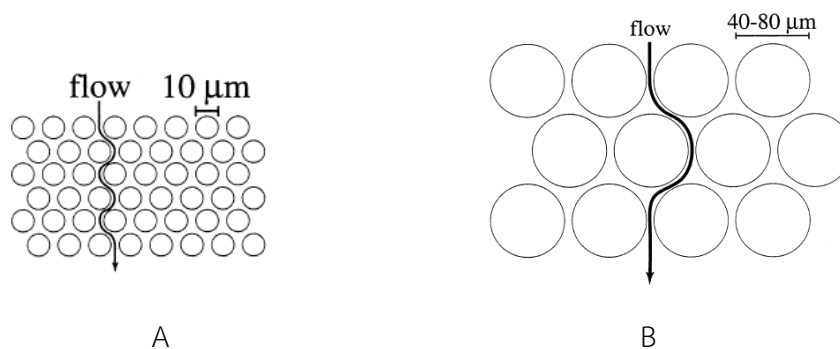


Figure 2.11 Sorbent particles in (A) SPE disk and (B) SPE cartridge [49]

In summary, the advantages and disadvantages of four types of SPE formats are compared in Table 2.2.

Table 2.2 Comparison of formats in SPE

Format	Advantage	Disadvantage
Cartridge	<ul style="list-style-type: none"> combining several columns low cost 	<ul style="list-style-type: none"> slow flow rate high void volume high backpressure
Pipette-tip	<ul style="list-style-type: none"> very small volume of sample and elution solvents shorter extraction time easy automation ability to treat many samples by using a multichannel micropipette 	<ul style="list-style-type: none"> large amount of plastic waste plugging

Format	Advantage	Disadvantage
Stir bar	<ul style="list-style-type: none"> • low sample volume • Simplicity of operation • rapidity 	<ul style="list-style-type: none"> • Specialized equipment (a thermal desorption unit)
Disk	<ul style="list-style-type: none"> • small volume of elution solvents • faster flow rates • large surface area • less-time consuming 	<ul style="list-style-type: none"> • smaller breakthrough volume • more expensive than cartridges

2.4.3 Sorbents in SPE

The main applicability of SPE is used as extraction by adsorption of sorbent. There are a large number of sorbents to use in extraction as a result of selectivity with the analytes. The most frequently used groups of sorbents are chemically modified silica gel, polymer sorbents, nanostructured materials, and molecularly imprinted polymers.

2.4.3.1 Silica and bonded silica sorbent

Silica gel is a good adsorbing agent and is widely used, because it does not swell or strain. Moreover, it has good mechanical strength and can undergo heat treatment. The silica surface is heterogeneous, with a variety of different types of silanol groups (Si-OH) present. Silica can be used as a sorbent in SPE even without modification. Nevertheless, to increase applicability and option of silica gel, the silica surface is modified by bonding a wide variety of functional groups to the surface; for instance octadecyl (C18), octyl (C8), aminopropyl (NH₂), and ionic or mixed-mode (C8/cation exchange). The chemically modified silica gel is expected to select with the analytes and improve of extraction efficiency.

2.4.3.2 Polymer sorbents

Polymers are widely used as the sorbent because the polymers have moderate surface areas and highly crosslinked increasing surface areas which result in higher retention. Polymeric resins contain a different functional group i.e. acetyl, hydroxymethyl, and benzoyl and have been introduced to increase selectivity and recovery. These modified polymer resins are hydrophilicity or hydrophobicity depend on category of polymers chosen that are specific with the analytes.

2.4.3.3 Nanostructured materials

Nanomaterials are used in many fields of science and technology such as additive, reinforcement, and SPE. Nanomaterials have been introduced for using as SPE owing to the nanometer scale of their particle size, and their utility in miniaturization. Nanostructured materials can be applied as sorbents in two configurations: directly used as raw materials and modified materials.

The advantages of nanostructured materials:

- Easy derivatization procedures.
- High surface-to-volume ratio.
- Good thermal, mechanical and electronic properties.

The important products of nanostructured materials are graphite, carbon nanotubes, and electrospun nanofibers [11].

2.4.3.4 Molecularly imprinted polymers

Molecularly imprinted polymers (MIPs) are synthesized by highly crosslinked polymers in the presence of a template molecule. This molecule is removed and the polymer can be used as a selective binding medium for the analyte or structurally related compounds. MIPs can resist heating to temperatures higher than 120°C and are very stable with organic solvents, strong acids, and bases. MIPs are used in many applications as separation materials, enzyme mimics for catalytic applications, recognition elements in biosensors, and antibody/receptor

binding site mimics. MIPs are provided to improve the selectivity and sensitivity of analytical methods.

2.5 Analysis of PAHs

PAHs are usually trace compounds in various samples such as food and environment. Factually, the analytes have to be removed from the large different constituents. In the present, there are a few popular techniques used for extraction and purification PAHs from the sample including solid phase extraction (SPE) [2,50,51], and solid phase microextraction (SPME) [52-57]. Then, the analytical determination is carried out by liquid chromatography (LC), or gas chromatography (GC) with different detector.



CHAPTER III

EXPERIMENTAL

3.1 Materials

3.1.1 Preparation of electrospun CNTs-Nylon6 composite nanofibers by electrospinning technique

- 1) Nylon6 (particle size 3.00 mm) (Sigma Aldrich, Germany)
- 2) Carbon nanotubes (CNTs; i.d. 10 nm) (Nanogenaration, Thailand)
- 3) Formic acid, 85% (Carlo Erba, France)

3.1.2 Extraction of PAHs in water

- 1) Polycyclic aromatic hydrocarbons (PAHs) (Dr.Ehrenstorfer, Germany)
- 2) Decafluorobiphenyl (Sigma-Aldrich, UK)
- 2) Cyclohexane (Carlo Erba, France)
- 3) Acetonitrile (ACN) (Merck, Germany)
- 4) Hexane (Mallinckrodt, UK)
- 5) Acetone (Merck, Germany)
- 6) Methanol (MeOH) (Merck, Germany)
- 7) Ultrapure water (Milli-Q, Millipore, Germany)

3.2 Methodology

3.2.1 Preparation of electrospun CNTs-Nylon6 composite nanofibers

The CNTs-Nylon6 solution for electrospinning was prepared by dispersed CNTs in 5 mL of formic acid using the sonication for 90 minutes. Then, Nylon6 was added and constantly stirred at 50°C for 1 hour.

The electrospinning system was setup as shown in Figure 3.1. The CNTs-Nylon6 solution was loaded into 3 mL plastic syringe with a blunt stainless needle (20G) and connected to the anode of high voltage power supply. The aluminium foil was used as a collector and connected to the cathode. A voltage of 28 kV (power supply series 230, BERTAN, Hicksville, New York, USA) was applied. The flow rate of the CNTs-Nylon6 solution was controlled and fixed at 2.0 $\mu\text{L}/\text{min}$ by a syringe pump (Prosense B.V., NE-1000, USA). Different concentrations of Nylon6 (15, 20, 25 and 30% w/v), amounts of CNTs (0, 0.33, 0.66, 0.83% w/w) and collector distance (11 to 17 cm) were investigated in the optimization process. The electrospun CNTs-Nylon6 composite nanofibers were cut in a circular format with a diameter of 13 mm (Figure 3.2) and stored in a desiccator.

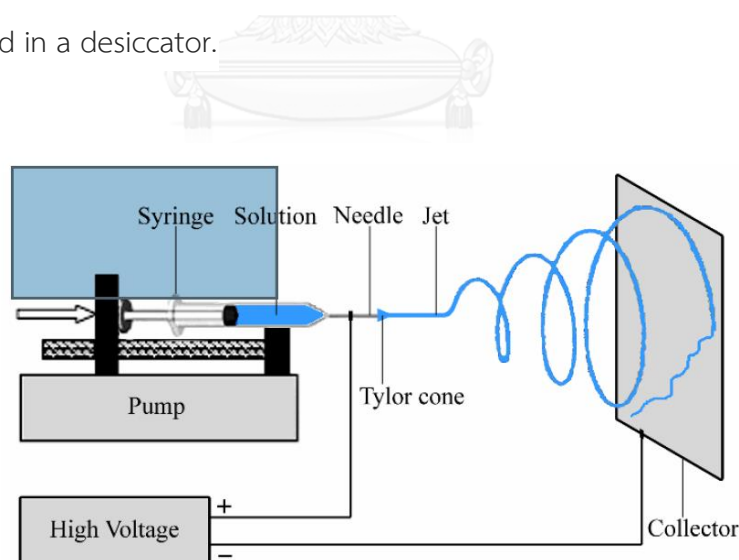


Figure 3.1 Schematic of electrospinning apparatus [58]

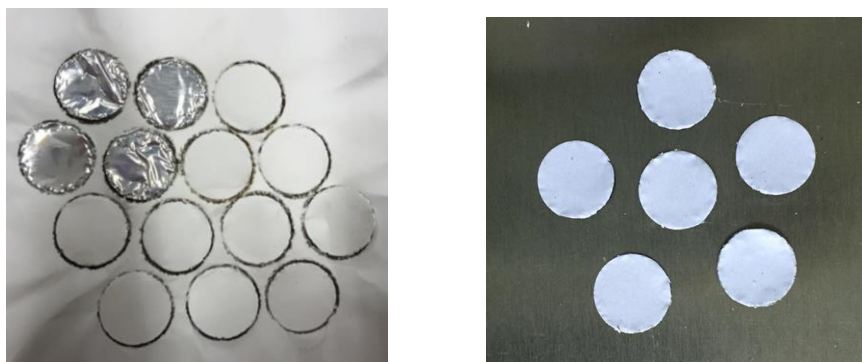


Figure 3.2 13 mm SPE disk format of electrospun CNTs-Nylon6 composite nanofibers

3.2.2 Characterization of electrospun CNTs-Nylon6 composite nanofibers

3.2.2.1 Scanning electron microscopy (SEM)

The morphology of the electrospun CNTs-Nylon6 composite membrane was characterized by scanning electron microscopy (SEM, JEOL, JSM-6480LV). The diameter of fibers was measured from the SEM images by Image J software as the average values with standard deviation (n=20).

3.2.2.2 Transmission electron microscopy (TEM)

The dispersion and alignment of CNTs in the electrospun CNTs-Nylon6 composite membrane was examined by transmission electron microscopy (TEM, JEOL, JEM-2010).

3.2.2.3 Thermogravimetric analysis (TGA)

The amount of CNTs in the nanofibers was determined by thermogravimetric analysis (TGA, PerkinElmer, Pyris1). Samples were heated from 50 °C to 800 °C with a heating rate of 25 °C/min.

3.2.2.4 Differential scanning calorimetry (DSC)

The crystallinity of the electrospun fibrous Nylon6 membrane was compared with the electrospun fibrous CNTs-Nylon6 composite membrane by differential scanning calorimeter (DSC, Mettler Toledo, DSC1). Reference and sample pan were heated from 30 °C to 350 °C with a heating rate of 20 °C/min.

3.2.2.5 Nitrogen physisorption measurement

Surface area of the electrospun CNTs-Nylon6 composite membrane was studied and compared with electrospun Nylon6 membrane by the Brunauer, Emmett and Teller technique (BET) theory.

3.2.3 Analysis of PAHs by GC-MS

PAHs solutions were analyzed by GC-MS system consisting of:

- Gas chromatograph (Agilent, GC 7890A, USA)
- Mass spectrometer (Agilent, 7000 Triple Quad, USA)
- Autosampler (Agilent, 7693, USA)
- Autoinjector (Agilent, G4513A, China)

The conditions of GC-MS analysis are shown in Table 3.1 and 3.2.

Table 3.1 GC condition

Parameters	Conditions
Oven temperature	60 °C (2 min) to 250 °C at 5°C/min (hold 15 min) and 250 °C to 300 °C at 10 °C/min (hold 5 min)
Injection	Splitless, 2.4 min, 300°C, 0.5 µL
Detector	Mass Spectrometry (SIM mode), 280°C
Carrier gas	Helium, (u=40 cm/sec)
Column	HP-5MS, 30m x 0.25 mm x 0.25 µm

Table 3.2 MS condition

Range	Time (min)	Mass to charge ratio (m/z)
1	0 - 5	128, 102, 64
2	5 - 15	82, 67, 55
3	15 - 18	153, 152, 76, 63
4	18 - 22	170, 166, 139, 85
5	22 - 25	178, 152, 89, 76
6	25 - 31	202, 200, 101
7	31 - 37	228, 226, 114, 113
8	37 - 43	252, 126, 125
9	43 - 54	278, 276, 139, 138, 137, 125

3.2.4 Extraction of PAHs by electrospun CNTs-Nylon6 composite nanofibers

3.2.4.1 Preparation of PAHs solutions

Sixteen PAHs were studied naphthalene, acenaphthene, acenaphthylene, fluorene, phenanthrene, anthracene, fluoranthene, pyrene, benzo[a]anthracene, chrysene, benzo[b]fluoranthene, benzo[k]fluoranthene, benzo(a)pyrene, dibenzo(a,h)anthracene, benzo[g,h,i]perylene and indeno[1,2,3-cd]pyrene. 10 mg/L of mixed PAHs standard solution in cyclohexane was prepared by diluting 1 mL of 100 mg/L of mixed standard solution to 10 mL with cyclohexane. This solution was used for preparation of calibration curve and spiked samples.

Seven concentrations of mixed PAHs standard solution, 0.05, 0.10, 0.20, 0.30, 0.50, 1.0 and 2.0 mg/L, were prepared for the calibration curve by diluting from 10 mg/L of mixed PAHs standard solutions.

3.2.4.2 Extraction procedure

The electrospun fibrous CNTs-Nylon6 composite membrane was placed in filter holder (Figure 3.3) and pretreated with 5 mL of methanol and then 5 mL of Milli-Q water by SPE manifold (SPE-24G column processors, J.T. Baker, USA).

Next, the 25 mL water sample was loaded through this sorbent and dried by N₂ gas for 30 minutes. Then, the sorbent was eluted by desorption solvent. The extract solution was dried to dryness by N₂ gas. Finally, 20 µL of decafluorobiphenyl was added and diluted to 1 mL with cyclohexane for further analysis by GC-MS. Steps for PAHs extraction was shown in Figure 3.4



Figure 3.3 Filter holder



Figure 3.4 Steps of PAHs extraction by electrospun CNTs-Nylon6 composite membrane

3.2.4.3 Optimization of membrane material

The types of membrane materials, 25 and 30 %w/v of Nylon6 and various amounts of CNTs in composite membrane, were studied by followed the procedure in 3.2.4.2 and compared with the commercial C18 silica bonded phase SPE cartridge (100 mg/3 mL, Vertical, Thailand). The prepared membranes were summarized in Table 3.3. Peak area of PAHs was identified to determine the optimized sorbent for extraction of PAHs.

Table 3.3 Abbreviations of sorbent

Nylon6 (%)	CNTs (%)	Sorbent
25	-	25N
	0.33	25N0.33C
	0.66	25N0.66C
	0.83	25N0.83C
30	-	30N
	0.33	30N0.33C
	0.66	30N0.66C
	0.83	30N0.83C

3.2.4.4 Optimization of types of desorption solvent

The types of desorption solvent were examined by followed the procedure in 3.2.4.2. The studied solvents were hexane, cyclohexane, acetone, acetonitrile, and mixed solvent of acetone and acetonitrile. Peak area of PAHs was identified to determine the optimized solvent for desorption.

3.2.4.5 Optimization of volume of the desorption solvent

The volume of desorption solvent was studied by varied at 0.5, 1.0 and 1.5 mL of the optimized desorption solvent. Peak area of PAHs was identified to determine the optimized volume of desorption solvent.

3.2.4.6 Optimization of sorbent weight

The effect of sorbent weight on extraction efficiency was examined by varied at 3.0, 4.0, 5.0 and 6.0 mg of the electrospun CNTs-Nylon6 composite nanofibers. The extraction procedure was mentioned in 3.2.4.2 and used the optimum condition of type and volume of desorption solvent.

3.2.4.7 Recovery of PAHs extraction

The Milli-Q water was spiked at the concentration of 8 µg/L of mixed PAHs and followed the procedure in 3.2.4.2 with optimum condition for extraction of PAHs by the electrospun fibrous CNTs-Nylon6 composite membrane. The concentration of PAHs was obtained from calibration curve. The extraction recovery was then calculated as follow;

$$\% \text{ Recovery} = (\text{Concentration of recovered PAHs} / \text{Concentration of spiked PAHs}) \times 100\%$$

3.2.4.8 Method of detection (MOD) and method of quantitation (MOQ)

The method of detection (MOD) was defined as the concentration of PAHs giving 3 times of the signal to noise ratio, while the method of quantitation (MOQ) was 10 times of the signal to noise ratio. The concentration was then calculated from the calculation curve.

3.2.4.9 Reproducibility

Reproducibility was calculated from 10 replicates of the extraction of mixed PAHs spiked into milli-Q water at 6.0 and 10.0 µg/L and followed the procedure in 3.2.4.2 with optimum condition for extraction of PAHs by the electrospun fibrous CNTs-Nylon6 composite membrane examined.

3.2.5 Extraction of PAHs in water sample

Plastic bottled drinking water was sampling from the market. The water samples were filtered and extracted using the optimized extraction conditions of PAHs by the electrospun fibrous CNTs-Nylon6 composite membrane. The suitability of the proposed method was evaluated by recoveries.

CHAPTER IV

RESULTS AND DISCUSSION

This chapter is divided into three major sections. First, the optimization and characterization of the electrospun CNTs-Nylon6 composite nanofibers were studied. Then, the extraction of PAHs in water using the electrospun CNTs-Nylon6 composite membrane was optimized. Finally, the electrospun CNTs-Nylon6 composite membrane is applied for determination of PAHs in water samples.

4.1 Optimization and characterization of the electrospun CNTs-Nylon6 composite fibers

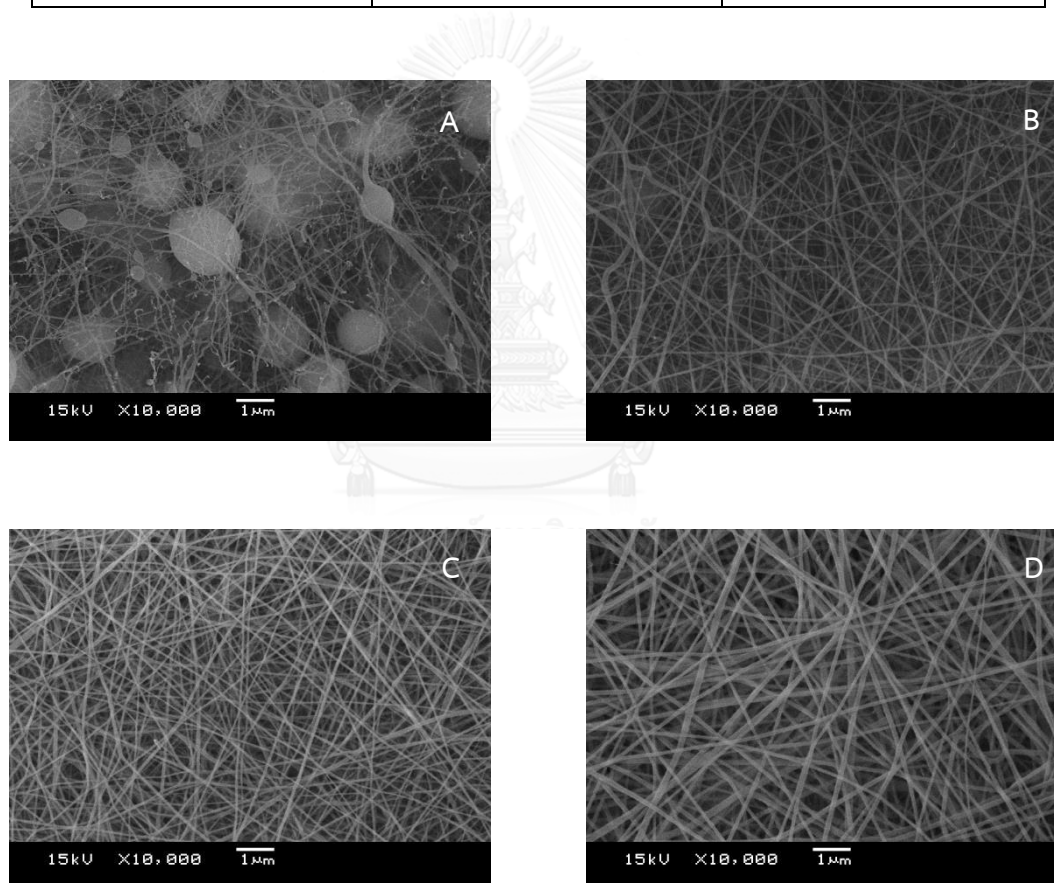
4.1.1 Optimization of electrospun CNTs-Nylon6 composite nanofibers

4.1.1.1 Effect of Nylon6 concentration

The SEM images of CNTs-Nylon6 nanofibers at various Nylon6 concentrations (15, 20, 25 and, 30 %w/v in formic acid) with 0.2% w/w of CNTs were shown in Figure 4.1. The morphology and diameter of fiber were summarized in Table 4.1. The concentration of Nylon6 largely affected the morphology of the CNTs-Nylon6 nanofibers on account of the change of viscosity of the CNTs-Nylon6 solution. The Nylon6 concentration below 25 %w/v result bead-liked fibers (Figure 4.1A and 4.1B) relating to low viscosity of CNTs-Nylon6 solution. Though, 25 and 30 %w/v of Nylon6 result smoother and finer fibers. Therefore, the CNTs-Nylon6 nanofibers at 25 and 30 %w/v of Nylon were fabricated and further studied as a SPE sorbent.

Table 4.1 Morphology of CNTs-Nylon6 nanofibers at various Nylon6 concentrations

Nylon6 concentration (%w/v)	Fiber morphology	Average diameter (nm)
15	Fibers with bead	55 ± 13
20	Bead-liked fibers	58 ± 10
25	Fine fibers	62 ± 8
30	Fine fibers	85 ± 8

**Figure 4.1** SEM images of the electrospun CNTs-Nylon6 composite nanofibers (A) 15% (B) 20% (C) 25% (D) 30% w/v of Nylon6 with 0.2% w/w of CNTs.

4.1.1.2 Effect of collector distance

The CNTs-Nylon6 composite nanofibers were fabricated using 30%w/v of Nylon6 and 0.33%w/w of CNTs at various collector distances. Increasing collector distance could help a better stretching of nanofibers and a complete evaporation of the solvent. The SEM images of 30% w/v of Nylon6 with 0.33% w/w of CNTs at various collector distances were shown in Figure 4.2. Fine and smooth fibers were obtained at all collector distance. In addition, the average diameters of CNTs-Nylon6 composite nanofibers (Table 4.2) were 126, 101 and 83 nm for a collector distance of 11, 12 and 13 cm, respectively. Increasing the collector distance led to smaller fiber diameters. Therefore, the optimum collector distance to fabricate CNTs-Nylon6 composite nanofibers was 13 cm in order to obtain small diameter of fibers.

Table 4.2 Average diameters of electrospun CNTs-Nylon6 composite nanofibers at 30%w/v of Nylon6 and 0.33%w/w of CNTs (n=20).

Collector distance (cm)	Average diameter (nm)
11	126 ± 10
12	101 ± 9
13	83 ± 9

However, the collector distance of 13 cm was not optimized for other amounts of CNTs in CNTs-Nylon6 composite nanofibers. Increasing the amount of CNTs in the polymer solution caused the increase of electrical charge at spinning droplet which fastens the polymer jet to the collector. Therefore, collector distance needs to be optimized for certain amounts of CNTs. The longer collector distance was required for a higher content of CNTs. The optimum of collector distance at various amounts of CNTs was summarized in Table 4.3.

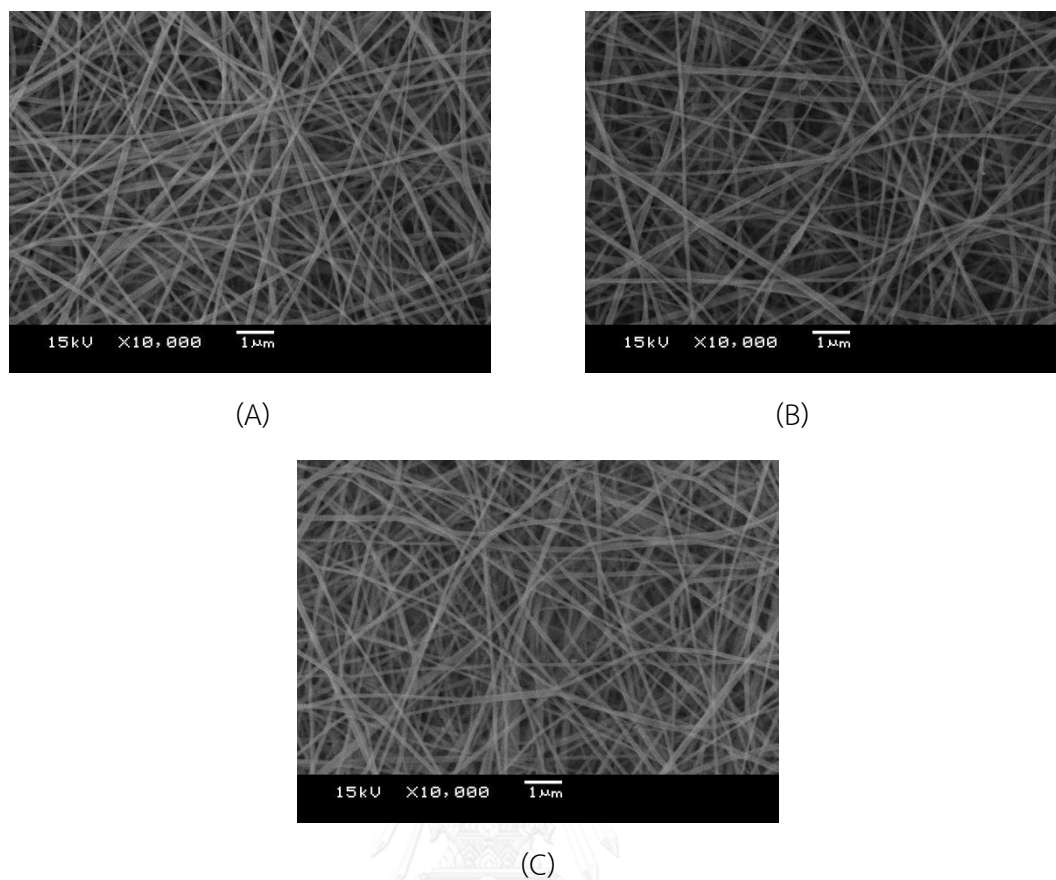


Figure 4.2 SEM images of the electrospun CNTs-Nylon6 composite nanofibers 30% w/v of Nylon6 with 0.33% w/w of CNTs, collector distance at (A) 11 cm, (B) 12 cm and (C) 13 cm.

Table 4.3 The optimum of the collector distance for fabricated electrospun Nylon6 and CNTs-Nylon6 composite nanofibers.

CNTs amount (%w/w)	Optimum collector distance (cm)
0	10
0.33	13
0.66	15
0.83	17

4.1.1.3 Effect of CNTs amount

Increasing CNTs into the CNTs-Nylon6 solution would affect a conductivity of the solution because of electrical properties of CNTs. The longer collector distance was required for a higher content of CNTs. However, the addition of CNTs more than 0.83 %w/w could not fabricate because of the exceeding of solution conductivity to maintain the spinning jet. The SEM images and average diameters of the optimum condition of the electrospun CNTs-Nylon6 composite were shown in Figure 4.3 and Table 4.4, respectively.

Table 4.4 Average diameters of CNTs-Nylon6 composite nanofibers (nm) for the optimum of collector distance. (n=20)

Nylon6 Concentration (%w/v)	Amount of CNTs (%w/w)	Diameters of CNTs-Nylon6 composite nanofibers (Mean \pm SD, nm)
25	0	74 \pm 13
	0.33	59 \pm 9
	0.66	68 \pm 11
	0.83	70 \pm 14
30	0	117 \pm 12
	0.33	83 \pm 12
	0.66	97 \pm 15
	0.83	102 \pm 12

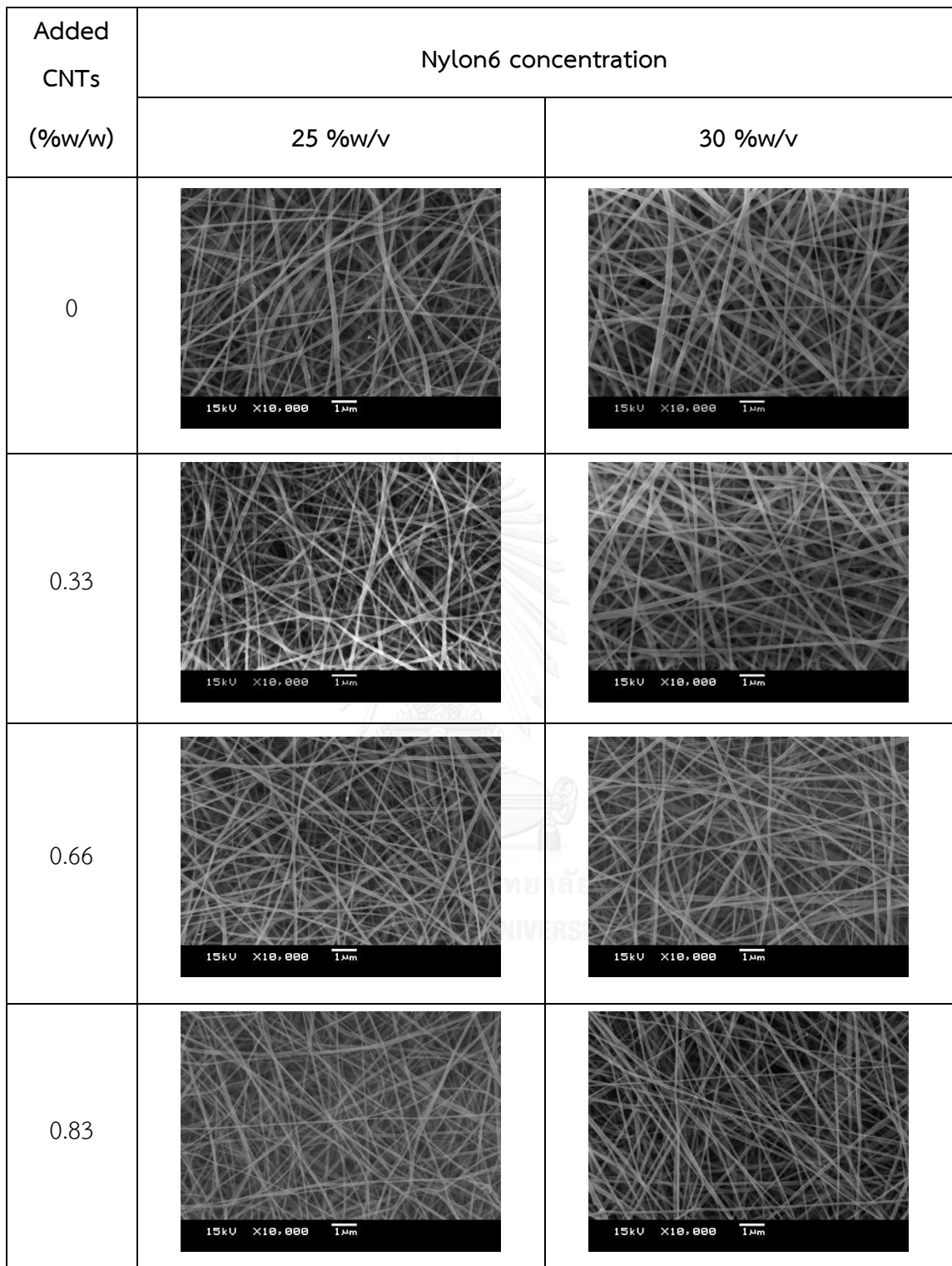


Figure 4.3 SEM images of the electrospun CNTs-Nylon6 composite nanofibers at various concentrations of Nylon6 and CNTs.

4.1.2 Characterization of electrospun CNTs-Nylon6 composite nanofibers

4.1.2.1 Transmission electron microscopy (TEM)

From TEM images in Figure 4.4, CNTs were incorporated into the fibers and aligned along the long axis of Nylon6 nanofibers for 30 %w/v of Nylon6 nanofibers, on the contrary, dispersion of CNTs in 25 %w/v of Nylon6 was not complete. This results rather small diameters of 25 %w/v of Nylon6 nanofibers so the aggregation of CNTs was observed within the nanofibers.

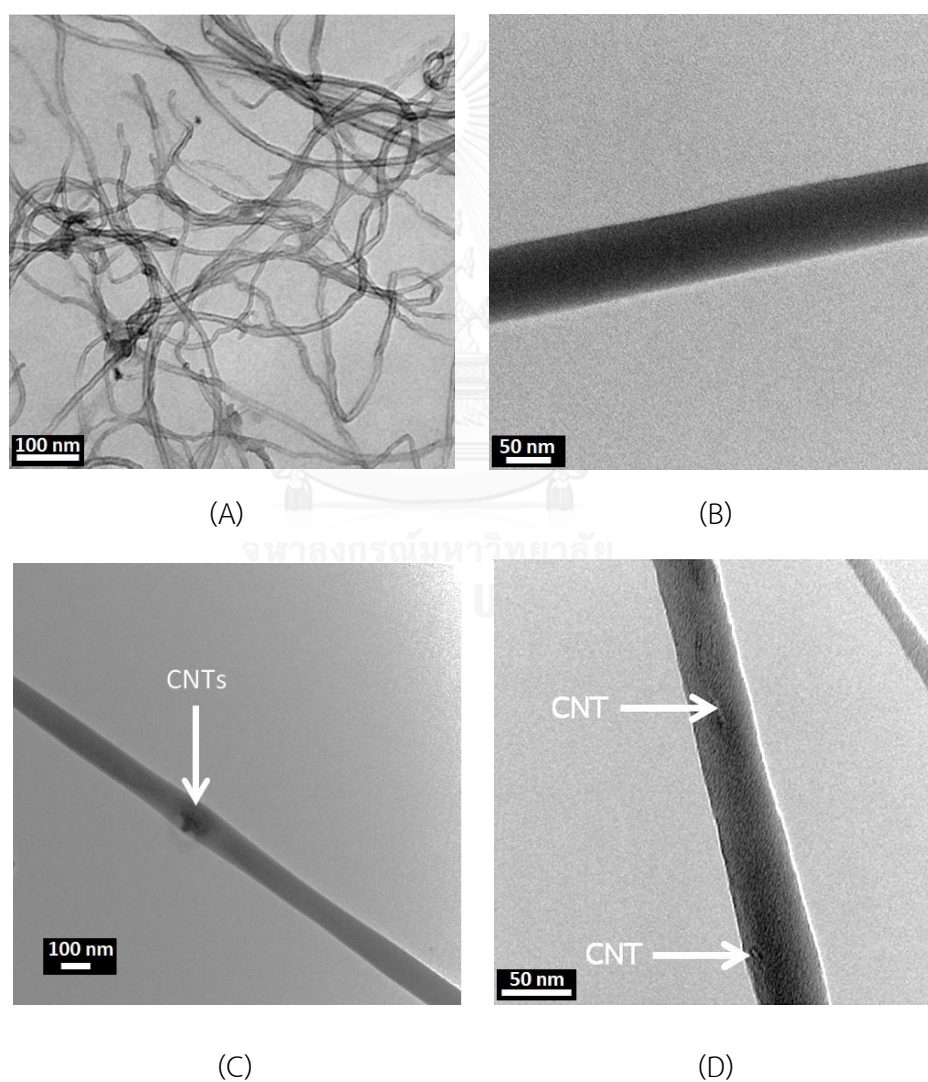


Figure 4.4 TEM images of (A) CNTs, (B) pure Nylon6, (C) 25 %w/v and (D) 30 %w/v of Nylon6 with 0.83 %w/w of CNTs.

The random samples on the membrane of the electrospun CNTs-Nylon6 composite nanofibers were examined. From the Figure 4.5, the CNTs incorporate in all of the fiber samples. This can imply that the CNTs thoroughly disperse in the electrospun CNTs-Nylon6 composite nanofibers.

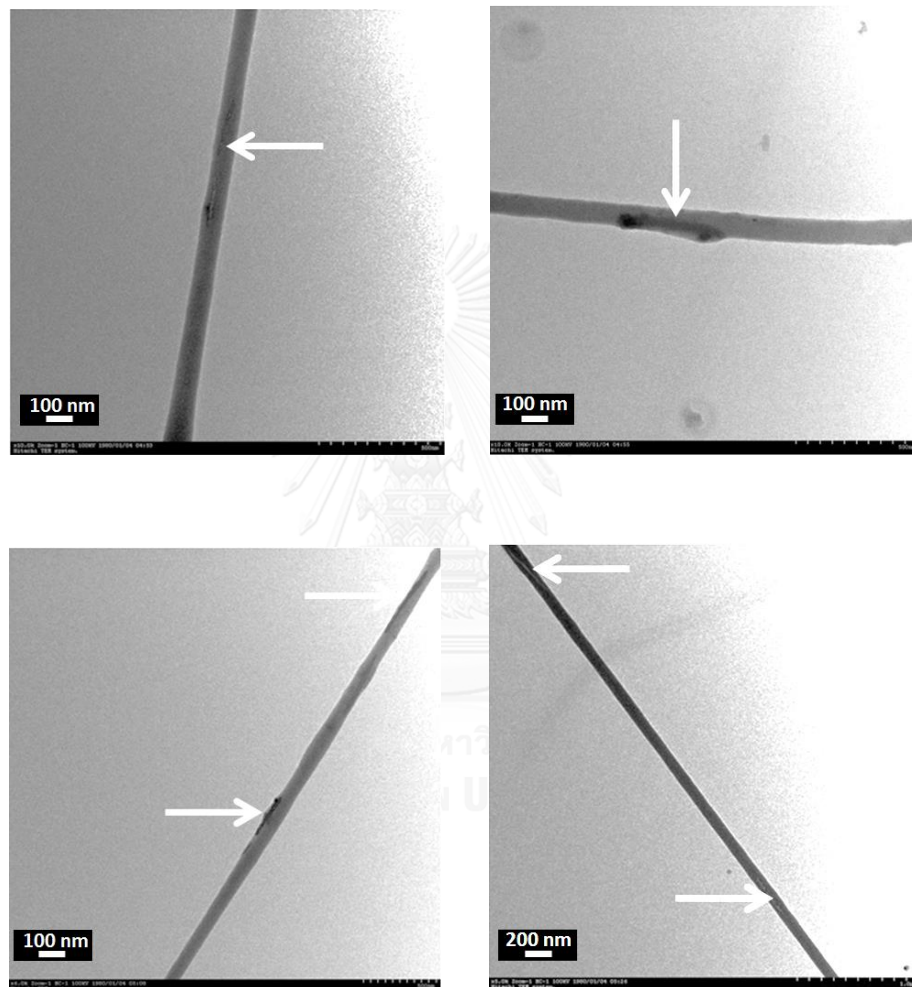
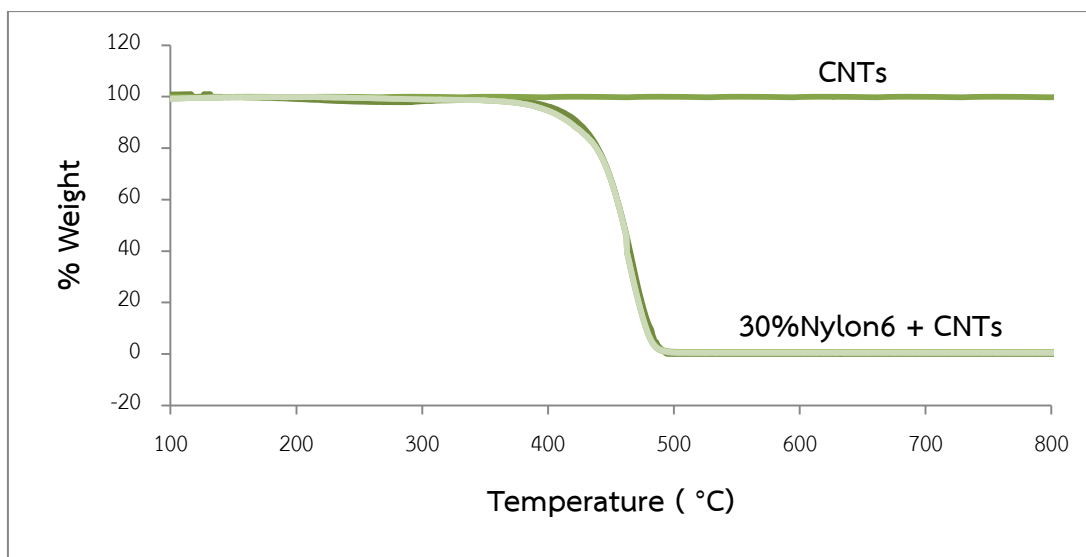


Figure 4.5 The dispersion of CNTs in the electrospun 30 %w/v of Nylon6 fibers with 0.83 %w/w of CNTs nanofibers.

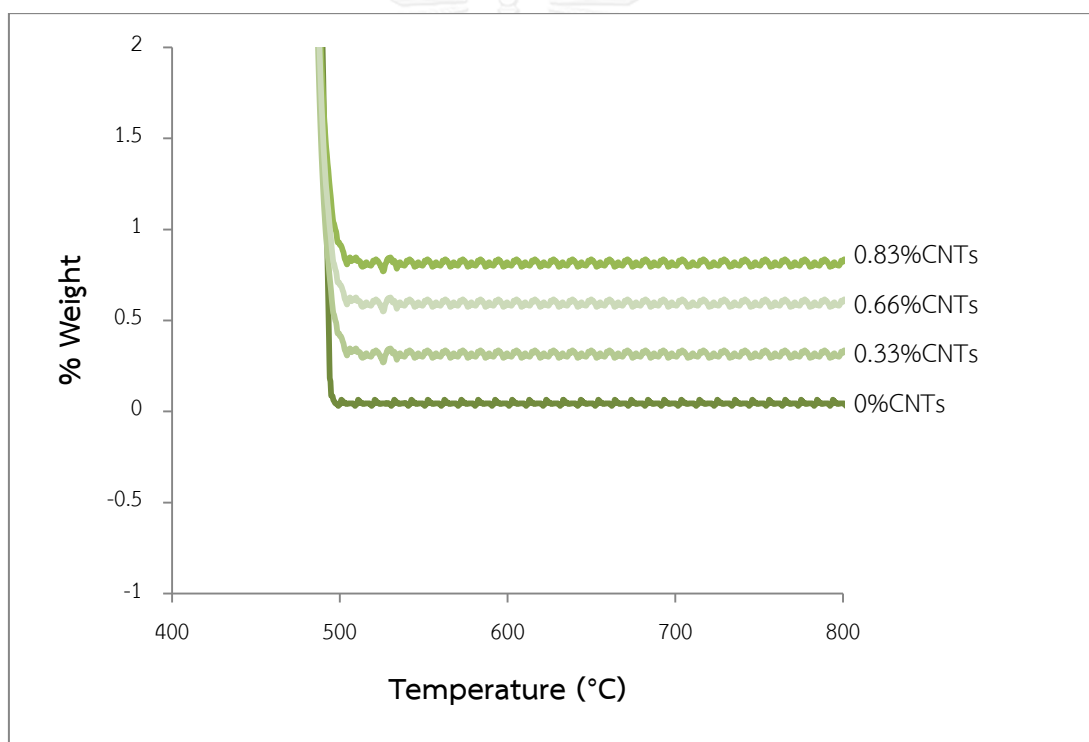
4.1.2.2 Thermogravimetric analyzer (TGA)

The amount of CNTs in the fibers was further examined by TGA. Figure 4.6 and 4.7 show TGA curves of the electrospun Nylon6 and CNTs-Nylon6 composite nanofibers. Under a nitrogen atmosphere, weight loss of the electrospun Nylon6 and CNTs-Nylon6 composite nanofibers showed the one-step mechanism. A slow decomposition begins at 400°C and the first weight loss corresponding to the temperature of thermal degradation was found at 500°C that was owing to the presence of Nylon6 material. The first-step weight loss of the electrospun CNTs-Nylon6 composite nanofibers was just observed to be similar to the electrospun Nylon6 fibers; afterward leaving behind the CNT residues owing to the composing temperature for CNTs material is very high.

The CNT residues were the CNTs that remained in the nanofibers and used to confirm the amount of CNTs incorporating into the fibers. From TGA curves (Figure 4.6B and 4.7B), the electrospun Nylon6 nanofibers added 0.33, 0.66 and 0.83 %w/w of CNTs remained the CNTs residue of 0.33, 0.66 and 0.83 %weight, respectively, hence the amount of CNTs incorporate into the nanofibers accorded with the amount of CNTs added into the Nylon6 solution.

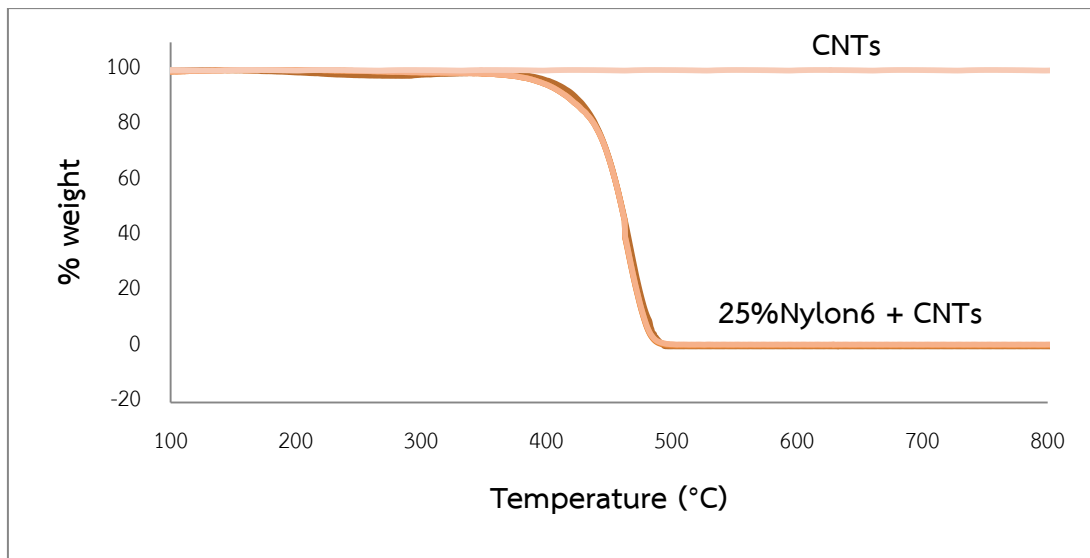


(A)

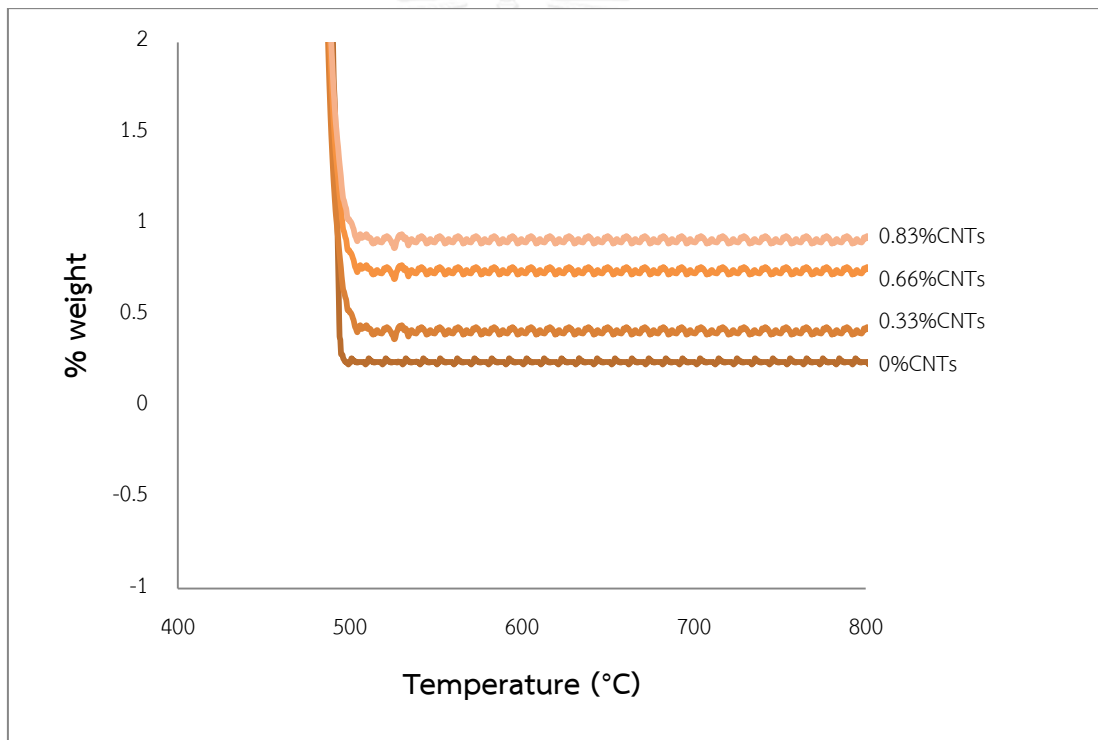


(B)

Figure 4.6 TGA curves of (A) 30 %w/v of Nylon6 with CNTs and pure CNTs. The heating speed was 25°C/min. (B) Enlarge image of TGA curves for 30 %w/v of Nylon6 with CNTs at 400-800 °C.



(A)



(B)

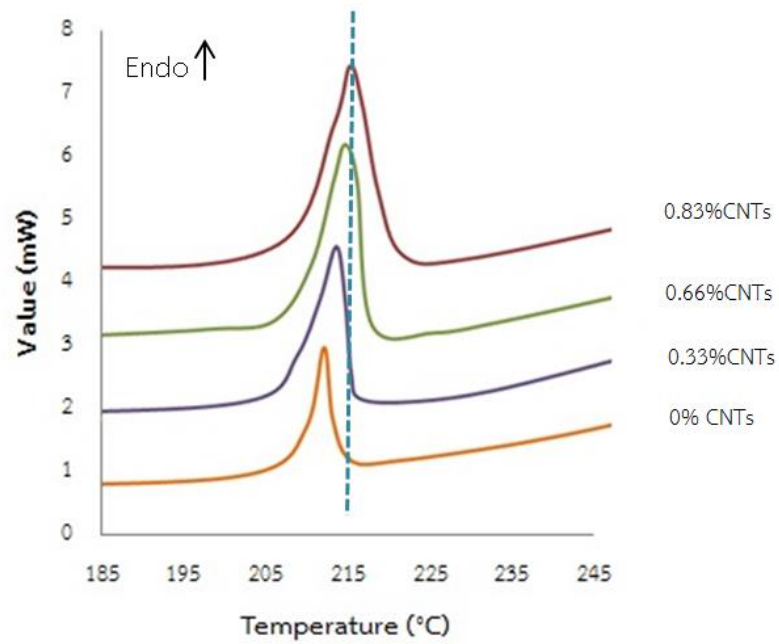
Figure 4.7 TGA curves of (A) 25 %w/v of Nylon6 with CNTs and pure CNTs. The heating speed was 25°C/min. (B) Enlarge image of TGA curves for 25 %w/v of Nylon6 with CNTs at 400-800 °C.

4.1.2.3 Differential scanning calorimetry (DSC)

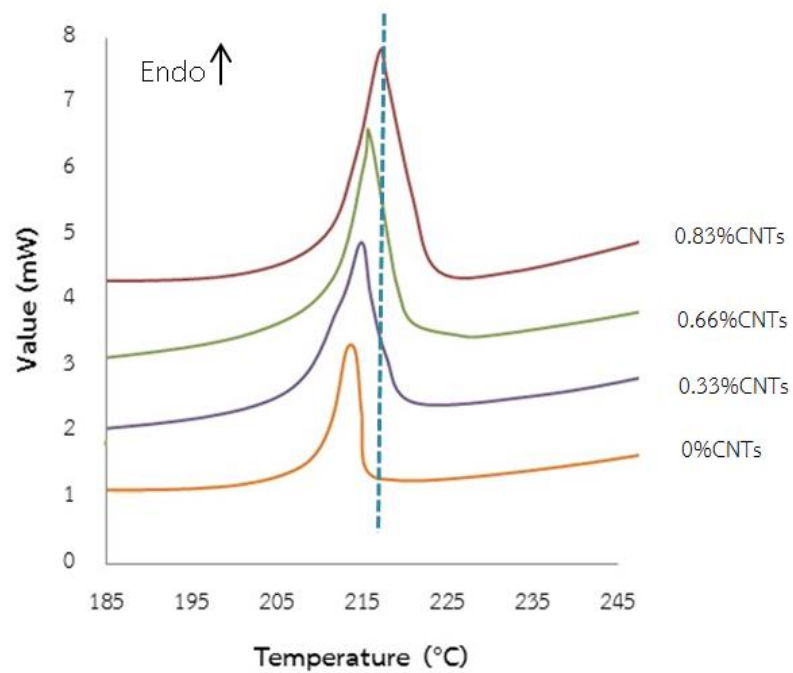
DSC was employed to study the effect of CNTs on the crystallinity of Nylon6. DSC thermograms of CNTs-Nylon6 composite nanofibers are shown in Figure 4.8 and the T_m and melting ΔH values are listed in Table 4.5. From Figure 4.8 and Table 4.5, the T_m and melting ΔH of nanofibers increased (shifted to higher temperature) when the CNTs content increased. This is implied that the increased amount of nuclei crystallising in the matrix owing to addition of CNTs. The CNTs material also blocked the Nylon6 chains mobility that resulted in an accelerated nucleation process.

Table 4.5 Thermal properties of nanofibers electrospun from Nylon6 and CNTs/Nylon6 composite.

Nylon6 (%w/v)	CNTs (%w/w)	T_m (°C)	Melting ΔH (J/g)
25	-	213.3	75.3
	0.33	214.9	82.8
	0.66	215.4	84.6
	0.83	216.3	86.9
30	-	212.4	73.6
	0.33	213.6	80.6
	0.66	215.0	82.6
	0.83	215.3	84.7



(A)



(B)

Figure 4.8 DSC thermograms of electrospun CNTs-Nylon6 nanofibers: (A) 25%w/v of Nylon6 and (B) 30%w/v of Nylon6.

4.1.2.4 Nitrogen physisorption measurement

Figure 4.9 illustrates nitrogen adsorption-desorption isotherms for the electrospun CNTs-Nylon6 composite (Figure 4.9A) and Nylon6 nanofibers (Figure 4.9B). The isotherm exhibits H3 type hysteresis loop starting from relative pressure of 0.4 while at a lower relative pressure it exhibits type I behavior according to IUPAC classification. Such a hysteresis loop in the isotherm demonstrates the microporous and mesoporous structure of the sample. The vertical turn up between the relative pressure of 0.9 and 1.0 could be due to the additional macroporous structure. The isotherm for the electrospun CNTs-Nylon6 composite was similar to that for Nylon6 nanofibers. This confirms that the CNTs incorporate into the fibers and do not affect the structure of the electrospun Nylon6 nanofibers.

The BET specific surface area of the electrospun CNTs-Nylon6 composite nanofibers is about $149 \text{ m}^2/\text{g}$ compared to the electrospun Nylon6 nanofibers which are about $139 \text{ m}^2/\text{g}$. The electrospun CNTs-Nylon6 composite nanofibers have more specific surface area resulting from the smaller diameters of the fibers.

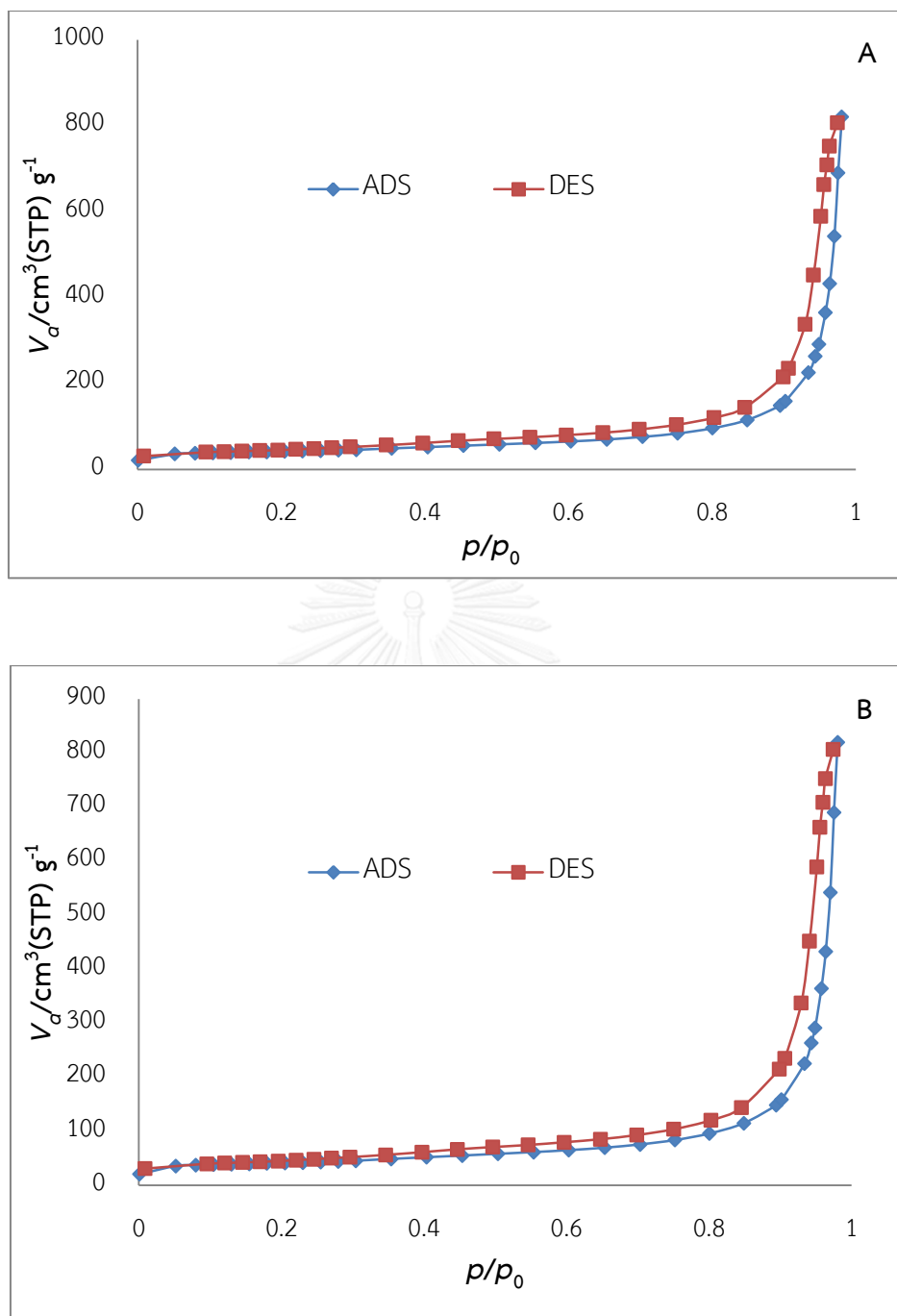


Figure 4.9 The nitrogen adsorption-desorption isotherm of (A) the electrospun CNTs-Nylon6 composite nanofibers and (B) the electrospun Nylon6 nanofibers.

4.2 The extraction of PAHs in water using the electrospun CNTs-Nylon6 composite nanofibers

In this section, the extraction of PAHs in water was followed the procedure in 3.2.3.2. Extraction of spiked water with the concentration of 8 $\mu\text{g/L}$ PAHs was performed. 4.0 mg of electrospun Nylon6 (25 and 30 %w/v) sorbent and electrospun CNTs-Nylon6 composite sorbent were used to study and optimize the extraction efficiency and then compared with the commercial C18 silica bonded phase SPE cartridge (100 mg/3 mL, Vertical, Thailand). The abbreviation of sorbents with various amounts of Nylon6 and CNTs was listed in Table 3.3.



4.2.1 Effect of membrane material

The recovery of 16 PAHs with different sorbents are compared in Figure 4.10 and summarized in Table 4.6. Nylon6 had the functional group both hydrophilic and hydrophobic in its molecule. Therefore, Nylon6 sorbent could interact with small and large molecules of PAHs by Van der Waals and dipole-dipole force, respectively, while C18 sorbent could interact by Van der Waals force only with PAHs. The percentage recoveries of PAHs obtained from 30N sorbent were 38.1-101.6 which was similar to C18 silica bonded phase SPE (%recovery of 38.7-103.4). In addition, the percentage recoveries of PAHs by using 25N sorbent were 40.2-103.3 which were slightly higher than 30N sorbent and C18 silica bonded phase SPE cartridge. This might be an account of smaller diameters of nanofibers in 25N sorbent.

The electrospun CNTs-Nylon6 composite sorbent exhibited a better performance than Nylon6 sorbent and C18 silica bonded phase SPE, especially for large molecule of PAHs (more than 3 rings). Increasing the amount of CNTs could improve percentage recoveries for extraction PAHs since the CNTs could interact with PAHs by physical adsorption and π - π interaction. The percentage recoveries of electrospun CNTs-Nylon6 composite sorbent were increased from 38.1-101.6 to

52.2-101.9 for 30N0.83C sorbent and from 40.2-103.3 to 49.8-103.5 for 25N0.83C sorbent.

In comparison of electrospun CNTs-Nylon6 composite sorbent at the same amount of the CNTs content but different concentration of Nylon6 (25 and 30 %w/v), the percentage recoveries of almost all PAHs extracted by electrospun CNTs-30%w/v Nylon6 composite sorbent were higher than electrospun CNTs-25%w/v Nylon6 composite sorbent. This would be the result of the aggregation of CNTs in electrospun CNTs-25%w/v Nylon6 composite nanofibers causing a poor dispersion of CNTs in the fibers. On the other hand, the dispersion of CNTs in electrospun CNTs-30%w/v Nylon6 composite sorbent was good resulting to the better extraction efficiency.



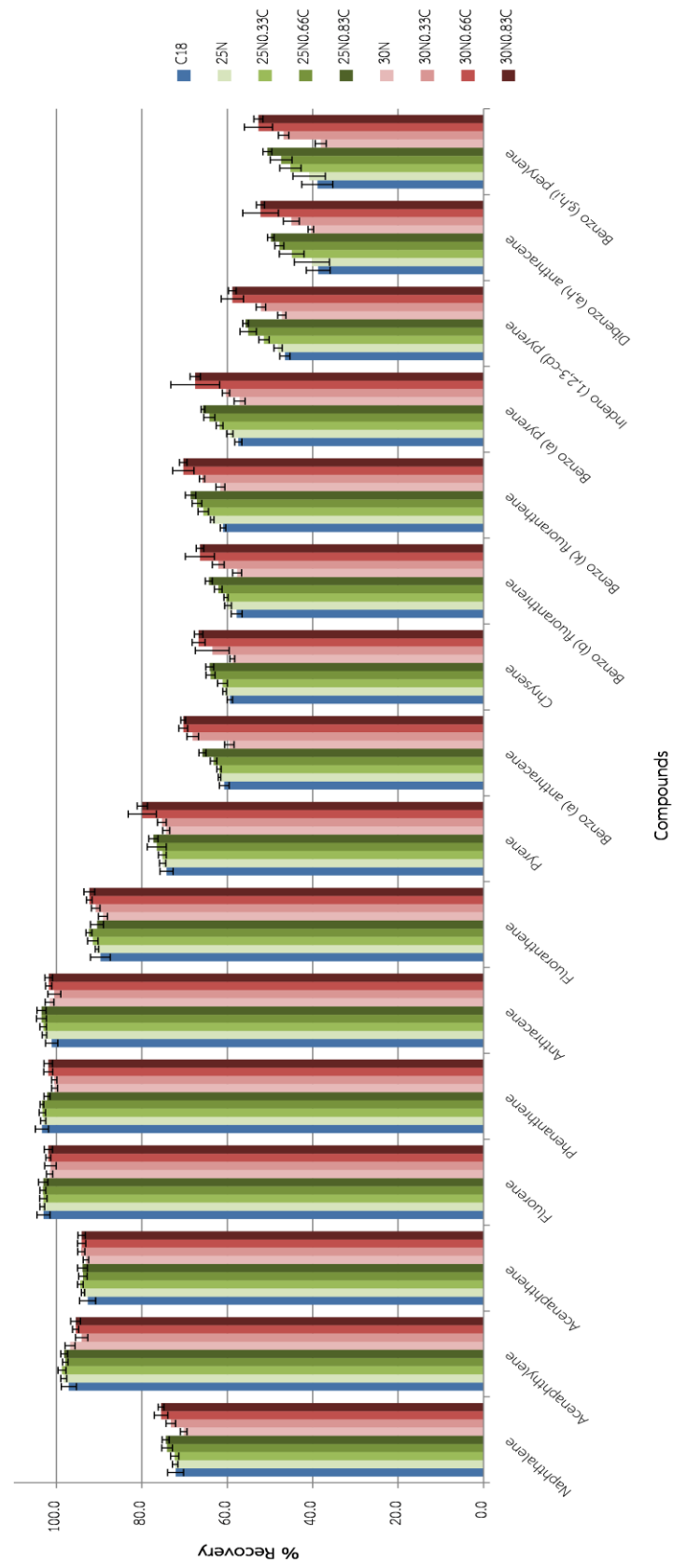


Figure 4.10 Percentage recoveries for the extraction of PAHs from spiked water at 8 µg/L by different sorbents.

Table 4.6 Percentage recoveries and standard deviations for the extraction of PAHs from spiked water at 8 µg/L by different sorbents

Name	% Recovery																	
	C18		25N		25N0.33C		25N0.66C		25N0.83C		30N		30N0.33C		30N0.66C		30N0.83C	
	%Recovery	SD	%Recovery	SD	%Recovery	SD	%Recovery	SD	%Recovery	SD	%Recovery	SD	%Recovery	SD	%Recovery	SD	%Recovery	SD
Naphthalene	72.1	1.9	72.2	0.6	72.3	1.0	74.1	1.2	74.4	0.8	70.2	0.8	73.2	1.1	75.5	1.6	75.5	0.7
Acenaphthylene	97.1	1.8	98.3	0.7	98.7	0.9	97.9	0.6	98.2	0.8	96.8	1.2	94.1	1.4	95.5	0.7	95.5	1.1
Acenaphthene	92.7	1.9	93.8	0.4	94.4	0.7	93.8	1.0	93.9	1.1	93.1	0.6	94.2	0.8	94.1	0.9	94.1	0.8
Fluorene	103.0	1.5	103.3	0.6	103.1	0.9	103.2	0.7	103.1	1.1	101.6	0.7	101.4	1.3	101.9	0.6	101.9	1.0
Phenanthrene	103.4	1.6	103.1	0.6	103.3	0.8	103.4	0.4	102.2	0.7	100.4	0.7	100.5	0.6	101.9	1.1	101.9	1.0
Anthracene	101.1	1.4	102.8	0.5	103.1	0.8	103.5	1.2	103.5	1.1	101.6	1.0	100.5	1.5	101.8	0.7	101.8	0.9
Fluoranthene	89.7	2.3	90.5	0.4	91.5	1.2	92.4	0.7	90.5	1.5	89.1	1.1	90.8	1.0	92.3	0.7	92.3	1.3
Pyrene	74.2	1.5	75.1	0.7	75.2	0.9	76.5	2.2	77.3	1.0	74.3	0.8	75.3	1.0	79.9	3.3	79.9	1.2
Benzo (a) anthracene	60.7	1.1	61.8	0.3	61.9	0.5	63.2	0.8	65.8	0.8	59.5	1.1	68.1	1.4	70.3	1.0	70.3	0.6
Chrysene	59.4	0.6	60.6	0.4	61.1	1.1	63.9	1.0	64.1	0.9	58.8	0.6	63.5	4.0	66.7	1.5	66.7	1.0
Benzo (b) fluoranthrene	57.8	1.3	59.8	0.8	60.3	0.5	62.1	0.9	64.3	0.8	57.7	1.1	62.1	1.4	66.4	3.4	66.4	0.9
Benzo (k) fluoranthene	61.0	0.6	63.5	0.4	65.6	1.2	67.1	1.1	68.6	1.2	61.6	1.1	65.9	0.6	70.3	2.5	70.3	0.9
Benzo (a) pyrene	57.4	0.8	59.4	0.8	61.8	0.8	64.2	1.3	65.7	0.4	57.1	1.3	60.3	0.8	67.5	5.7	67.5	1.2
Indeno (1,2,3-cd) pyrene	46.5	1.2	48.1	1.0	51.4	1.2	55.1	1.9	55.7	0.7	47.2	1.0	52.1	1.1	58.8	2.6	58.8	0.9
Dibenzo (a,h) anthracene	38.7	2.8	40.2	4.1	44.9	2.9	47.8	1.1	49.8	0.8	40.4	0.6	45.0	1.9	52.2	4.2	52.2	0.9
Benzo (g,h,i) perylene	38.9	3.6	40.8	3.8	45.2	2.5	47.4	2.6	50.6	1.1	38.1	1.3	46.8	1.2	52.7	3.3	52.7	1.0

4.2.2 Desorption solvent

Because a wide range polarity of PAHs, the desorption solvent should be optimized to desorb both small and large molecules of PAHs. The solvents that suitable for both solubility and polarity were examined which are hexane, cyclohexane, methanol, acetone, acetonitrile, and mixture of acetone and acetonitrile in the ratio of 1:1, 1:2 and 2:1 (v/v). The results of percentage recoveries eluted by different solvents were compared in Figure 4.11 and summarized in Table 4.7. Hexane and cyclohexane showed good recoveries for small PAHs molecules (< 4 rings); conversely, the percentage recoveries of large PAHs molecules were low. Since non-polar solvents could interact well with the non-polar compounds, hexane and cyclohexane were then good desorption solvents for the small PAHs molecules. For large PAHs molecules, they could interact with the CNTs by π - π interaction which was strong interaction. Therefore, increasing the polarity of desorption solvent could be enhanced the elution strength for large PAHs molecule. Methanol, acetone, and acetonitrile were then evaluated. Methanol and acetone showed slightly lower percentage recoveries than hexane and cyclohexane for small PAHs molecules and similar values for large PAHs molecules. As a result, the polarity of methanol and acetone was not suitable for small PAHs molecule and also not enough to elute large PAHs molecule. For acetonitrile, it showed better percentage recoveries for large PAHs molecules since acetonitrile could interact with aromatic rings of PAHs by π - π interaction. However, the percentage recoveries for small PAHs molecule were dropped. As a result, mixed solvent was examined. Mixture of acetone and acetonitrile was selected regarding of miscibility and elution strength. 1:1 (v/v) of acetone and acetonitrile gave the best percentage recoveries for all PAHs because acetone could elute small PAHs molecules and acetonitrile could elute large PAHs molecules.

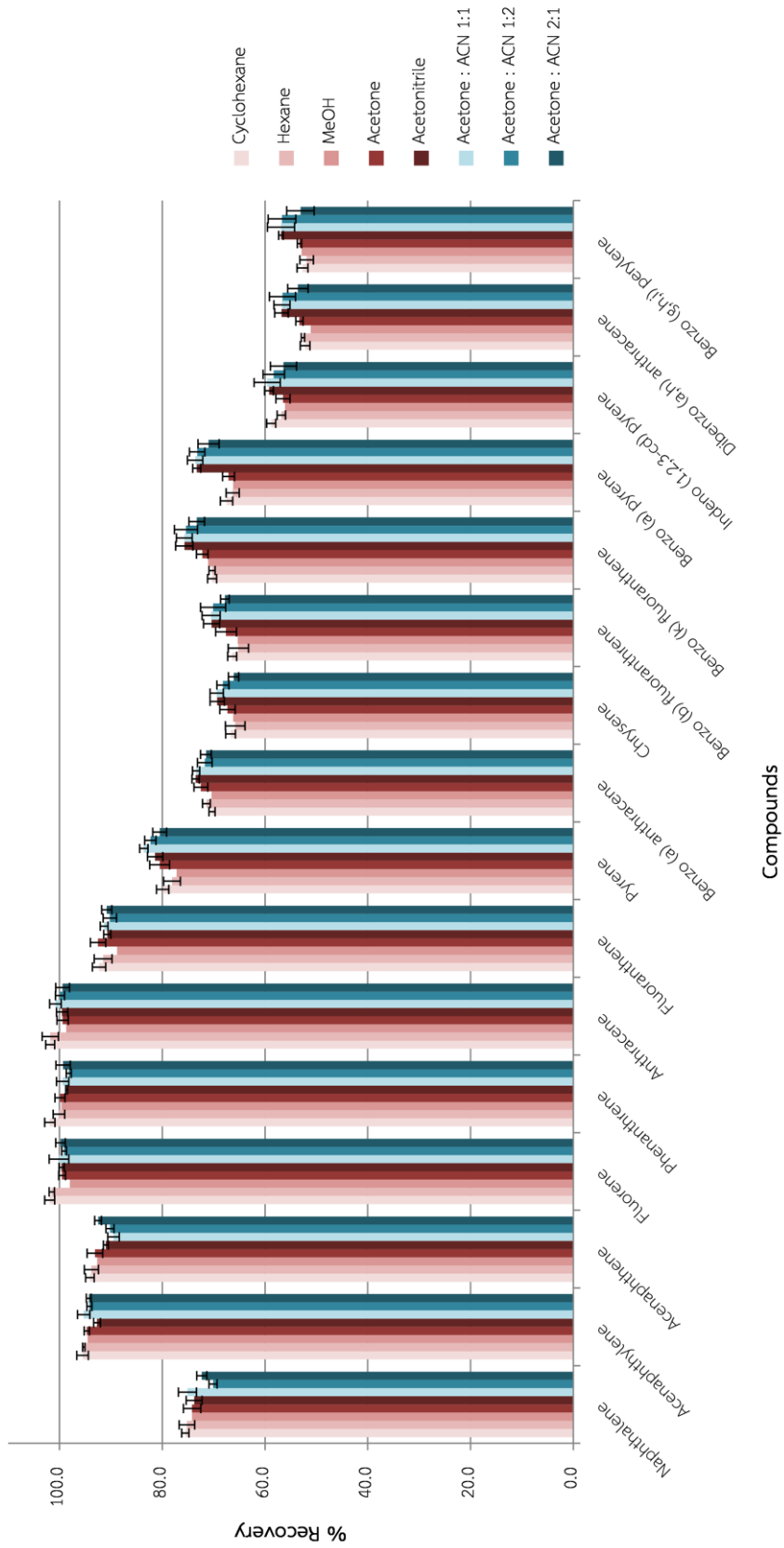


Figure 4.11 Effect of desorption solvent on the extraction of PAHs from spiked water at 8 µg/L.

Table 4.7 Percentage recoveries and standard deviations of the extraction of PAHs from spiked water at 8 µg/L by 30N0.83C sorbent and eluting with different solvents.

Name	% Recovery																	
	Cyclohexane		Hexane		Methanol		Acetone		Acetonitrile		1:1 of Acetone:ACN		1:2 of Acetone:ACN		2:1 of Acetone:ACN			
	%Recovery	SD	%Recovery	SD	%Recovery	SD	%Recovery	SD	%Recovery	SD	%Recovery	SD	%Recovery	SD	%Recovery	SD	%Recovery	SD
Naphthalene	75.5	0.7	75.2	1.5	74.2	1.7	74.2	1.6	73.8	1.0	75.1	1.8	70.1	0.8	72.3	1.0		
Acenaphthylene	95.5	1.1	95.3	0.2	94.5	0.5	94.7	0.7	92.7	0.4	95.3	1.2	94.2	0.5	94.3	0.5		
Acenaphthene	94.1	0.8	93.8	1.4	92.7	1.5	93.1	0.5	91.0	1.8	89.5	1.1	90.2	0.8	92.5	0.7		
Fluorene	101.9	1.0	101.5	0.5	98.0	0.7	99.5	0.5	99.6	1.1	100.1	1.9	99.1	0.5	99.8	0.9		
Phenanthrene	101.9	1.0	100.1	1.1	99.6	1.0	99.9	0.2	98.6	0.3	99.4	1.2	98.2	0.5	99.3	1.4		
Anthracene	101.8	0.9	101.8	1.6	98.7	1.1	99.4	1.1	99.5	0.3	100.8	1.1	99.9	0.9	99.4	1.3		
Fluoranthene	92.3	1.3	91.5	1.7	88.8	1.5	92.5	0.7	90.7	1.7	91.3	0.8	90.2	1.3	90.8	1.0		
Pyrene	79.9	1.2	78.1	1.6	77.2	1.9	80.5	1.5	81.4	1.4	83.6	0.8	82.3	1.1	80.5	1.3		
Benzo (a) anthracene	70.3	0.6	71.4	0.8	70.4	1.3	72.5	0.7	73.5	1.7	73.4	0.7	71.7	1.4	71.5	1.0		
Chrysene	66.7	1.0	65.8	1.9	66.2	1.5	67.3	1.4	69.3	0.3	69.4	1.3	68.2	1.2	66.1	1.0		
Benzo (b) fluoranthene	66.4	0.9	65.2	2.0	65.3	2.0	67.6	1.6	70.4	0.8	70.5	1.8	70.1	2.5	67.8	0.8		
Benzo (k) fluoranthene	70.3	0.9	70.3	0.6	71.1	1.1	72.2	1.7	75.7	0.9	75.7	1.6	75.4	2.3	73.3	1.5		
Benzo (a) pyrene	67.5	1.2	66.3	1.3	66.2	1.1	67.1	0.8	73.3	0.5	73.6	1.5	73.2	1.5	71.0	2.1		
Indeno (1,2,3-cd) pyrene	58.8	0.9	56.8	0.8	56.1	1.4	56.5	0.9	59.2	0.2	59.6	2.6	58.3	2.1	56.4	2.6		
Dibenzo (a,h) anthracene	52.2	0.9	52.6	0.3	51.1	0.7	53.3	1.3	56.8	1.5	56.7	1.6	56.6	2.6	53.6	2.0		
Benzo (g,h,i) perylene	52.7	1.0	51.9	1.3	52.9	0.4	53.3	0.4	56.9	1.7	56.9	2.7	56.7	2.7	53.1	2.7		

4.2.3 Volume of the desorption solvent

The volume of 1:1 (v/v) mixture of acetone and acetonitrile as desorption solvent was evaluated to maximize extraction efficiency. The optimum desorption volume was varied at 0.5, 1.0 and 1.5 mL. From Figure 4.12 and Table 4.8, the volume of 1:1 (v/v) mixture of acetone and acetonitrile at 1.0 mL was the best volume for the elution of PAHs from the sorbent. At 0.5 mL of 1:1 (v/v) mixture of acetone and acetonitrile, the percentage recoveries were very low because the volume of the desorption solvent was not enough to elute PAHs from the sorbent. However, the percentage recoveries of the elution of PAHs from the sorbent by 1.0 and 1.5 mL of 1:1 (v/v) mixture of acetone and acetonitrile were not different. Therefore, 1.0 mL of 1:1 (v/v) mixture of acetone and acetonitrile was applied for the elution PAHs from the sorbent. Since 1.0 mL of desorption solvent was enough to elute PAHs from the sorbent and could reduce time in the evaporation of the solvents step.



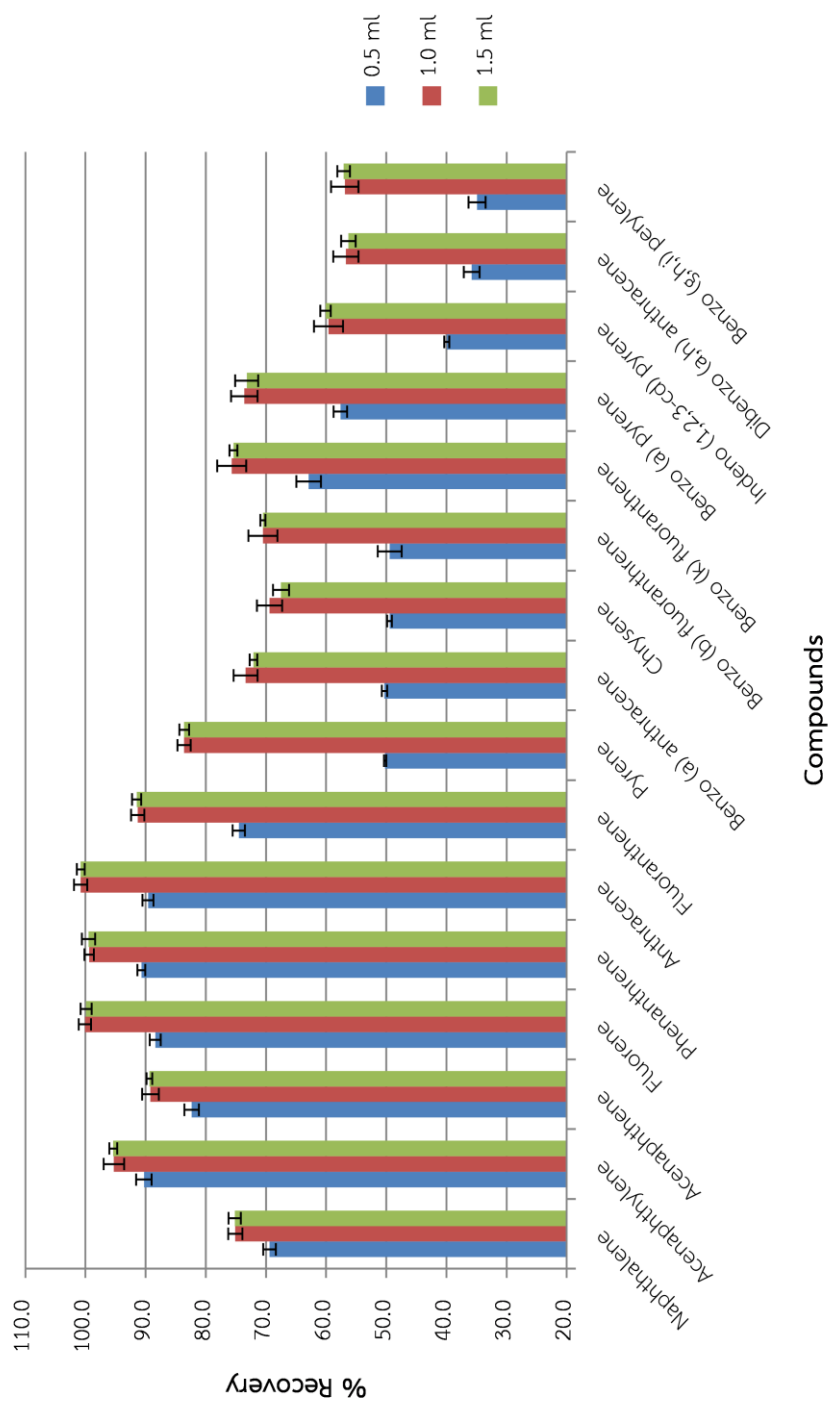


Figure 4.12 Percentage recoveries of PAHs from at 8 µg/L spiked in to Milli-Q water by extraction with different volumes of 1:1 (v/v) mixture of acetone and acetonitrile for elution. Elute with 1:1 (v/v) mixture of acetone and acetonitrile by different volume.

Table 4.8 Percentage recoveries and standard deviations of extraction PAHs from at 8 µg/L spiked in to Milli-Q water by 30N0.83C sorbent and eluted with different volumes of 1:1 (v/v) mixture of acetone and acetonitrile.

Name	% Recovery					
	0.5 mL		1.0 mL		1.5 mL	
	%Recovery	SD	%Recovery	SD	%Recovery	SD
Naphthalene	69.4	1.0	75.1	1.8	75.2	1.0
Acenaphthylene	90.3	1.3	95.3	1.2	95.4	0.6
Acenaphthene	82.4	1.2	89.5	1.1	89.4	0.5
Fluorene	88.4	0.9	100.1	1.9	99.9	0.9
Phenanthrene	90.7	0.7	99.4	1.2	99.5	1.1
Anthracene	89.6	0.9	100.8	1.1	100.8	0.7
Fluoranthene	74.5	1.0	91.3	0.8	91.5	0.8
Pyrene	50.2	0.2	83.6	0.8	83.6	0.8
Benzo (a) anthracene	50.3	0.5	73.4	0.7	72.1	0.6
Chrysene	49.5	0.4	69.4	1.3	67.5	1.3
Benzo (b) fluoranthrene	49.4	2.0	70.5	1.8	70.5	0.4
Benzo (k) fluoranthene	62.9	2.1	75.7	1.6	75.4	0.6
Benzo (a) pyrene	57.6	1.1	73.6	1.5	73.2	1.9
Indeno (1,2,3-cd) pyrene	40.0	0.4	59.6	2.6	60.1	0.9
Dibenzo (a,h) anthracene	35.8	1.3	56.7	1.6	56.3	1.2
Benzo (g,h,i) perylene	34.9	1.4	56.9	2.7	57.1	1.0

4.2.4 Weight of the electrospun CNTs-Nylon6 composite nanofibers

In this section, the weight of the sorbent was optimized. The amount of SPE disk was varied at 3.0, 4.0, 5.0 and 6.0 mg of 30N0.83C sorbent. Extraction of spiked water with 8 $\mu\text{g/L}$ of PAHs was performed. 1.0 mL of 1:1 (v/v) mixture of acetone and acetonitrile was used for eluting step. 3.0 mg of SPE disk showed the worst performance because the capacity of SPE disk was not enough to adsorb with analytes as shown in Figure 4.13 and summarized in Table 4.9. When the weight of the SPE disk was increased, the extraction efficiency was improved. Nevertheless, the weight of SPE disk more than 4.0 mg (5.0 and 6.0 mg) could not improve because of the exceeding of capacity of the sorbent. Thereby, 4.0 mg of 30N0.83C sorbent was applied to use for the extraction in water samples.



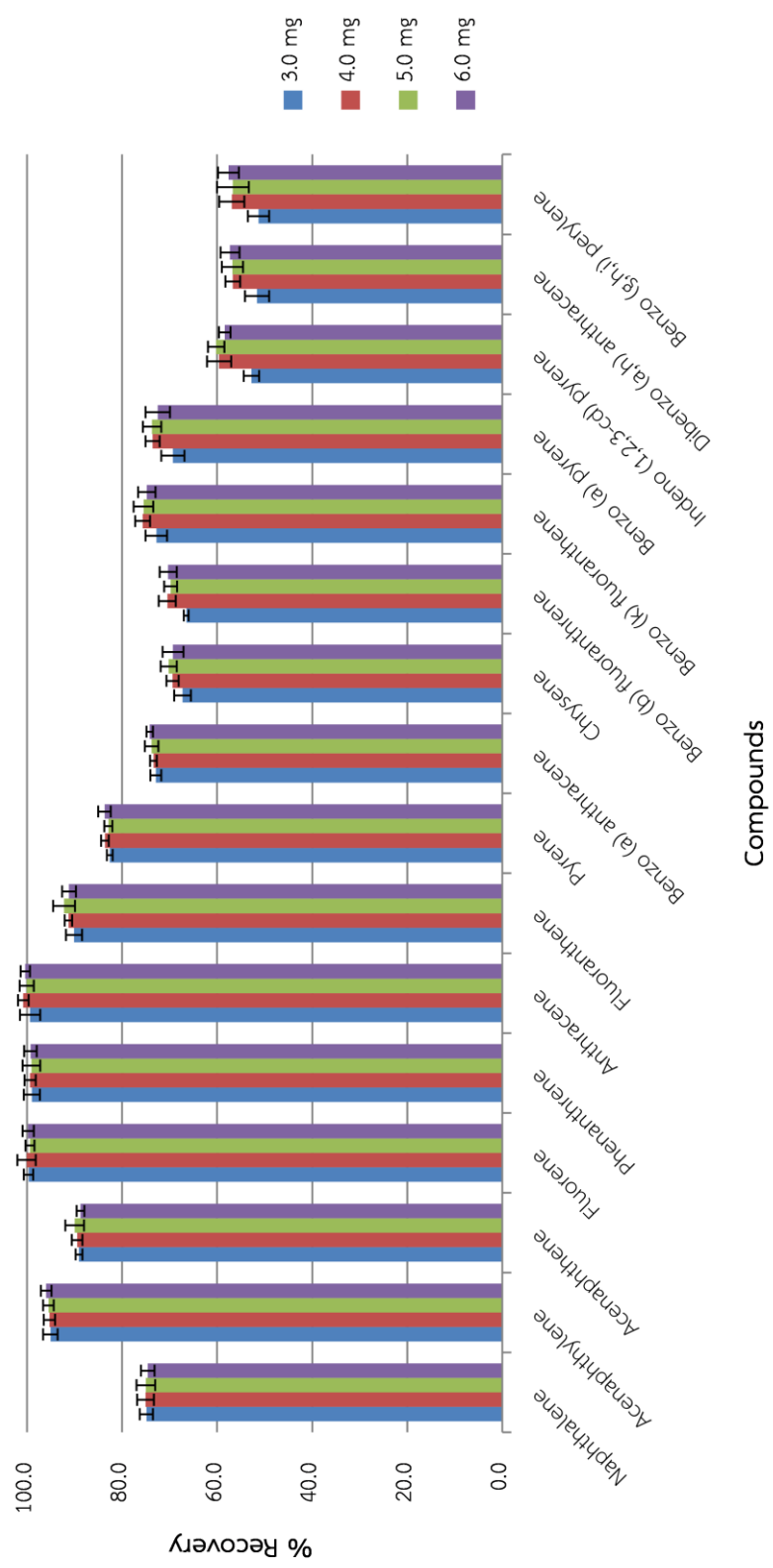


Figure 4.13 Percentage recoveries of PAHs from at 8 µg/L spiked in to Milli-Q water by extraction with different weights of 30N0.83C sorbent and eluted by 1.0 mL of 1:1 (v/v) mixture of acetone and acetonitrile.

Table 4.9 Percentage recoveries and standard deviations of extraction PAHs from at 8 µg/L spiked in to Milli-Q water by different weights of 30N0.83C sorbent.

Name	% Recovery							
	3.0 mg		4.0 mg		5.0 mg		6.0 mg	
	%Recovery	SD	%Recovery	SD	%Recovery	SD	%Recovery	SD
Naphthalene	74.9	1.4	75.1	1.8	75.0	2.0	74.6	1.4
Acenaphthylene	95.1	1.5	95.3	1.2	95.5	1.1	96	1.1
Acenaphthene	89.1	0.7	89.5	1.1	90.0	2.0	88.8	0.8
Fluorene	99.7	1.0	100.1	1.9	99.4	1.0	99.8	1.2
Phenanthrene	99.0	1.7	99.4	1.2	99.1	1.9	99.3	1.3
Anthracene	99.4	2.1	100.8	1.1	100.1	1.5	100.4	1.0
Fluoranthene	90.1	1.7	91.3	0.8	92.2	2.3	91.2	1.5
Pyrene	82.6	0.6	83.6	0.8	82.9	0.9	83.7	1.3
Benzo (a) anthracene	72.9	1.2	73.4	0.7	73.8	1.4	74.2	0.7
Chrysene	67.3	1.8	69.4	1.3	70.2	1.7	69.3	2.2
Benzo (b) fluoranthrene	66.5	0.5	70.5	1.8	69.8	1.4	70.3	1.8
Benzo (k) fluoranthene	72.8	2.3	75.7	1.6	75.5	2.1	74.8	1.8
Benzo (a) pyrene	69.3	2.4	73.6	1.5	73.7	1.9	72.5	2.6
Indeno (1,2,3-cd) pyrene	52.8	1.6	59.6	2.6	60.2	1.7	58.4	1.2
Dibenzo (a,h) anthracene	51.6	2.5	56.7	1.6	56.8	2.2	57.3	2.0
Benzo (g,h,i) perylene	51.3	2.3	56.9	2.7	56.7	3.4	57.6	2.2

The optimum condition for the extraction of PAHs in water by electrospun CNTs-Nylon6 composite nanofibers was summarized in Table 4.10.

Table 4.10 The optimum condition for the extraction of PAHs in water by electrospun CNTs-Nylon6 composite nanofibers.

Optimum condition	Result
Type of sorbent	30%w/v of Nylon6 with 0.83%w/w of CNTs (30N0.83C)
Type of desorption solvent	1:1 (v/v) mixture of acetone and acetonitrile
Volume of desorption solvent	1 mL
Weight of sorbent	4.0 mg

4.3 Method validation

The determination of PAHs in water by solid-phase extraction using electrospun CNTs-Nylon6 composite nanofibers as a sorbent followed the condition in Table 4.10 was validated. The method of detection (MOD) and method of quantitation (MOQ) were illustrated in Table 4.11 which were 0.2-3.0 $\mu\text{g/L}$ and 0.5-6.0 $\mu\text{g/L}$, respectively. The reproducibility of the method was evaluated from relative standard deviation (RSD) of 10 replicates extraction of spiked water at 6, 8 and 10 $\mu\text{g/L}$ PAHs. The result was shown in Table 4.12. %RSDs lower than 5 were obtained for all spiked concentrations which were acceptable by AOAC (not more than 21% [59]).

Table 4.11 Method of detection (MOD) and method of quantitation (MOQ) for developed method.

Name	MOD ($\mu\text{g/L}$)	MOQ ($\mu\text{g/L}$)
Naphthalene	0.2	0.5
Acenaphthylene	0.2	0.5
Acenaphthene	0.2	0.5
Fluorene	0.4	1.2
Phenanthrene	0.4	1.2
Anthracene	0.4	1.2
Fluoranthene	0.2	0.8
Pyrene	0.2	0.8
Benzo (a) anthracene	1.2	2.5
Chrysene	1.2	2.5
Benzo (b) fluoranthrene	3.0	6.0
Benzo (k) fluoranthene	3.0	6.0
Benzo (a) pyrene	3.0	6.0
Indeno (1,2,3-cd) pyrene	3.0	6.0
Dibenzo (a,h) anthracene	3.0	6.0
Benzo (g,h,i) perylene	3.0	6.0

Table 4.12 Percentage recoveries and RSD for the extraction of PAHs from spiked water at 6, 8 and 10 µg/L PAHs (n=10).

Name	6 µg/L		8 µg/L		10 µg/L	
	Recovery (%)	RSD (%)	Recovery (%)	RSD (%)	Recovery (%)	RSD (%)
Naphthalene	74.0	1.2	75.1	2.4	74.6	1.2
Acenaphthylene	95.5	0.5	95.3	1.3	97.5	0.4
Acenaphthene	88.5	0.6	89.5	1.3	88.0	0.7
Fluorene	98.4	0.6	100.1	1.9	99.0	0.6
Phenanthrene	98.5	0.9	99.4	1.2	98.7	0.6
Anthracene	98.9	0.7	100.8	1.1	99.0	0.4
Fluoranthene	91.6	1.4	91.3	0.8	92.8	0.6
Pyrene	84.2	0.9	83.6	1.0	84.5	0.7
Benzo (a) anthracene	74.6	1.4	73.4	1.0	74.6	0.8
Chrysene	69.3	1.7	69.4	1.9	69.4	0.8
Benzo (b) fluoranthrene	69.5	2.2	70.5	2.5	69.1	0.9
Benzo (k) fluoranthene	74.6	1.7	75.7	2.0	74.0	0.7
Benzo (a) pyrene	73.2	2.0	73.6	2.0	73.8	0.8
Indeno (1,2,3-cd) pyrene	57.7	2.1	59.6	4.3	57.7	1.0
Dibenzo (a,h) anthracene	56.5	2.0	56.7	2.8	56.6	1.2
Benzo (g,h,i) perylene	56.7	2.4	56.9	4.7	56.7	1.4

Comparison of PAHs recoveries for this method with other methods (Table 4.13), the recoveries of small PAHs molecule for extraction by using CNTs and C18 cartridge were similar to 30N0.83C sorbent in this research. Whereas, the percentage recoveries of large PAHs molecule for extraction by using 30N0.83C sorbent were lower than CNTs and C18 cartridge because of the smaller amount of sorbent. Other parameters of the method were compared in Table 4.14. Nevertheless, the volume of desorption solvent for our material was less than other methods. In addition, reproducibility for this method was good since %RSDs lower than 5 were obtained.

Table 4.13 Comparison of PAHs recoveries from other researches to our sorbent.

Name	CNTs [13] (150 mg)		C18 [12] (500 mg)		Sorbent in this research 30N0.83C	
	Recovery (%)	RSD (%)	Recovery (%)	RSD (%)	Recovery (%)	RSD (%)
Naphthalene	80.5	10.2	59.2	13.3	75.1	2.4
Acenaphthylene	89.0	12.1	58.5	14.8	95.3	1.3
Acenaphthene	94.5	9.2	60.8	16.1	89.5	1.3
Fluorene	101.5	2.6	68.0	14.0	100.1	1.9
Phenanthrene	98.5	6.8	74.4	13.3	99.4	1.2
Anthracene	74.5	6.5	70.7	14.0	100.8	1.1
Fluoranthene	105.0	2.7	76.4	10.5	91.3	0.8
Pyrene	80.5	9.9	77.0	13.0	83.6	1.0
Benzo (a) anthracene	86.0	5.7	-	-	73.4	1.0
Chrysene	82.0	5.2	-	-	69.4	1.9
Benzo (b) fluoranthrene	84.5	1.4	86.9	9.8	70.5	2.5
Benzo (k) fluoranthene	82.0	3.8	-	-	75.7	2.0
Benzo (a) pyrene	94.0	3.9	99.8	8.2	73.6	2.0
Indeno (1,2,3-cd) pyrene	127.0	1.2	-	-	59.6	4.3
Dibenzo (a,h) anthracene	87.5	7.4	-	-	56.7	2.8
Benzo (g,h,i) perylene	85.0	5.6	88.3	3.3	56.9	4.7

Table 4.14 Comparison of method from other researches.

Conditions	CNTs	C18	30N0.83C
Weight of sorbent	150 mg	500 mg	4 mg
Volume of sample	500 mL	10 mL	25 mL
Volume of desorption solvent	15 mL	3 mL	1 mL
% Recovery (small PAHs molecule)	74.5 – 105.0%	58.5 – 77.0 %	75.1 – 100.8%
% Recovery (large PAHs molecule)	82.0 – 127.0%	86.9 – 99.8%	56.7 – 75.7%
%RSD	1.2 – 12.1%	3.0 – 16.1%	0.8 – 4.7%

4.4 Applied the electrospun CNTs-Nylon6 composite nanofibers for determination of PAHs in water samples

Drinking water samples were extracted using the optimized extraction conditions of the 30N0.83C membrane. PAHs were detected in the samples (Figure 4.14-Figure 4.19). The samples were spiked and recoveries were calculated. The percentage recoveries of PAHs at 10 µg/L spiked in the samples ranged from 54.2-101.6% that indicates no matrix interferences (Table 4.15-Table 4.17)

Table 4.15 Percentage recoveries of PAHs at 10 µg/L spiked in drinking water sample 1.

Name	Concentration detected in sample (µg/L)	Concentration detected at 10 µg/L spiked in sample (mg/L)	Recovery (%)
Naphthalene	0.60	0.2	75.2
Acenaphthylene	ND	0.2	94.7
Acenaphthene	ND	0.2	90.1
Fluorene	ND	0.3	99.3
Phenanthrene	ND	0.3	99.6
Anthracene	ND	0.3	99.7
Fluoranthene	ND	0.2	92.2
Pyrene	ND	0.2	84.3
Benzo (a) anthracene	ND	0.2	74.1
Chrysene	ND	0.2	68.5
Benzo (b) fluoranthrene	ND	0.2	69.8
Benzo (k) fluoranthene	ND	0.2	76.1
Benzo (a) pyrene	ND	0.2	72.6
Indeno (1,2,3-cd) pyrene	ND	0.2	58.3
Dibenzo (a,h) anthracene	ND	0.1	56.1
Benzo (g,h,i) perylene	ND	0.1	56.4

Table 4.16 Percentage recoveries of PAHs at 10 µg/L spiked in drinking water sample 2.

Name	Concentration detected in sample (µg/L)	Concentration detected at 10 µg/L spiked in sample (mg/L)	Recovery (%)
Naphthalene	0.62	0.2	73.6
Acenaphthylene	ND	0.2	96.1
Acenaphthene	ND	0.2	90.3
Fluorene	1.2	0.3	98.4
Phenanthrene	ND	0.3	98.9
Anthracene	ND	0.3	101.6
Fluoranthene	ND	0.2	89.3
Pyrene	ND	0.2	81.5
Benzo (a) anthracene	ND	0.2	73.4
Chrysene	ND	0.2	70.3
Benzo (b) fluoranthrene	ND	0.2	72.7
Benzo (k) fluoranthene	ND	0.2	74.3
Benzo (a) pyrene	ND	0.2	72.2
Indeno (1,2,3-cd) pyrene	ND	0.1	57.3
Dibenzo (a,h) anthracene	ND	0.1	54.4
Benzo (g,h,i) perylene	ND	0.1	56.8

Table 4.17 Percentage recoveries of PAHs at 10 µg/L spiked in drinking water sample 3.

Name	Concentration detected in sample (µg/L)	Concentration detected at 10 µg/L spiked in sample (mg/L)	Recovery (%)
Naphthalene	0.60	0.2	77.1
Acenaphthylene	0.52	0.2	93.2
Acenaphthene	0.50	0.2	87.3
Fluorene	ND	0.3	100.6
Phenanthrene	ND	0.3	101.3
Anthracene	ND	0.3	98.7
Fluoranthene	ND	0.2	88.5
Pyrene	ND	0.2	84.6
Benzo (a) anthracene	ND	0.2	71.4
Chrysene	ND	0.2	97.7
Benzo (b) fluoranthrene	ND	0.2	70.3
Benzo (k) fluoranthene	ND	0.2	76.6
Benzo (a) pyrene	ND	0.2	73.4
Indeno (1,2,3-cd) pyrene	ND	0.2	58.3
Dibenzo (a,h) anthracene	ND	0.1	55.1
Benzo (g,h,i) perylene	ND	0.1	54.2

ND = Not detected

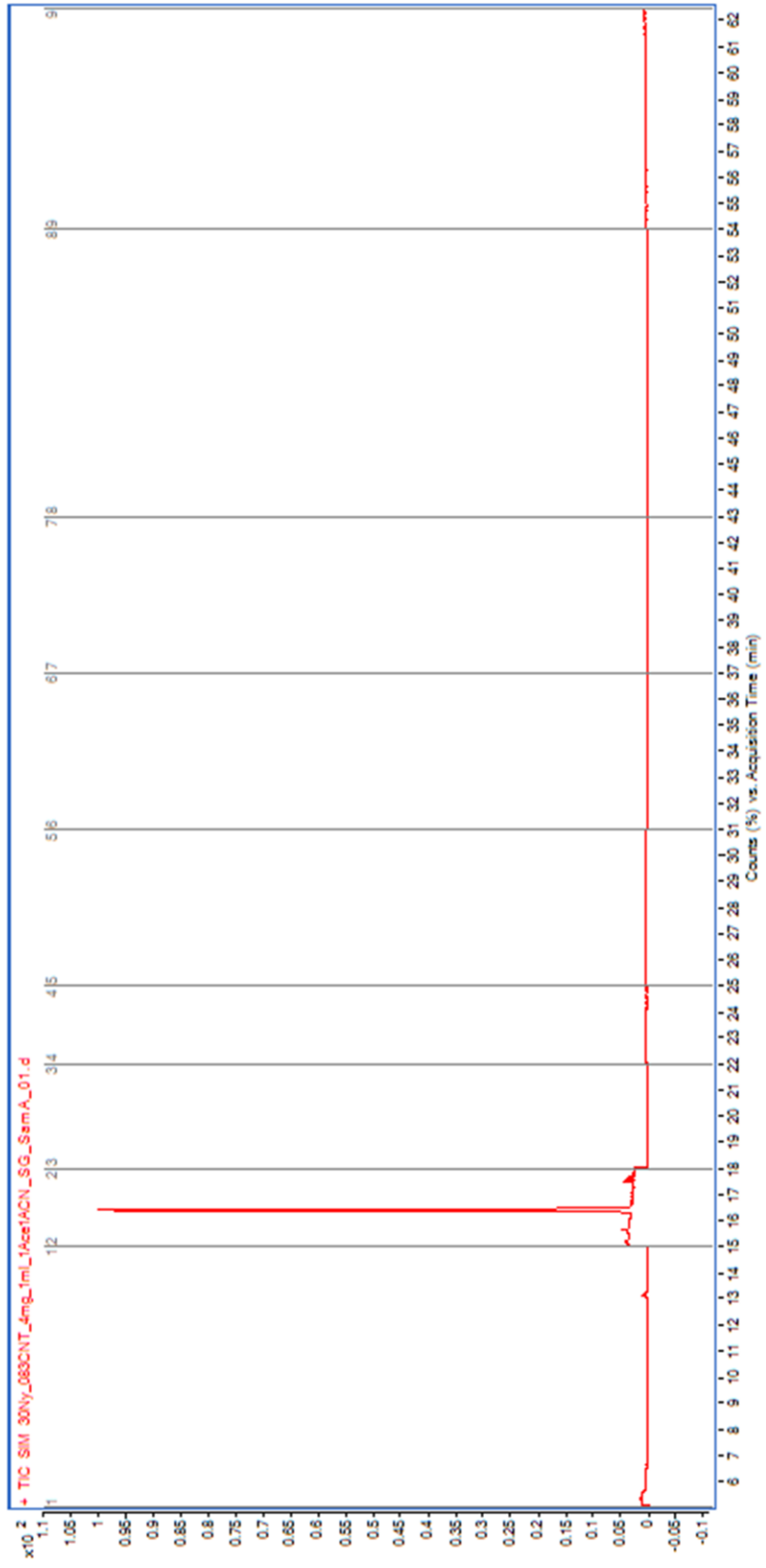


Figure 4.14 Chromatogram of PAHs from extraction of drinking water sample 1.

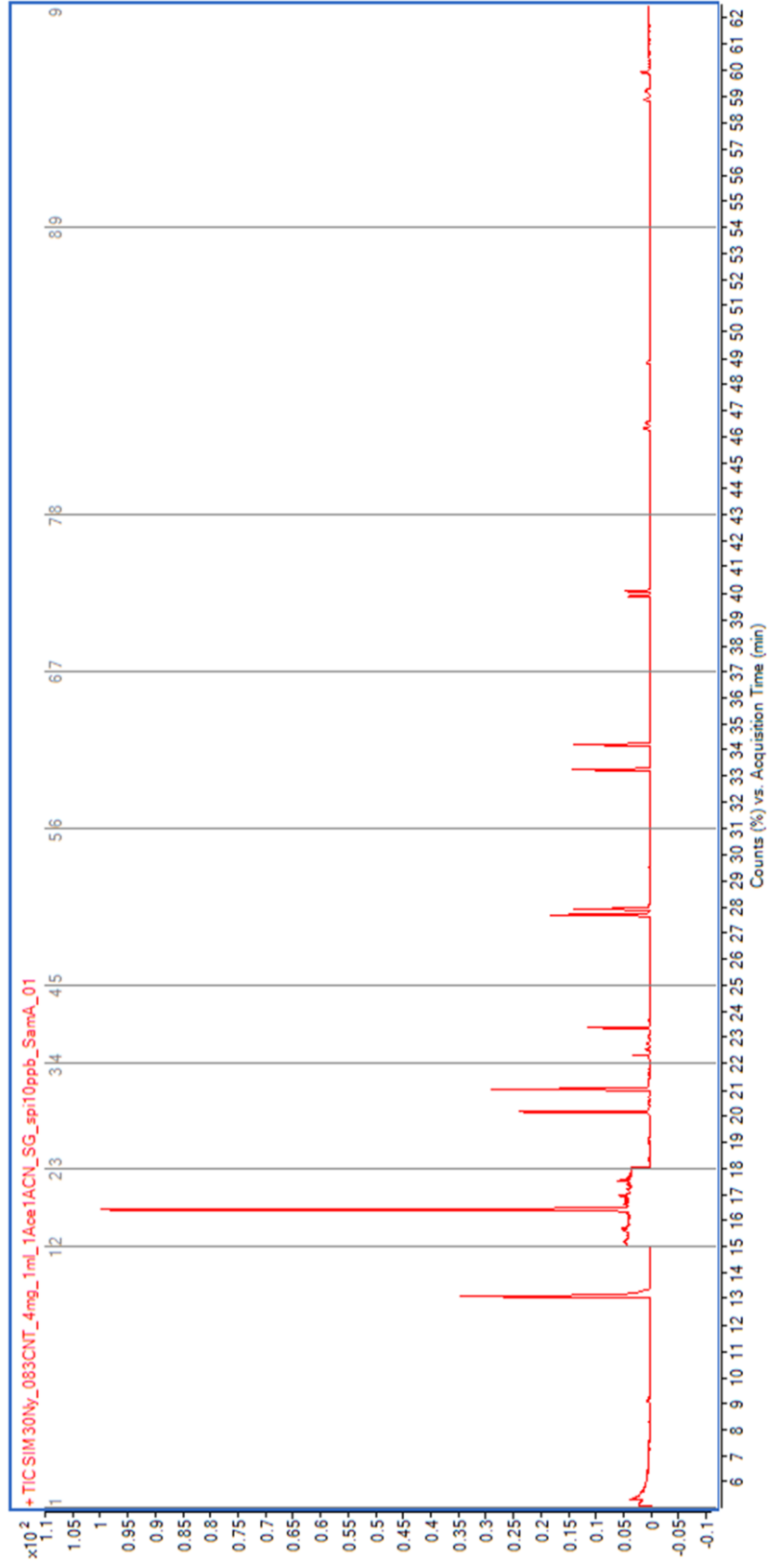


Figure 4.15 Chromatogram of PAHs from extraction of drinking water sample 1 was spiked PAHs at 10 $\mu\text{g/L}$.

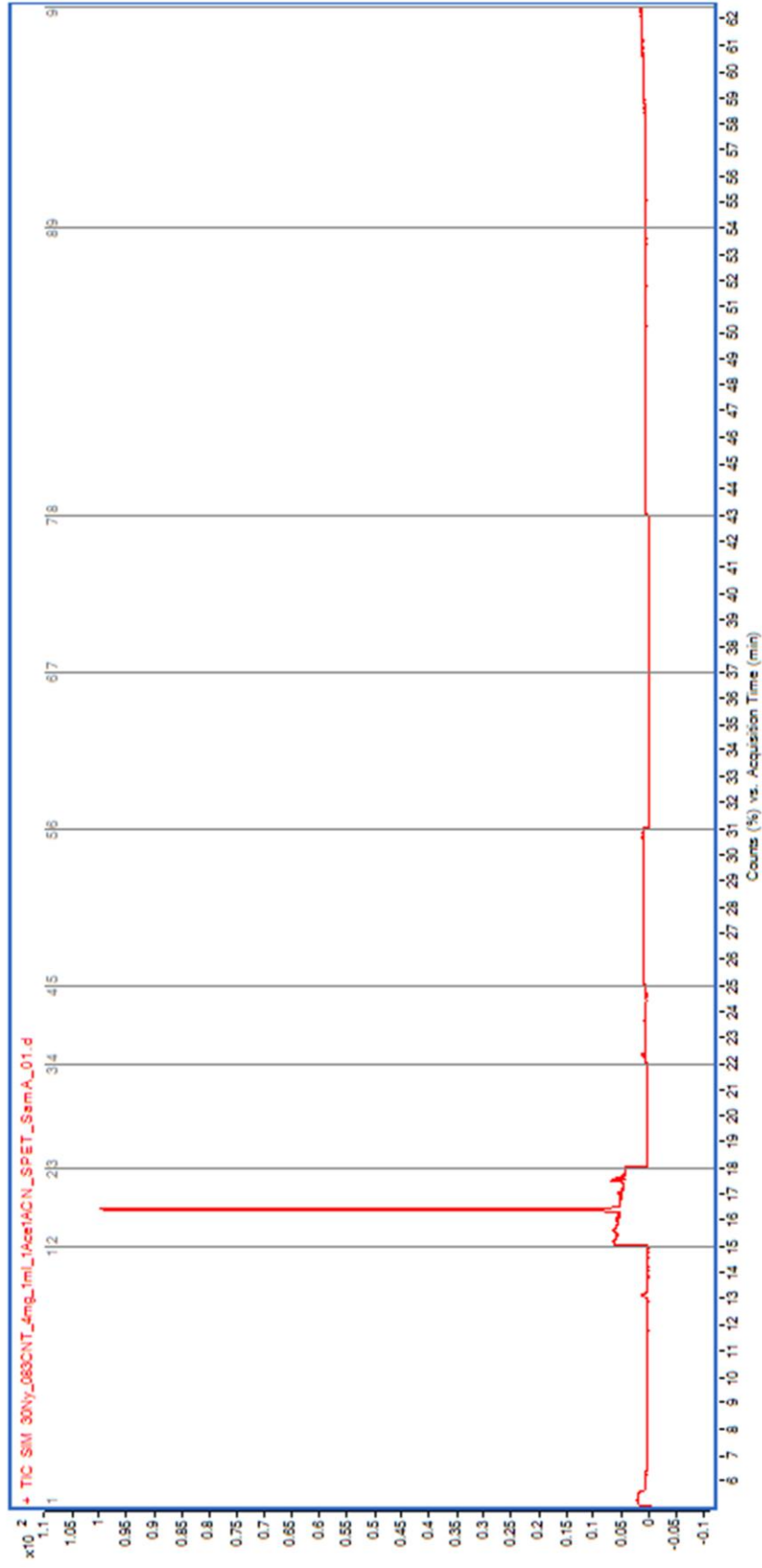


Figure 4.16 Chromatogram of PAHs from extraction of drinking water sample 2.

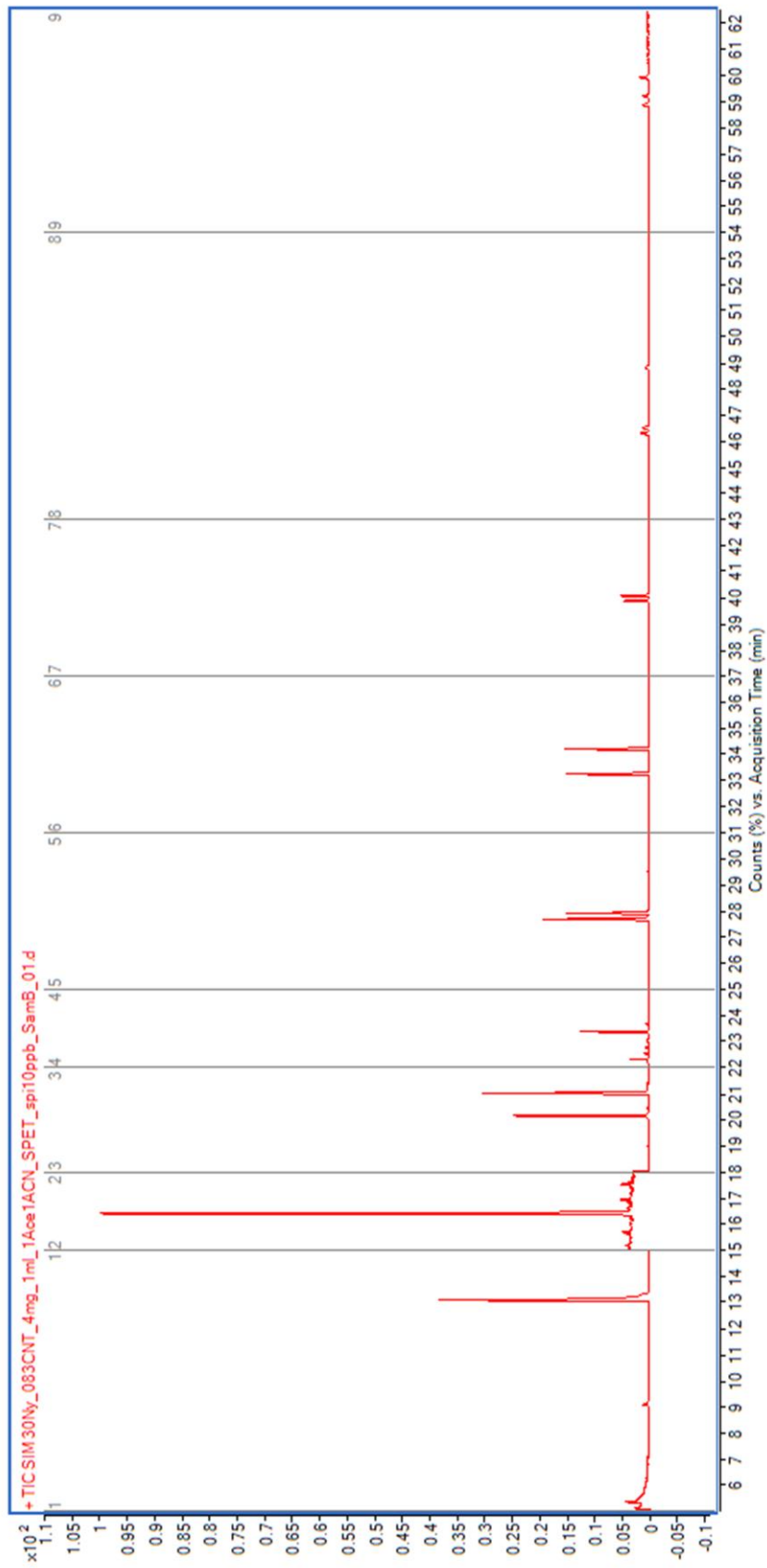


Figure 4.17 Chromatogram of PAHs from extraction of drinking water sample 2 was spiked PAHs at 10 $\mu\text{g/L}$.

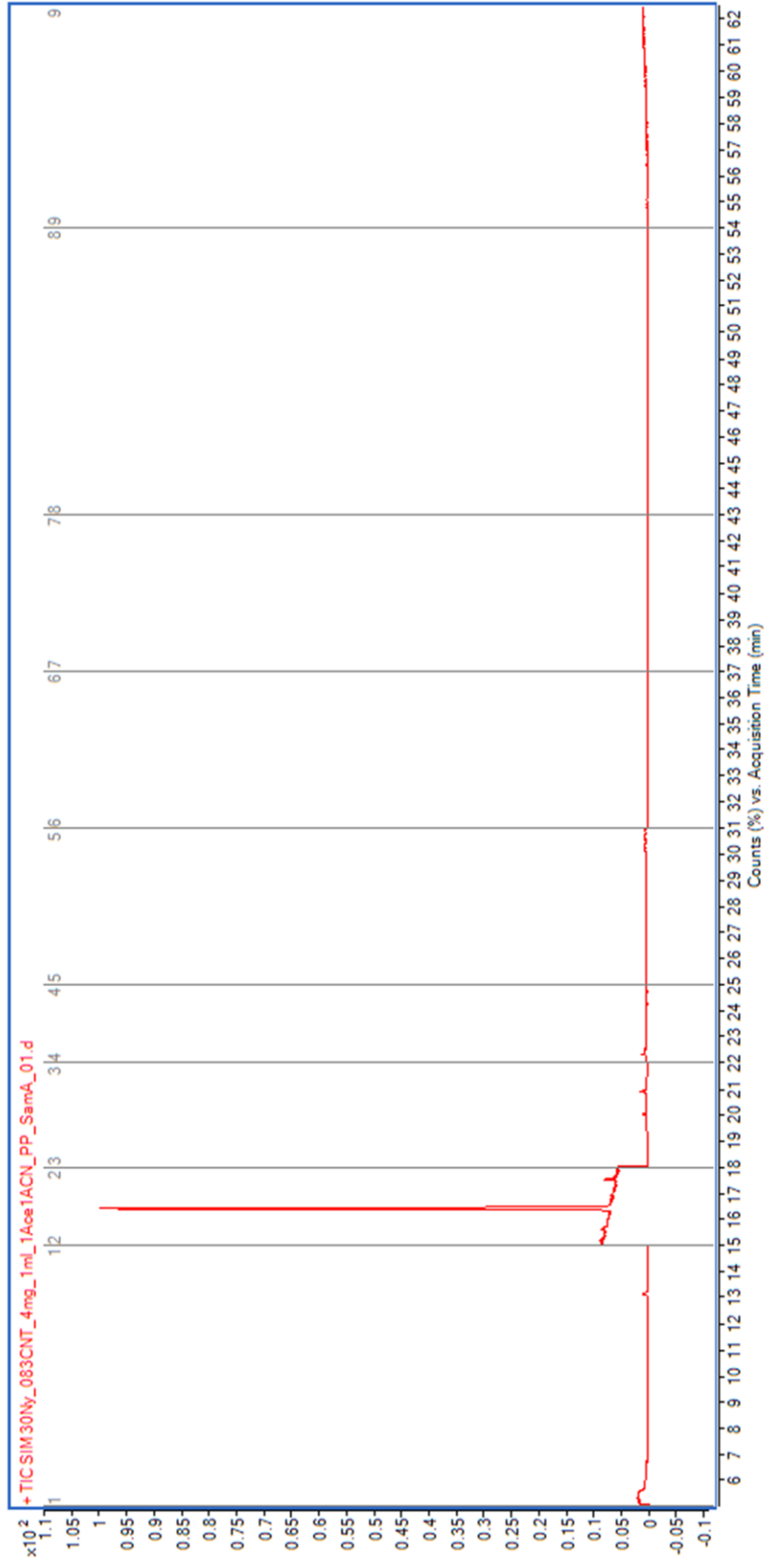


Figure 4.18 Chromatogram of PAHs from extraction of drinking water sample 3.

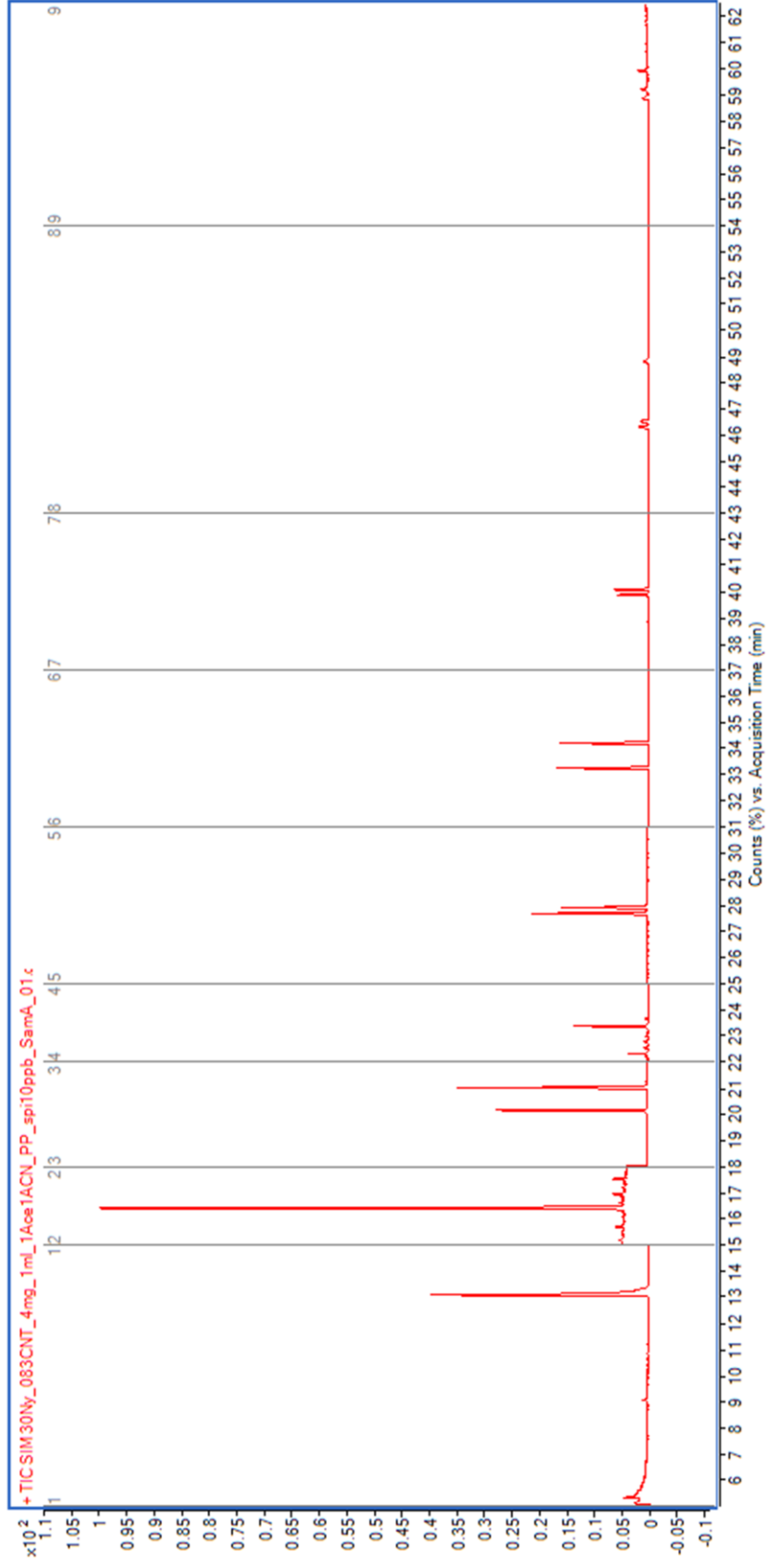


Figure 4.19 Chromatogram of PAHs from extraction of drinking water sample 3 was spiked PAHs at 10 $\mu\text{g/L}$.

CHAPTER V

CONCLUSIONS

5.1 Conclusions

The electrospun fibrous CNTs-Nylon6 composite membrane as SPE sorbent was prepared and used for extraction of PAHs in water samples. The preparation of electrospun CNTs-Nylon6 composite fibers and the extraction of PAHs by this sorbent were shown in Figure 5.1 and Figure 5.2, respectively. The electrospun CNTs-Nylon6 composite nanofibers were successfully fabricated to apply as a sorbent for SPE. The CNTs content in CNTs-Nylon6 composite nanofibers aligned along the long axis and thoroughly dispersed in Nylon6 nanofibers. The decreasing of Nylon6 concentration led to smaller fiber diameters relating to low viscosity of CNTs-Nylon6 solution. The optimum of the collector distance was increased as increasing the amount of CNTs added because of electrical properties of CNTs. The amount of CNTs incorporating into the nanofibers accorded with the amount of CNTs added into the Nylon6 solution. In addition, the electrospun Nylon6-CNTs composite nanofibers were available in micropore, mesopore and macropore and had a high specific surface area. Therefore, the electrospun Nylon6-CNTs which prepared from 25 and 30 %w/v of Nylon6 with various amounts of CNTs were used to study for the extraction of PAHs in water samples. As the result, the optimum conditions for extraction PAHs in water samples were using 4.0 mg of 30 %w/v of Nylon6 with 0.83 %w/w of CNTs, 1 mL of 1:1 (v/v) mixture of acetone and acetonitrile as the desorption solvent. The small and large molecules of PAHs was eluted by π - π interaction from acetone and acetonitrile, respectively, and 1.0 mL of 1:1 (v/v) mixture of acetone and acetonitrile was enough to elute PAHs from the sorbent and could reduce time in the evaporation of the solvents step. The percentage recoveries of the extraction of PAHs from 8 μ g/L spiked water at optimum conditions were in the range of 56.7 – 100.8% with the RSD less than 5 that were acceptable. The MOD and MOQ ranged 0.2 – 3.0 μ g/L and 0.5 – 6.0 μ g/L, respectively. Finally, the optimum conditions were

applied to the analysis of water samples. The percentage recoveries of PAHs at 10 $\mu\text{g/L}$ spiked in water samples ranged from 54.2-101.6%.

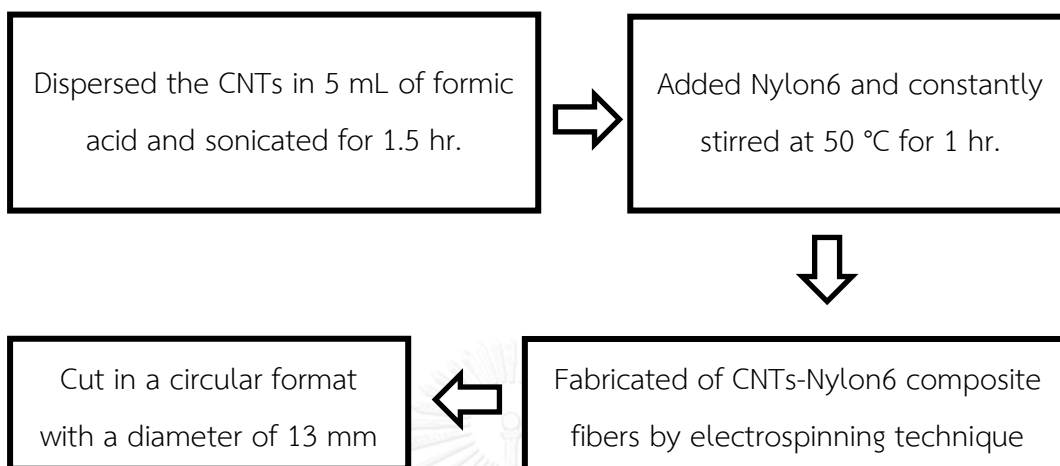


Figure 5.1 Flow chart of CNTs-Nylon6 composite fibers preparation by electrospinning technique

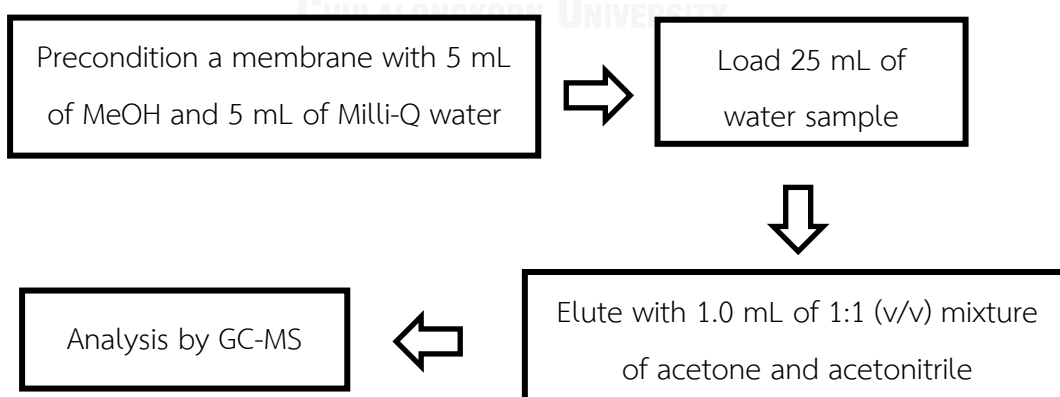


Figure 5.2 Flow chart of extraction of PAHs in water samples

5.2 Suggestion of future work

The electrospun CNTs-Nylon6 composite fibers were a good adsorbent for extraction. The electrospun polymer fibers were high specific area so they are popular to use as a sorbent. Moreover, the CNTs which could interact with a variety force, for example, van der Waals force, π - π interaction, and electrostatic force could improve the better extraction efficiency. In the future work, sorbent could be specified with other analytes for various interested compounds by functionalization of CNTs. This would develop selectivity that could be lead to improving the good extraction efficiency.



REFERENCES

- [1] Barranco, A., et al. Solid-Phase Clean-Up in The Liquid Chromatographic Determination of Polycyclic Aromatic Hydrocarbons in Edible Oils. Journal of Chromatography A 988(1) (2003): 33-40.
- [2] Bogusz, M.J., El Hajj, S.A., Ehaideb, Z., Hassan, H., and Al-Tufail, M. Rapid Determination of Benzo(A)Pyrene in Olive Oil Samples with Solid-Phase Extraction and Low-Pressure, Wide-Bore Gas Chromatography–Mass Spectrometry and Fast Liquid Chromatography with Fluorescence Detection. Journal of Chromatography A 1026(1-2) (2004): 1-7.
- [3] Gomez-Ruiz, J.A., Cordeiro, F., Lopez, P., and Wenzl, T. Optimisation and Validation of Programmed Temperature Vaporization (Ptv) Injection in Solvent Vent Mode for The Analysis of The 15+1 EU-Priority PAHs by GC-MS. Talanta 80(2) (2009): 643-50.
- [4] Teixeira, V.H., Casal, S., and Oliveira, M.B.P.P. Pahs Content in Sunflower, Soybean and Virgin Olive Oils: Evaluation in Commercial Samples and During Refining Process. Food Chemistry 104(1) (2007): 106-112.
- [5] Namera, A., Nakamoto, A., Saito, T., and Miyazaki, S. Monolith as A New Sample Preparation Material: Recent Devices and Applications. Journal of Separation Science 34(8) (2011): 901-24.
- [6] Purcaro, G., Moret, S., and Conte, L.S. Overview on Polycyclic Aromatic Hydrocarbons: Occurrence, Legislation and Innovative Determination in Foods. Talanta 105 (2013): 292-305.
- [7] Moja, S.J. and Mtunzi, F. Application of Solid Phase Extraction (SPE) Method in Determining Polycyclic Aromatic Hydrocarbons (PAHs) in River Water Samples Journal of Environmental Chemistry and Ecotoxicology 5(11) (2013): 278-283.
- [8] Kanchanamayoon, W. and Tatrahun, N. Determination of Polycyclic Aromatic Hydrocarbons in Water Samples by Solid Phase Extraction and Gas Chromatography. World Journal of Chemistry 3(2) (2008): 51-54.

- [9] Ravelo-Perez, L.M., Herrera-Herrera, A.V., Hernandez-Borges, J., and Rodriguez-Delgado, M.A. Carbon Nanotubes: Solid-Phase Extraction. Journal of chromatography. A 1217(16) (2010): 2618-41.
- [10] Ma, J., Xiao, R., Li, J., Yu, J., Zhang, Y., and Chen, L. Determination of 16 Polycyclic Aromatic Hydrocarbons in Environmental Water Samples by Solid-Phase Extraction Using Multi-Walled Carbon Nanotubes as Adsorbent Coupled with Gas Chromatography-Mass Spectrometry. Journal of chromatography. A 1217(34) (2010): 5462-9.
- [11] Guo, L. and Lee, H.K. Development of Multiwalled Carbon Nanotubes Based Micro-Solid-Phase Extraction for The Determination of Trace Levels of Sixteen Polycyclic Aromatic Hydrocarbons in Environmental Water Samples. Journal of chromatography. A 1218(52) (2011): 9321-9327.
- [12] Huang, Z.-M., Zhang, Y.Z., Kotaki, M., and Ramakrishna, S. A Review on Polymer Nanofibers by Electrospinning and Their Applications in Nanocomposites. Composites Science and Technology 63(15) (2003): 2223-2253.
- [13] Wannatong, L., Sirivat, A., and Supaphol, P. Effects of Solvents on Electrospun Polymeric Fibers: Preliminary Study on Polystyrene. Polymer International 53(11) (2004): 1851-1859.
- [14] Mottaghitlab, V. and Haghi, A.K. A Study on Electrospinning of Polyacrylonitrile Nanofibers. Korean Journal of Chemical Engineering 28(1) (2010): 114-118.
- [15] Yördem, O.S., Papila, M., and Menciloğlu, Y.Z. Effects of Electrospinning Parameters on Polyacrylonitrile Nanofiber Diameter: An Investigation by Response Surface Methodology. Materials & Design 29(1) (2008): 34-44.
- [16] Xu, Q., et al. Electrospun Nylon6 Nanofibrous Membrane as SPE Adsorbent for the Enrichment and Determination of Three Estrogens in Environmental Water Samples. Chromatographia 71(5-6) (2009): 487-492.
- [17] Xu, Q., Yin, X., Wu, S., Wang, M., Wen, Z., and Gu, Z. Determination of Phthalate Esters in Water Samples Using Nylon6 Nanofibers Mat-Based Solid-

- Phase Extraction Coupled to Liquid Chromatography. Microchimica Acta 168(3-4) (2010): 267-275.
- [18] Wu, S.-Y., et al. Determination of Bisphenol A in Plastic Bottled Drinking Water by High Performance Liquid Chromatography with Solid-membrane Extraction Based on Electrospun Nylon 6 Nanofibrous Membrane. Chinese Journal of Analytical Chemistry 38(4) (2010): 503-507.
- [19] Feng, L., Li, S.H., Zhai, J., Song, Y.L., Jiang, L., and Zhu, D.B. Template Based Synthesis of Aligned Polyacrylonitrile Nanofibers Using A Novel Extrusion Method. Synthetic Metals 135-136 (2003): 817-818.
- [20] Wang, S., et al. Template-Assisted Synthesis of Porous Molybdenum Dioxide Nanofibers and Nanospheres by Redox Etching Method. Journal of Crystal Growth 290(1) (2006): 96-102.
- [21] Suzuki, A. and Arino, K. Polypropylene Nanofiber Sheets Prepared by CO₂ Laser Supersonic Multi-Drawing. European Polymer Journal 48(7) (2012): 1169-1176.
- [22] Suzuki, A., Mikuni, T., and Hasegawa, T. Nylon 66 Nanofibers Prepared by CO₂ Laser Supersonic Drawing. Journal of Applied Polymer Science (2014).
- [23] Xing, X., Wang, Y., and Li, B. Nanofiber Drawing and Nanodevice Assembly in Poly(trimethylene Terephthalate). Optical Society of America 16(14) (2008): 10815-10822.
- [24] Ichimori, T., Mizuma, K., Uchida, T., Yamazaki, S., and Kimura¹, K. Morphological Diversity and Nanofiber Networks of Poly(p-oxybenzoyl) Generated by Phase Separation During Copolymerization. Journal of Applied Polymer Science 128 (2013): 1282-1290.
- [25] Shao, J., Chen, C., Wang, Y., Chen, X., and Du, C. Early Stage Evolution of Structure and Nanoscale Property of Nanofibers in Thermally Induced Phase Separation Process. Reactive and Functional Polymers 72(10) (2012): 765-772.
- [26] Ramakrishna, S. An Introduction to Electrospinning and Nanofibers. World Scientific, 2005.
- [27] Smith, L.A. and Ma, P.X. Nano-Fibrous Scaffolds for Tissue Engineering. Colloids and Surfaces. B, Biointerfaces 39(3) (2004): 125-131.

- [28] Subbiah, T., Bhat, G.S., Tock, R.W., Parameswaran, S., and Ramkumar, S.S. Electrospinning of Nanofibers. Journal of Applied Polymer Science 96(2) (2005): 557-569.
- [29] Frenot, A. and Chronakis, I.S. Polymer Nanofibers Assembled by Electrospinning. Current Opinion in Colloid & Interface Science 8(1) (2003): 64-75.
- [30] Lin, J., Wang, X., Ding, B., Yu, J., Sun, G., and Wang, M. Biomimicry via Electrospinning. Critical Reviews in Solid State and Materials Sciences 37(2) (2012): 94-114.
- [31] Matsumoto, H. and Tanioka, A. Functionality in Electrospun Nanofibrous Membranes Based on Fiber's Size, Surface Area, and Molecular Orientation. Membranes (Basel) 1(3) (2011): 249-64.
- [32] Supaphol, P., Suwanton, O., Sangsanoh, P., Srinivasan, S., Jayakumar, R., and Nair, S.V. Electrospinning of Biocompatible Polymers and Their Potentials in Biomedical Applications. Advanced Polymer Science 246 (2011): 213-239.
- [33] Valizadeh, A. and Mussa Farkhani, S. Electrospinning and Electrospun Nanofibres. IET Nanobiotechnol 8(2) (2014): 83-92.
- [34] Kim, J.-S. and Wneker, D.H. Polybenzimidazole Nanofiber Produced By Electrospinning. Polymer Engineering and Science 39(5) (1999): 849-854.
- [35] Bhardwaj, N. and Kundu, S.C. Electrospinning: A Fascinating Fiber Fabrication Technique. Biotechnology Advances 28(3) (2010): 325-47.
- [36] Tatiana C. Rohner, Lion, N., and Girault, H.H. Electrochemical and Theoretical Aspects of Electro Spray Ionisation. Physical Chemistry Chemical Physics 6(12) (2004): 3056-3068.
- [37] Hohman, M.M., Shin, M., Rutledge, G., and Brenner, M.P. Electrospinning and Electrically Forced Jets. I. Stability Theory. Physics of Fluids 13(8) (2001): 2201.
- [38] Haghi, A.K. and Akbari, M. Trends in Electrospinning of Natural Nanofibers. Physica Status Solidi (A) 204(6) (2007): 1830-1834.
- [39] Hohman, M.M., Shin, M., Rutledge, G., and Brenner, M.P. Electrospinning and Electrically Forced Jets. II. Applications. Physics of Fluids 13(8) (2001): 2221.

- [40] Rodriguez-Mozaz, S., Lopez de Alda, M.J., and Barcelo, D. Advantages and Limitations of On-Line Solid Phase Extraction Coupled to Liquid Chromatography-Mass Spectrometry Technologies Versus Biosensors for Monitoring of Emerging Contaminants in Water. Journal of chromatography A 1152(1-2) (2007): 97-115.
- [41] Pedrouzo, M., Reverté, S., Borrull, F., Pocurull, E., and Marcé, R.M. Pharmaceutical Determination in Surface and Wastewaters Using High-Performance Liquid Chromatography-(Electrospray)-Mass Spectrometry. Journal of Separation Science 30(3) (2007): 297-303.
- [42] Telepchak, M.J., August, T.F., and Chaney, G. Forensic and Clinical Application of Solid Phase Extraction. Humana Press, 2004.
- [43] Baggiani, C., Anfossi, L., and Giovannoli, C. Solid Phase Extraction of Food Contaminants Using Molecular Imprinted Polymers. Analytica Chimica Acta 591(1) (2007): 29-39.
- [44] Liska, I. Fifty Years of Solid-Phase Extraction in Water Analysis –Historical Development and Overview. Journal of Chromatography A 885 (2000): 3-16.
- [45] Płotka-Wasyłka, J., Szczepanska, N., de la Guardia, M., and Namiesnik, J. Modern Trends in Solid Phase Extraction: New Sorbent Media. Trends in Analytical Chemistry 77 (2016): 23-43.
- [46] Solid Phase Extraction Columns [Online]. Available from: <http://www.greyhoundchrom.com/topic/31-solid-phase-extraction-columns.aspx> [March 15, 2016]
- [47] Agilent Bond Elut OMIX [Online]. Available from: <https://www.agilent.com/cs/library/primers/public/5990-9049EN-Omix-Sept11-lo.pdf> [March 15, 2016]
- [48] Empore™ C18 90 mm Extraction Disc, Model 2315, 10 pack, 3 packs per case per case [Online]. Available from: http://solutions.3m.com/wps/portal/3M/en_US/3M-Purification-Inc/3MPI-US/Products/~Empore-C18-90-mm-Extraction-Disc-Model-2315-10-pack-3-packs-per-case-per-case?N=8691596+4294874097&rt=d [March 15, 2016]

- [49] Thurman, E.M. and Snavely, K. Advances in Solid-Phase Extraction Disks for Environmental Chemistry. Trends in Analytical Chemistry 19(1) (2000): 18-26.
- [50] Houessou, J.K., Benac, C., Delteil, C., and Camel, V.R. Determination of Polycyclic Aromatic Hydrocarbons in Coffee Brew Using Solid-Phase Extraction. Journal of Agricultural and Food Chemistry 53 (2005): 871-879.
- [51] Moreda, W., Rodríguez-Acuña, R., del Carmen Pérez-Camino, M., and Cert, A. Determination of High Molecular Mass Polycyclic Aromatic Hydrocarbons in Refined Olive Pomace and Other Vegetable Oils. Journal of the Science of Food and Agriculture 84(13) (2004): 1759-1764.
- [52] Bianchin, J.N., Nardini, G., Merib, J., Dias, A.N., Martendal, E., and Carasek, E. Simultaneous Determination of Polycyclic Aromatic Hydrocarbons and Benzene, Toluene, Ethylbenzene and Xylene in Water Samples Using A New Sampling Strategy Combining Different Extraction Modes and Temperatures in A Single Extraction Solid-Phase Microextraction-Gas Chromatography-Mass Spectrometry Procedure. Journal of chromatography A 1233 (2012): 22-9.
- [53] Cortazar, E., Zuloaga, O., Sanz, J., Raposo, J.C., Etxebarria, N., and Fernández, L.A. Multisimplex Optimisation of The Solid-Phase Microextraction-Gas Chromatographic-Mass Spectrometric Determination of Polycyclic Aromatic Hydrocarbons, Polychlorinated Biphenyls and Phthalates from Water Samples. Journal of Chromatography A 978 (2002): 165-175.
- [54] Doonga, R.-a., Changa, S.-m., and Sunb, Y.-c. Solid-Phase Microextraction for Determining The Distribution of Sixteen US Environmental Protection Agency Polycyclic Aromatic Hydrocarbons in Water Samples. Journal of Chromatography A 879 (2000): 177-188.
- [55] Potted, D.W. and Pawliszyn, J. Rapid Determination of Polyaromatic Hydrocarbons and Polychlorinated Biphenyls in Water Using Solid-Phase Microextraction and GC/MS. Journal of Environmental Science and Technology 28 (1994): 298-305.
- [56] Tang, B. and Isacson, U. Analysis of Mono- and Polycyclic Aromatic Hydrocarbons Using Solid-Phase Microextraction: State-of-the-Art. Energy & Fuels 22 (2008): 1425-1438.

- [57] Vichi, S., Pizzale, L., Conte, L.S., Buxaderas, S., and López-Tamames, E. Simultaneous Determination of Volatile and Semi-Volatile Aromatic Hydrocarbons in Virgin Olive Oil by Headspace Solid-Phase Microextraction Coupled to Gas Chromatography/Mass Spectrometry. Journal of Chromatography A 1090(1-2) (2005): 146-154.
- [58] Ziabari, M., Mottaghitlab, V., and Haghi, A.K. Application of Direct Tracking Method for Measuring Electrospun Nanofiber Diameter. Brazilian Journal of Chemical Engineering 26(01) (2009): 53-62.
- [59] AOAC Peer-Verified Methods Program, Manual on Policies and Procedures. in *Appendix F: Guidelines for Standard Method Performance Requirements*. 1998, AOAC International: Gaithersburg, MD, USA.





APPENDIX

จุฬาลงกรณ์มหาวิทยาลัย
CHULALONGKORN UNIVERSITY

Table A-1 Equation and R^2 value of calibration curve for PAHs

Name	Equation	R^2
Naphthalene	$y = 4.4534x - 0.3194$	0.9965
Acenaphthylene	$y = 1.9703x - 0.1307$	0.9978
Acenaphthene	$y = 2.9010x - 0.2569$	0.9951
Fluorene	$y = 0.9360x - 0.0644$	0.9972
Phenanthrene	$y = 1.4500x - 0.0903$	0.9976
Anthracene	$y = 1.1978x - 0.0826$	0.9971
Fluoranthene	$y = 1.1237x - 0.0600$	0.9985
Pyrene	$y = 1.1179x - 0.0582$	0.9984
Benzo(a)anthracene	$y = 0.5550x - 0.0516$	0.9968
Chrysene	$y = 0.6354x - 0.0604$	0.9960
Benzo(b)fluoranthene	$y = 0.3226x - 0.0305$	0.9971
Benzo(k)fluoranthene	$y = 0.2923x - 0.0324$	0.9954
Benzo(a)pyrene	$y = 0.2466x - 0.0242$	0.9969
Indeno(1,2,3-cd)pyrene	$y = 0.1455x - 0.0114$	0.9971
Dibenzo(a,h)anthracene	$y = 0.1232x - 0.0067$	0.9974
Benzo(g,h,i)perylene	$y = 0.1707x - 0.0097$	0.9979

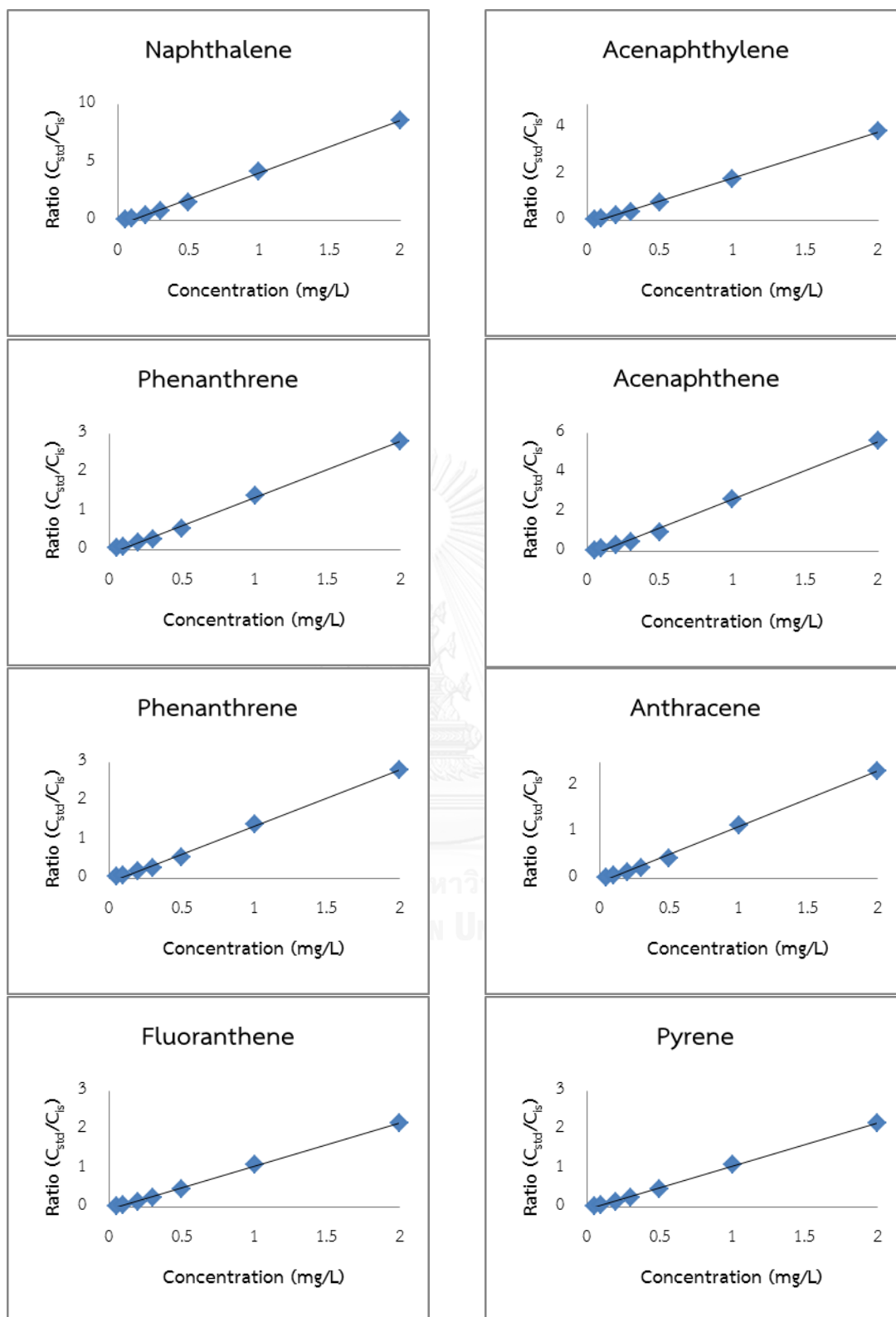


Figure A-1 Calibration curve of PAHs analysis by GC-MS

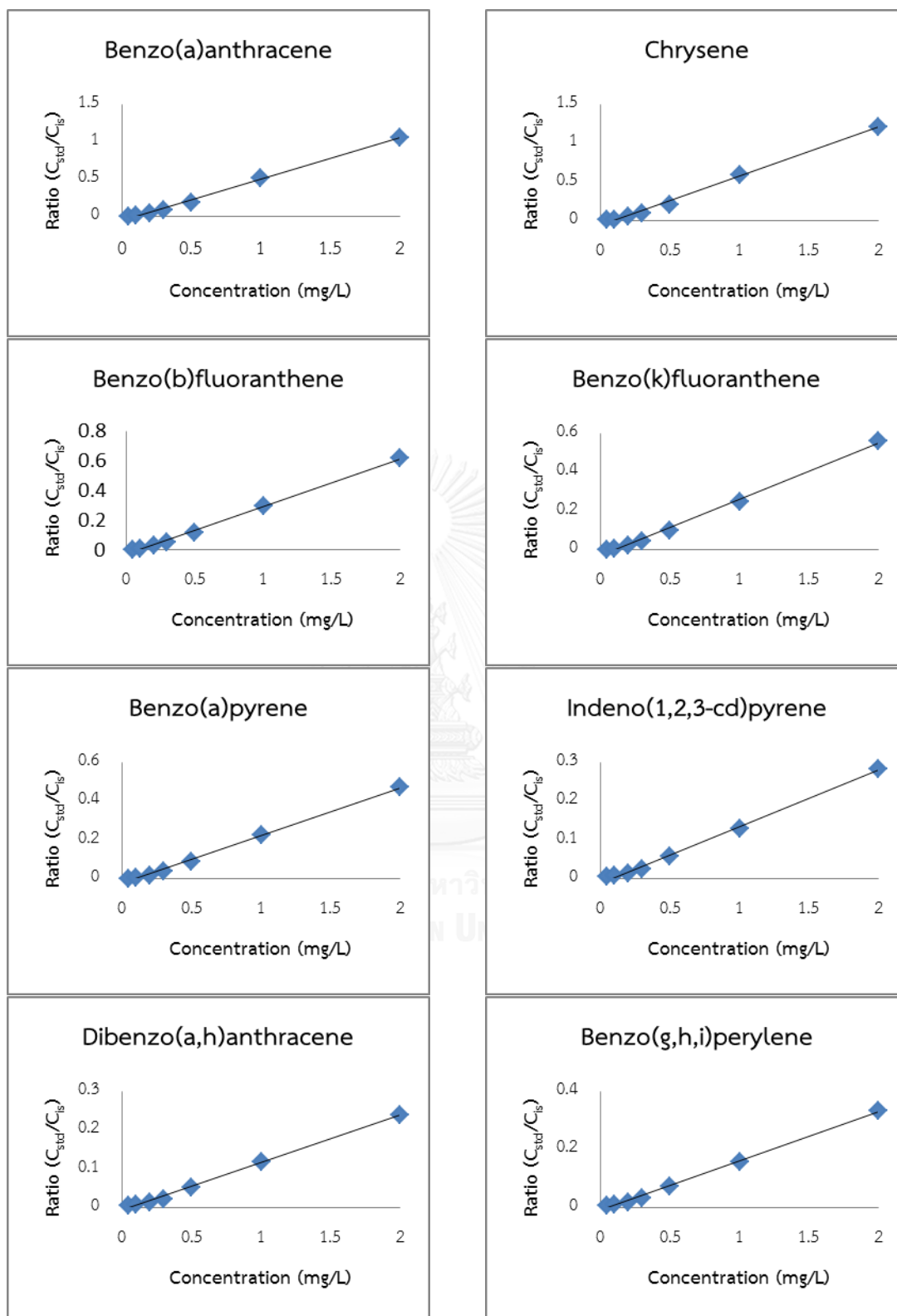


Figure A-1 Calibration curve of PAHs analysis by GC-MS (continue)

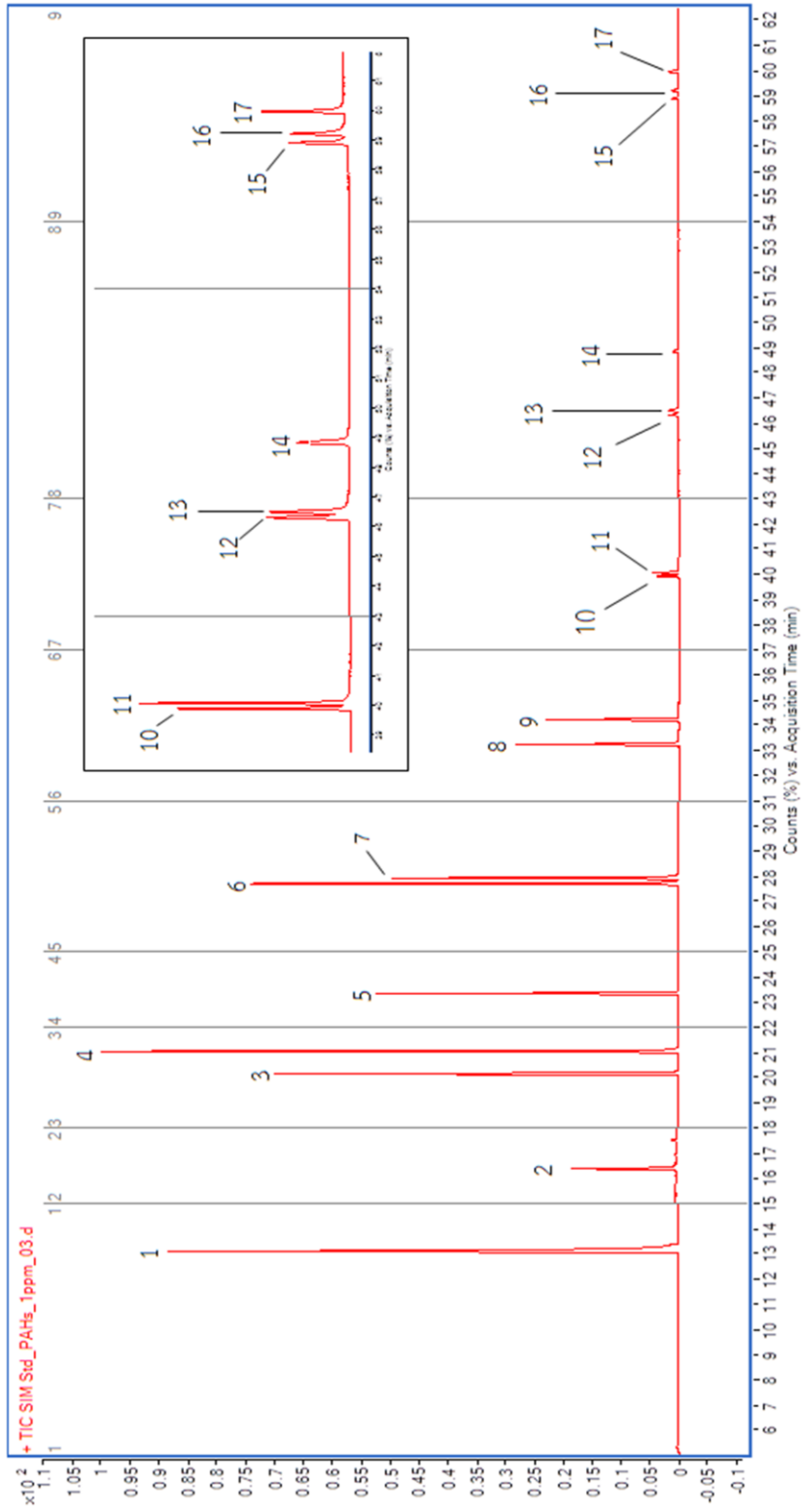


Figure A-2 GC chromatogram of mixed standard PAHs at 1 mg/L.

(Peak 1: Naphthalene, 2: Decafluorobiphenyl, 3: Acenaphthylene, 4: Acenaphthene, 5: Fluorene, 6: Phenanthrene, 7: Anthracene, 8: Fluoranthene, 9: Pyrene, 10: Benzo(a)anthracene, 11: Chrysene, 12: Benzo(b)fluoranthene, 13: Benzo(k)fluoranthene, 14: Benzo(a)pyrene, 15: Indeno(1,2,3-cd)pyrene, 16: Dibenzo(a,h)anthracene, 17: Benzo(g,h,i)perylene)

Table A-2 Retention time, Peak width and Resolution of PAHs

Peak Number	Compound Name	Retention Time (min)	Peak Width (min)	Resolution
1	Naphthalene	13.05	0.42	-
2	Decafluorobiphenyl	16.35	0.18	11.00
3	Acenaphthylene	20.1	0.23	18.29
4	Acenaphthene	20.98	0.25	3.67
5	Fluorene	23.32	0.16	11.41
6	Phenanthrene	27.67	0.18	25.59
7	Anthracene	27.88	0.2	1.11
8	Fluoranthene	33.21	0.18	28.05
9	Pyrene	34.17	0.17	5.49
10	Benzo(a)anthracene	39.86	0.19	31.61
11	Chrysene	40.04	0.18	0.97
12	Benzo(b)fluoranthene	46.26	0.21	31.90
13	Benzo(k)fluoranthene	46.46	0.18	1.03
14	Benzo(a)pyrene	48.78	0.27	10.31
15	Indeno(1,2,3-cd)pyrene	58.85	0.19	43.78
16	Dibenzo(a,h)anthracene	59.15	0.16	1.71
17	Benzo(g,h,i)perylene	59.90	0.16	4.69

Table A-3 Determined PAHs concentration in spiked water (8 µg/L) for extraction by different sorbents.

Name	C18		2.5N		30N		2.5N0.33C		2.5N0.66C		2.5N0.83C		30N0.33C		30N0.66C		30N0.83C	
	Mean	SD	Mean	SD	Mean	SD	Mean	SD	Mean	SD	Mean	SD	Mean	SD	Mean	SD	Mean	SD
Naphthalene	0.1442	0.0037	0.1444	0.0012	0.1404	0.0016	0.1446	0.0019	0.1482	0.0025	0.1488	0.0016	0.1464	0.0022	0.1510	0.0032	0.1510	0.0014
Acenaphthylene	0.1942	0.0036	0.1966	0.0013	0.1936	0.0023	0.1974	0.0019	0.1958	0.0013	0.1964	0.0016	0.1882	0.0029	0.1910	0.0015	0.1910	0.0023
Acenaphthene	0.1854	0.0037	0.1876	0.0007	0.1862	0.0012	0.1888	0.0013	0.1876	0.0020	0.1878	0.0023	0.1884	0.0017	0.1882	0.0019	0.1882	0.0017
Fluorene	0.2060	0.0031	0.2066	0.0011	0.2032	0.0015	0.2062	0.0017	0.2064	0.0014	0.2062	0.0022	0.2028	0.0027	0.2038	0.0012	0.2038	0.0020
Phenanthrene	0.2068	0.0031	0.2062	0.0012	0.2008	0.0014	0.2066	0.0015	0.2068	0.0008	0.2044	0.0014	0.2010	0.0012	0.2038	0.0021	0.2038	0.0020
Anthracene	0.2022	0.0029	0.2056	0.0010	0.2032	0.0021	0.2062	0.0016	0.2070	0.0023	0.2070	0.0021	0.2010	0.0030	0.2036	0.0014	0.2036	0.0018
Fluoranthene	0.1794	0.0047	0.1810	0.0008	0.1782	0.0021	0.1830	0.0025	0.1848	0.0014	0.1810	0.0030	0.1816	0.0020	0.1846	0.0013	0.1846	0.0026
Pyrene	0.1484	0.0031	0.1502	0.0015	0.1486	0.0016	0.1504	0.0019	0.1530	0.0044	0.1546	0.0021	0.1506	0.0021	0.1598	0.0066	0.1598	0.0024
Benzo (a) anthracene	0.1214	0.0023	0.1236	0.0006	0.1190	0.0022	0.1238	0.0010	0.1264	0.0015	0.1316	0.0016	0.1362	0.0027	0.1406	0.0021	0.1406	0.0011
Chrysene	0.1188	0.0013	0.1212	0.0009	0.1176	0.0011	0.1222	0.0023	0.1278	0.0021	0.1282	0.0018	0.1270	0.0079	0.1334	0.0031	0.1334	0.0019
Benzo (b) fluoranthrene	0.1156	0.0025	0.1196	0.0016	0.1154	0.0021	0.1206	0.0010	0.1242	0.0018	0.1286	0.0017	0.1242	0.0028	0.1328	0.0068	0.1328	0.0018
Benzo (k) fluoranthrene	0.1220	0.0013	0.1270	0.0008	0.1232	0.0021	0.1312	0.0024	0.1342	0.0022	0.1372	0.0024	0.1318	0.0013	0.1406	0.0050	0.1406	0.0018
Benzo (a) pyrene	0.1148	0.0016	0.1188	0.0015	0.1142	0.0025	0.1236	0.0016	0.1284	0.0026	0.1314	0.0009	0.1206	0.0017	0.1350	0.0115	0.1350	0.0024
Indeno (1,2,3-cd) pyrene	0.0930	0.0024	0.0962	0.0020	0.0944	0.0019	0.1028	0.0024	0.1102	0.0038	0.1114	0.0013	0.1042	0.0023	0.1176	0.0052	0.1176	0.0018
Dibenzo (a,h) anthracene	0.0774	0.0056	0.0804	0.0082	0.0808	0.0013	0.0898	0.0058	0.0956	0.0021	0.0996	0.0015	0.0900	0.0037	0.1044	0.0084	0.1044	0.0019
Benzo (g,h,i) perylene	0.0778	0.0073	0.0816	0.0076	0.0762	0.0026	0.0904	0.0050	0.0948	0.0051	0.1012	0.0021	0.0936	0.0025	0.1054	0.0066	0.1058	0.0021

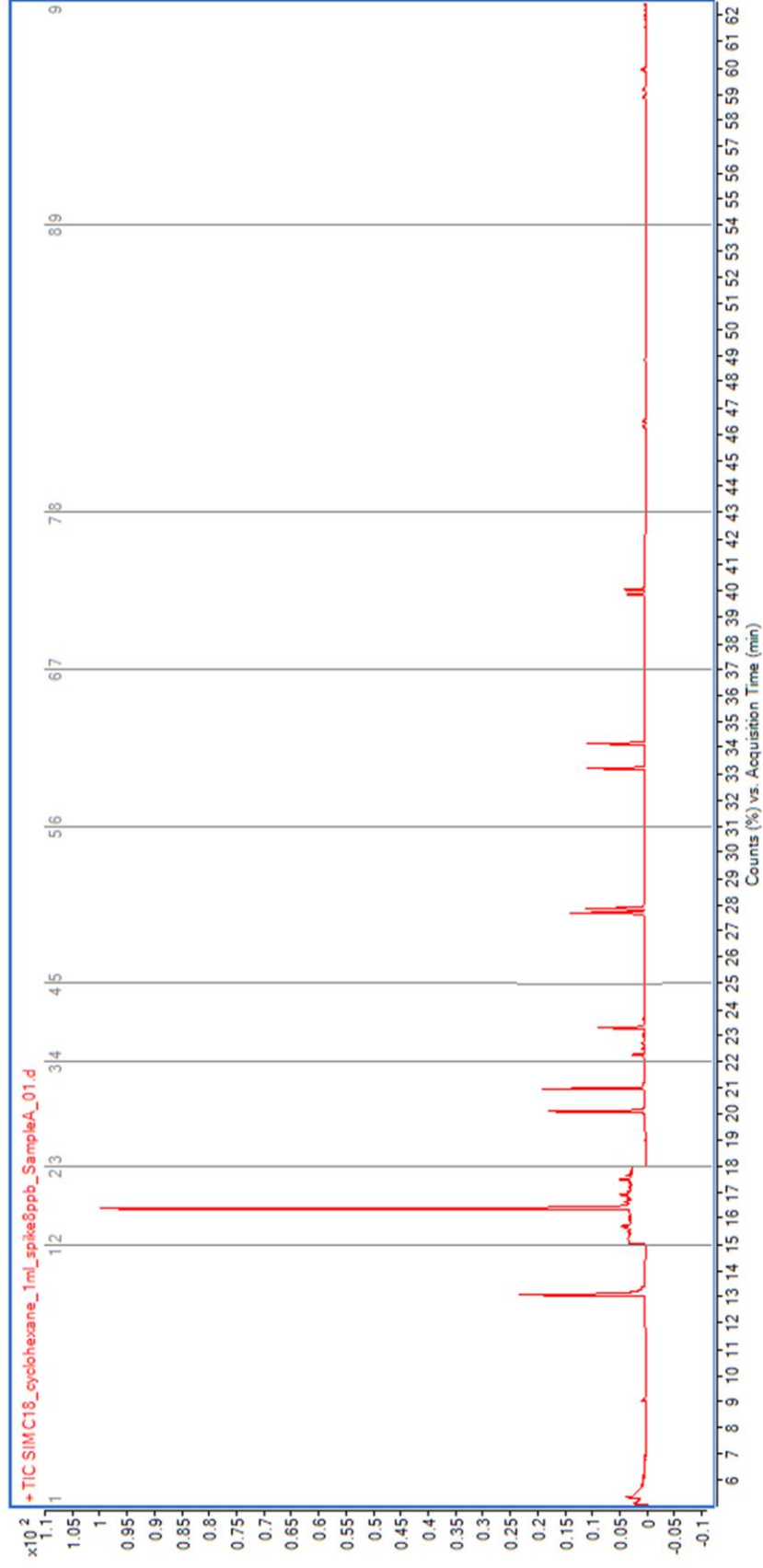


Figure A-3 Chromatogram of PAHs from the extraction of 8 µg/L spiked water by C18 SPE.

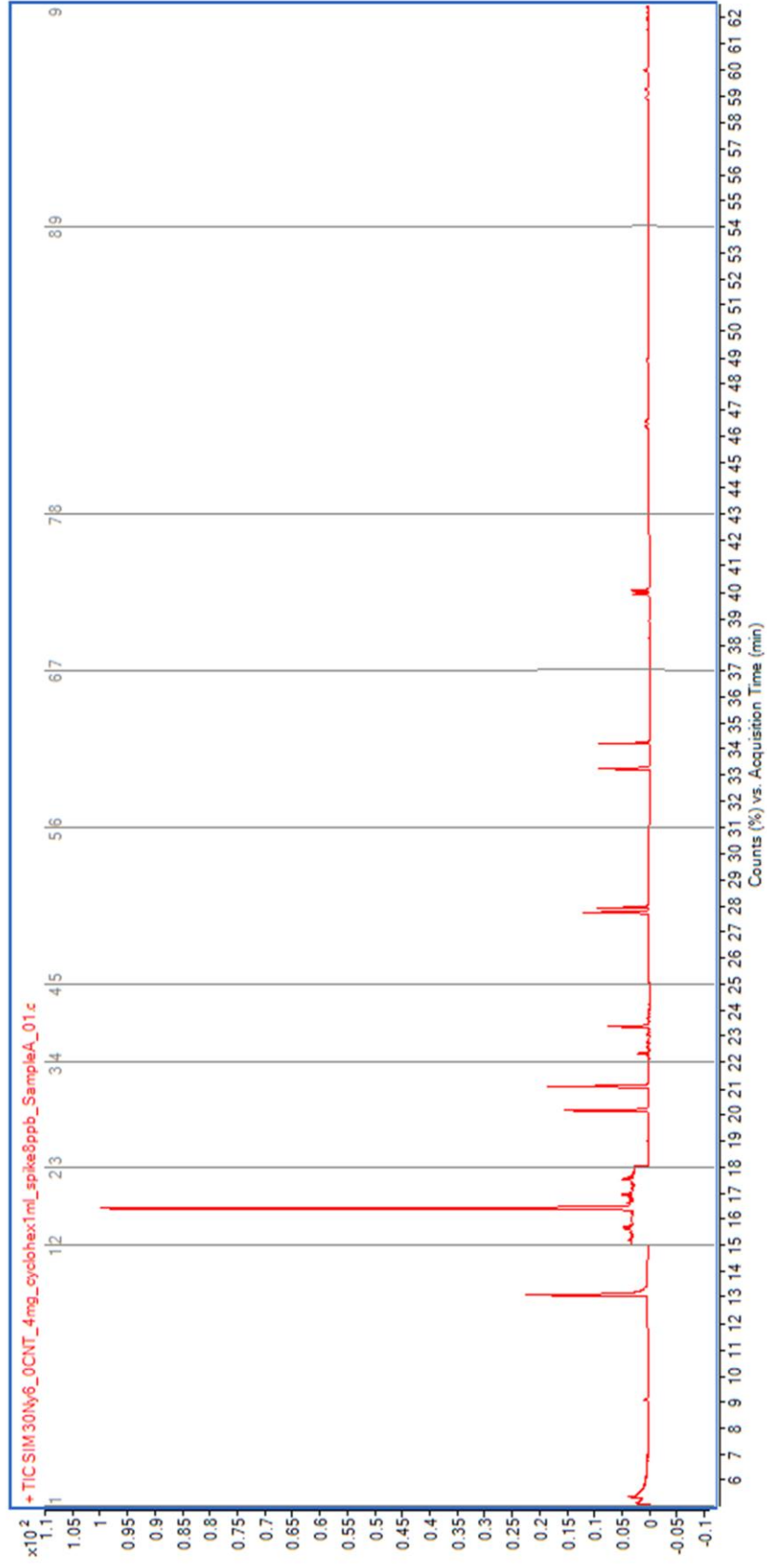


Figure A-4 Chromatogram of PAHs from the extraction of 8 µg/L spiked water by Nylon6 nanofibers (30N).

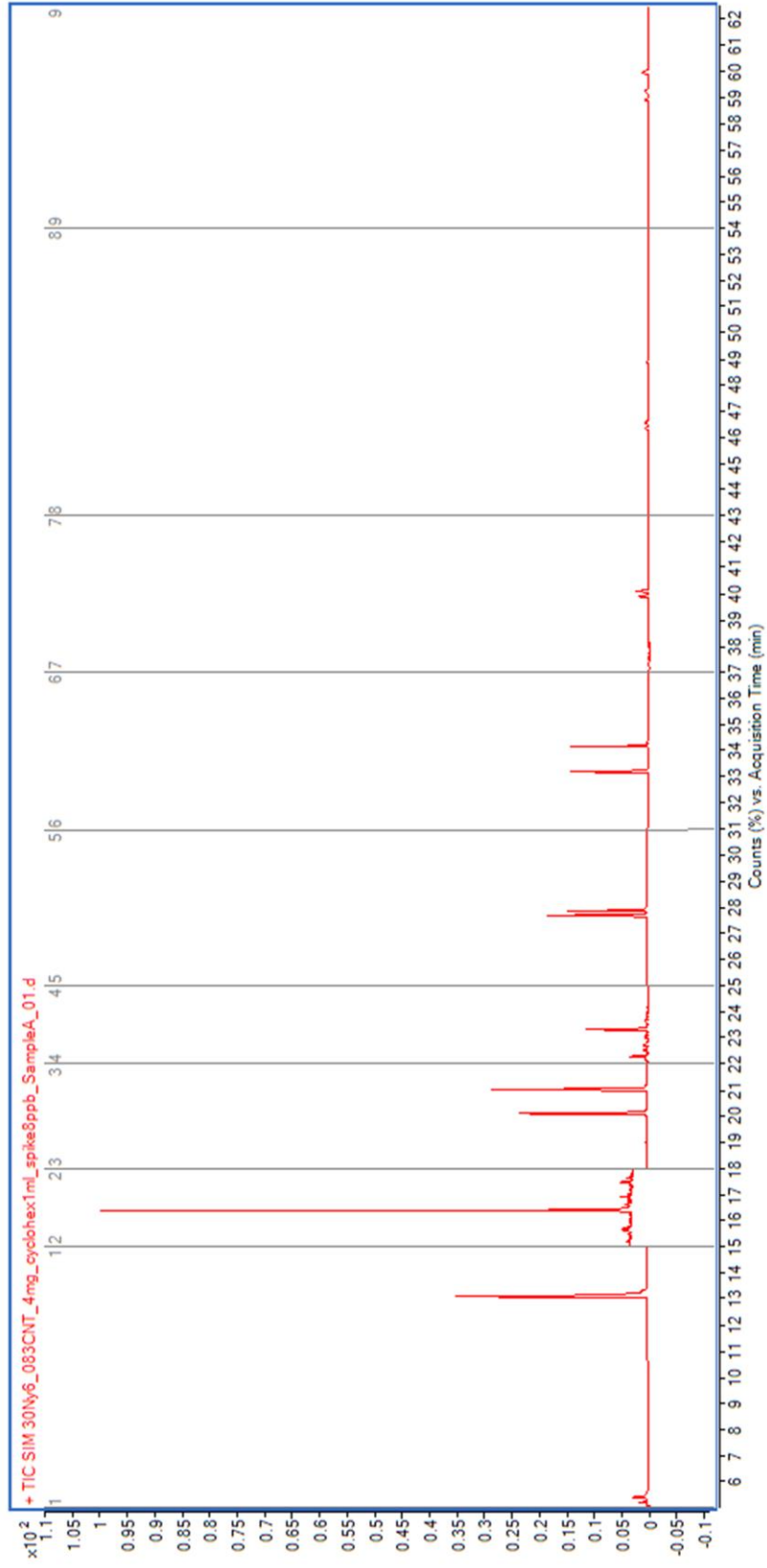


Figure A-5 Chromatogram of PAHs from the extraction of 8 $\mu\text{g/L}$ spiked water by CNTs-Nylon6 composite nanofibers (30N0.33C).

Table A-4 Determined PAHs concentration in spiked water (8 µg/L) for extraction by 30N0.83C sorbent as the sorbent and eluting with different desorption solvents.

Name	Cyclohexane		Hexane		Methanol		Acetone		Acetonitrile		Acetone : ACN,1:1		Acetone : ACN,1:2		Acetone : ACN,2:1	
	Mean	SD	Mean	SD	Mean	SD	Mean	SD	Mean	SD	Mean	SD	Mean	SD	Mean	SD
Naphthalene	0.1510	0.0014	0.1504	0.0031	0.1484	0.0034	0.1484	0.0031	0.1476	0.0021	0.1502	0.0035	0.1402	0.0016	0.1446	0.0019
Acenaphthylene	0.1910	0.0023	0.1906	0.0004	0.1890	0.0010	0.1894	0.0013	0.1854	0.0007	0.1906	0.0024	0.1884	0.0010	0.1886	0.0010
Acenaphthene	0.1882	0.0017	0.1876	0.0027	0.1854	0.0030	0.1862	0.0010	0.1820	0.0036	0.1790	0.0023	0.1804	0.0016	0.1850	0.0013
Fluorene	0.2038	0.0020	0.2030	0.0010	0.1960	0.0013	0.1990	0.0010	0.1992	0.0022	0.2002	0.0038	0.1982	0.0010	0.1996	0.0019
Phenanthrene	0.2038	0.0020	0.2002	0.0023	0.1992	0.0020	0.1998	0.0004	0.1972	0.0006	0.1988	0.0024	0.1964	0.0010	0.1986	0.0028
Anthracene	0.2036	0.0018	0.2036	0.0032	0.1974	0.0022	0.1988	0.0022	0.1990	0.0006	0.2016	0.0023	0.1998	0.0017	0.1988	0.0027
Fluoranthene	0.1846	0.0026	0.1830	0.0035	0.1776	0.0030	0.1850	0.0014	0.1814	0.0034	0.1826	0.0015	0.1804	0.0026	0.1816	0.0019
Pyrene	0.1598	0.0024	0.1562	0.0033	0.1544	0.0038	0.1610	0.0030	0.1628	0.0028	0.1672	0.0016	0.1646	0.0022	0.1610	0.0027
Benzo (a) anthracene	0.1406	0.0011	0.1428	0.0016	0.1408	0.0027	0.1450	0.0014	0.1470	0.0034	0.1468	0.0014	0.1434	0.0028	0.1430	0.0021
Chrysene	0.1334	0.0019	0.1316	0.0039	0.1324	0.0030	0.1346	0.0028	0.1386	0.0006	0.1388	0.0026	0.1364	0.0023	0.1322	0.0020
Benzo (b) fluoranthrene	0.1328	0.0018	0.1304	0.0040	0.1306	0.0041	0.1352	0.0031	0.1408	0.0017	0.1410	0.0035	0.1402	0.0049	0.1356	0.0017
Benzo (k) fluoranthene	0.1406	0.0018	0.1406	0.0012	0.1422	0.0023	0.1444	0.0034	0.1514	0.0019	0.1514	0.0031	0.1508	0.0045	0.1466	0.0030
Benzo (a) pyrene	0.1350	0.0024	0.1326	0.0025	0.1324	0.0023	0.1342	0.0016	0.1466	0.0010	0.1472	0.0030	0.1464	0.0030	0.1420	0.0041
Indeno (1,2,3-cd) pyrene	0.1176	0.0018	0.1136	0.0016	0.1122	0.0027	0.1130	0.0017	0.1184	0.0003	0.1192	0.0051	0.1166	0.0042	0.1128	0.0051
Dibenzo (a, h) anthracene	0.1044	0.0019	0.1052	0.0007	0.1022	0.0014	0.1066	0.0027	0.1136	0.0030	0.1134	0.0031	0.1132	0.0051	0.1072	0.0040
Benzo (g, h, i) perylene	0.1058	0.0021	0.1038	0.0026	0.1058	0.0009	0.1066	0.0009	0.1138	0.0033	0.1138	0.0053	0.1134	0.0053	0.1062	0.0053

Table A-5 Determined PAHs concentration in spiked water (8 µg/L) for extraction by 30N0.83C sorbent and eluting with different volumes of 1:1 (v/v) mixture of acetone and acetonitrile.

Name	0.5 mL		1.0 mL		1.5 mL	
	Mean	SD	Mean	SD	Mean	SD
Naphthalene	0.1388	0.0021	0.1502	0.0035	0.1504	0.0020
Acenaphthylene	0.1806	0.0026	0.1906	0.0024	0.1908	0.0013
Acenaphthene	0.1647	0.0024	0.1790	0.0023	0.1788	0.0010
Fluorene	0.1768	0.0018	0.2002	0.0038	0.1998	0.0019
Phenanthrene	0.1814	0.0013	0.1988	0.0024	0.1990	0.0023
Anthracene	0.1792	0.0018	0.2016	0.0023	0.2016	0.0013
Fluoranthene	0.1490	0.0021	0.1826	0.0015	0.1830	0.0016
Pyrene	0.1004	0.0004	0.1672	0.0016	0.1672	0.0017
Benzo (a) anthracene	0.1006	0.0009	0.1468	0.0014	0.1442	0.0012
Chrysene	0.0989	0.0008	0.1388	0.0026	0.1350	0.0027
Benzo (b) fluoranthrene	0.0989	0.0040	0.1410	0.0035	0.1410	0.0008
Benzo (k) fluoranthene	0.1258	0.0041	0.1514	0.0031	0.1508	0.0013
Benzo (a) pyrene	0.1153	0.0023	0.1472	0.0030	0.1464	0.0038
Indeno (1,2,3-cd) pyrene	0.0799	0.0009	0.1192	0.0051	0.1202	0.0017
Dibenzo (a,h) anthracene	0.0716	0.0026	0.1134	0.0031	0.1126	0.0024
Benzo (g,h,i) perylene	0.0698	0.0029	0.1138	0.0053	0.1142	0.0021

Table A-6 Determined PAHs concentration in spiked water (8 µg/L) for extraction by using different weights of 30N0.83C sorbent and eluting with 1 mL of 1:1 (v/v) mixture of acetone and acetonitrile.

Name	3.0 mg		4.0 mg		5.0 mg		6.0 mg	
	Mean	SD	Mean	SD	Mean	SD	Mean	SD
Naphthalene	0.1498	0.0028	0.1502	0.0035	0.1500	0.0019	0.1492	0.0029
Acenaphthylene	0.1902	0.0031	0.1906	0.0024	0.1910	0.0031	0.1920	0.0023
Acenaphthene	0.1782	0.0014	0.1790	0.0023	0.1805	0.0040	0.1775	0.0016
Fluorene	0.1994	0.0020	0.2002	0.0038	0.1988	0.0015	0.1996	0.0024
Phenanthrene	0.1980	0.0034	0.1988	0.0024	0.1982	0.0031	0.1986	0.0026
Anthracene	0.1988	0.0043	0.2016	0.0023	0.2002	0.0027	0.2008	0.0020
Fluoranthene	0.1802	0.0034	0.1826	0.0015	0.1844	0.0037	0.1824	0.0029
Pyrene	0.1652	0.0012	0.1672	0.0016	0.1658	0.0054	0.1674	0.0026
Benzo (a) anthracene	0.1458	0.0023	0.1468	0.0014	0.1476	0.0028	0.1484	0.0014
Chrysene	0.1346	0.0035	0.1388	0.0026	0.1404	0.0072	0.1386	0.0044
Benzo (b) fluoranthrene	0.1330	0.0010	0.1410	0.0035	0.1396	0.0023	0.1406	0.0036
Benzo (k) fluoranthene	0.1456	0.0046	0.1514	0.0031	0.1510	0.0030	0.1496	0.0036
Benzo (a) pyrene	0.1386	0.0049	0.1472	0.0030	0.1474	0.0027	0.1450	0.0052
Indeno (1,2,3-cd) pyrene	0.1056	0.0032	0.1192	0.0051	0.1204	0.0040	0.1168	0.0025
Dibenzo (a,h) anthracene	0.1032	0.0051	0.1134	0.0031	0.1136	0.0057	0.1146	0.0040
Benzo (g,h,i) perylene	0.1026	0.0045	0.1138	0.0053	0.1134	0.0071	0.1152	0.0044

VITA

Mr. Sirisak Tharasiripaitoon was born on May 9, 1989 in Bangkok, Thailand. He graduated with the degree of Bachelor of Science in Chemistry, Thammasat University in 2011. After that, he had worked at T.P. Drug Laboratories(1969) Co., Ltd. for 1 year and General Drug House Co., Ltd. for 8 months. In 2013, he has been a graduated student at Program of Petrochemistry and Polymer Science, Faculty of Science, Chulalongkorn University and become a member of Chromatography and Separation Research Unit (ChSRU). He finished his Master's degree of Science in 2016

Poster presentation and proceeding

"Characterization of Electrospun Nylon6-Carbon Nanotubes Composite Membrane for Solid Phase Extraction" Sirisak Tharasiripaitoon, Puttaruksa Varanusupakul. Poster presentation and proceeding, Pure and Applied Chemistry International Conference 2016 (PACCON 2016), Bangkok International Trade and Exhibition Centre (BITEC), Bangna, Bangkok, Thailand, 9-11 February, 2016.